THE EPITHELIAL NA^+ CHANNEL (ENAC) IN PANCREATIC ISLET β-CELLS REGULATES INSULIN SECRETION AND GLUCOSE METABOLISM

QUE YANTING

PhD

The Hong Kong Polytechnic University

2024

The Hong Kong Polytechnic University

Department of Biomedical Engineering

The epithelial Na^+ channel (ENaC) in pancreatic islet β-cells regulates insulin secretion and glucose metabolism

QUE Yanting

A thesis submitted in partial fulfillment of the requirements for the degree of Doctor of Philosophy

November 2023

CERTIFICATE OF ORIGINALITY

I hereby declare that this thesis is my own work and that, to the best of my knowledge and belief, it reproduces no material previously published or written, nor material that has been accepted for the award of any other degree or diploma, except where due acknowledgment has been made in the text.

_ ____(Signed)

___ QUE Yanting ____(Name of student)

Abstract

Insulin is exclusively produced and secreted by pancreatic islet β-cells, which plays a central role in regulating glucose metabolism. In response to blood glucose elevation or other physiological stimuli, β-cells are excited to trigger intracellular events such as Ca^{2+} mobilization and cAMP elevation leading to exocytosis of insulin granules, although the underlying molecular mechanisms are not fully understood. Previously, we identified a chloride channel CFTR in contributing to β-cell excitability and insulin secretion. In epithelial cells, it is well noted that CFTR closely interacts with the epithelial Na^+ channel (ENaC), which is best known for its role in epithelial Na^+ absorption. The present study aimed to elucidate whether and how ENaC is expressed in pancreatic islet β-cells to regulate insulin secretion and glucose metabolism.

In the first part of study, we analyzed human databases, primary rat/mouse pancreatic tissues as well as RINm5F, a rat β-cell line, which confirmed the expression of *Scnn1a*, *Scnn1b* and *Scnn1g* genes (encoding ENaC subunits, α, β and γ, respectively) in human and rodent β-cells. To our surprise, inhibiting this Na^+ channel by selective blockers, amiloride or benzamil, did not retard insulin secretion, but instead triggered a slow membrane depolarization with electrical bursts, elicited substantial Ca^{2+} oscillations and promoted insulin secretion in RINm5F or isolated mouse β-cells. siRNA-based knockdown of ENaCα, the rate-limiting subunit of ENaC, in RINm5F cells confirmed that deficiency of ENaC induced a significant increase in insulin

secretion. These findings suggested that ENaC in pancreatic islet β-cells is inversely correlated with insulin secretion.

The second part of the study was carried out to investigate the mechanism underlying the ENaC-mediated suppression of insulin secretion. Proteomic analysis of RINm5F cells through mass spectrometry showed ENaC knockdown altered glucose metabolism and cAMP-related insulin secretion signaling pathways, consistently suggesting a role of ENaC deficiency in exciting β-cells to release insulin. Further study confirmed that ENaC deficiency indeed caused an increase in intracellular cAMP levels. Pharmaceutical inhibition of the cAMP-synthesized enzyme adenyl cyclase (AC) by DDA or knockdown AC6/AC8 abolished the effects of ENaC deficiency including membrane depolarization, Ca^{2+} increases and insulin secretion. Manipulation of intracellular sodium levels together with recording cAMP signals revealed that high concentrations of sodium inhibit the cAMP response to its agonist forskolin. It therefore suggested that ENaC-mediated Na^{+} entry exerts an inhibitory effect on ACs activity and thus cAMP production which modulates multiple downstream events/factors to suppress modulating insulin secretion in β-cells.

Next, to evaluate the effect of ENaC on insulin secretion and glucose metabolism *in vivo*, a conditional knockout (cKO) mouse model with β-cell-specific knockout of ENaCα (*Scnn1a*$^{fl/fl}$, *Ins2*-Cre^{+}) was built, which exhibited disturbed responses in glucose tolerance in comparison with the loxp-negative Cre control mice

(*Scnn1a*$^{wt/wt}$, *Ins2*-Cre^{+}). The cKO mice, at young ages before puberty, exhibited insulin hypersecretion, hypoglycemia, enhanced PKA activation in islets as compared to the Cre control mice, although these changes were found diminished when the mice grew to mature ages (> 8-week-old). However, isolated islets from young or old cKO mice consistently showed hypersecretion of insulin *in vitro*.

Taken together, the present study has revealed a previously undefined role of ENaC in regulating β-cell function and insulin secretion: ENaC serves as a brake to restrain insulin secretion by inhibiting of cAMP production. Therefore, it provides new insights into the understanding the mechanism of insulin secretion in β-cells. Malfunction of ENaC could be a possible etiology of related disorder such as diabetes. The revealed novel role of ENaC in regulating cAMP production may have other implications beyond β-cell physiology.

List of Publications

Directly papers related to this work

1. **Yanting QUE**, Yong WU, Xiyang MA, Fulei WUCHU, Junjiang CHEN, Jinghui GUO, Ye Chun RUAN. ENaC suppresses cAMP production to protect pancreatic islet β cells from insulin hypersecretion. (In submission)
2. Yong WU, **Yanting QUE,** Junjiang CHEN, Lei SUN, Jinghui GUO, Ye Chun RUAN (2023). CFTR Modulates Hypothalamic Neuron Excitability to Maintain Female Cycle. *International Journal of Molecular Sciences*, *24*(16), 12572. *(Impact factor: 6.2, JCR - Q1 in Biochemistry & Molecular Biology)*
3. Fulei WUCHU *, Xiyang MA *, **Yanting QUE**, Junjiang CHEN, Ye Chun RUAN (2022). Biphasic regulation of CFTR expression by ENaC in epithelial cells: The involvement of Ca^{2+}-modulated cAMP production. *Frontiers in Cell and Developmental Biology*, *10*, 781762. *(Impact factor: 6.2, Q1 in Developmental Biology)* (*Co-first)
4. **Yanting QUE**, Xiyang MA, Yong WU, Junjiang CHEN, Jinghui GUO, Ye Chun RUAN (2023). SAT061 Deficiency Of ENaC Excites Pancreatic β Cells To Promote Insulin Secretion. *Journal of the Endocrine Society*, *7*(Supplement_1), bvad114-928.
5. Xiyang MA, Ruiyao XU, **Yanting QUE**, Junjiang CHEN, Ye Chun RUAN (2023). FRI389 Granulosa Cell-specific Knockout Of Scnn1a Disturbs Estrus Cycle And

Impairs Estrogen Production In Mice. *Journal of the Endocrine Society*, *7* (Supplement_1), bvad114-1583.

Conferences:

1. **Yanting QUE**, Ye Chun RUAN. Role of the epithelial Na^+ channel in pancreatic islet β cell insulin secretion. 4th ABCT Research Postgraduate Symposium in the Biology Discipline 2023 (Oral presentation)
2. **Yanting QUE**, Ye Chun RUAN. Inhibition of ENaC Excites Pancreatic β cells to Promote Insulin Secretion: A New Molecular Target for Diabetes Therapy Biomedical Engineering Conference 2023 (Poster presentation)
3. **Yanting QUE**, Xiyang MA, Yong WU, Junjiang CHEN, Jinghui GUO, Ye Chun RUAN. Deficiency of ENaC Excites Pancreatic β cells to Promote Insulin Secretion. Endocrine Society's Annual Meeting ENDO 2023 (Poster presentation)
4. **Yanting QUE**, Ye Chun RUAN. Role of epithelial sodium channel (ENaC) in insulin secretion and glucose metabolism. Three Minute Thesis (3MT) Competition 2023 (Oral presentation)
5. **Yanting QUE**, Ye Chun RUAN. Sodium environment and sodium channel genes in the regulation of insulin secretion. PAIR Conference 2023 (Poster presentation)
6. **Yanting QUE**, Ye Chun RUAN. Deficiency of ENaC excites pancreatic islet β cells to promote insulin secretion. 3rd ABCT Research Postgraduate Symposium in the Biology Discipline (2022) (Poster presentation)

Academic Awards:

1. Best Oral Presentation Award in 4th ABCT Research Postgraduate Symposium in the Biology Discipline. Role of the epithelial Na^+ channel in pancreatic islet β cell insulin secretion. (Aug 2023)
2. Best Poster Presentation Award in 3rd ABCT Research Postgraduate Symposium in the Biology Discipline. Deficiency of ENaC excites pancreatic islet β cells to promote insulin secretion. (Aug 2022)

Acknowledgements

This is a valuable and memorable journey in my life. I am very fortunate to have received love and support from my supervisor, colleagues, peers, and family throughout this process. Without their help, I wouldn't have been able to complete my PhD studies.

I would like to express my deepest gratitude to my supervisor, Dr. Sharon RUAN, for her professional supervision and unwavering mentorship in shaping my research from my initial stages when I felt like a blank canvas. From experimental design to academic writing, Dr. Ruan has provided me with countless opportunities to develop my skills and discover my strengths. Any achievements I have attained today are a direct result of her patient guidance, as she led me on a transformative journey of exploration and a relentless pursuit of truth, igniting a genuine passion for research within me. I am especially grateful for her steadfast commitment to reviewing and revising every word and sentence in the thesis, as it has taught me how to conduct good research and critical thinking. I also sincerely thank Dr. Ruan for her love, understanding and forever support in my life. She has been a beacon of light, guiding me to learn, explore, think, and embrace love. I am truly blessed and grateful to have such a precious relationship with her.

I would like to extend my sincere appreciation to all the members of Dr. Ruan’s research group, with whom we work together as a family. I am indebted to Dr. CHEN Junjiang

who has provided invaluable discussions, shared his knowledge, and offered much support not only in my research but also in my daily life throughout this journey. I would like to extend my heartfelt gratitude to Dr. GUO Jinghui and Mr. WU Yong for their invaluable teaching, tremendous assistance and contributions, particularly in the establishment of patch-clamp and islet isolation technologies that greatly supported this project.

I would like to sincerely thank my fellow lab members, Dr. HU Peijie and Dr. MA Xiyang, for their patient guidance and generous assistance whenever I needed it. I sincerely thank Dr. MA Xiyang and Ms. WUCHU Fulei for their contributions in initiating the groundwork for this project. I am grateful to XU Ruiyao, DU Yi, DU Wanting, CHU Muyan, and FENG Lin for their active involvement in my project, providing experimental assistance, friendly support, and encouraging words. I would thank Dr. WANG Shan for her dedicated efforts in revising my thesis and providing valuable suggestions on academic writing. I also thank other members ZHANG Xiaotian, CAI Xiaojun, and TANG Zhengqi for their help and advice. Their collaboration and camaraderie have made my research experience more enriching and enjoyable.

I would like to extend my sincere appreciation to my thesis committee members, Prof. SUN Lei, Prof. HUANG Ping Bo, Prof. Ko Wing Hung, for their precious time and valuable suggestions about the thesis.

I would like thank to Dr. TAN Yonghua, Dr. ZHAO Xin, Dr. Thomas Lee for offering me valuable suggestions and comments on my research proposal and confirmation registration.

I would also like to acknowledge the staff of the University of Life Science (ULS) and Centralized Animal Facilities (CAF) for their technical support, access to resources, and conducive research environment. Their assistance has facilitated the smooth progress of my research and contributed to the success of this thesis.

I would like to thank my parents for bringing me into this world and for their unconditional support and love.

I would like to extend a special thanks to my husband Dr. Shu Jing, for being a precious presence in my life, providing me with love, tolerance, understanding, and endless encouragement.

I humbly dedicate this thesis to all those who have inspired and supported me throughout my academic journey.

Table of Contents

List of figures

List of tables

List of abbreviations

Ach	Acetylcholine
ACs	Adenylyl Cyclases
AKT	Protein kinase B
Ami	Amiloride
ASICs	Acid-sensing Ion Channels
ASL	Airway Surface Liquid
ATP	Adenosine Triphosphate
Ben	Benzamil
cAMP	Cyclic Adenosine Monophosphate
cDNA	Complementary DNA
CAF	Centralized Animal Facilities
CF	Cystic Fibrosis
CFTR	Cystic Fibrosis Transmembrane Conductance Regulator
CRISPER	Clustered Regularly Interspaced Short Palindromic Repeats
DAB	3,3’-Diaminobenzidine
DDA	2',5'-dideoxyadenosine
DDA	Data-dependent acquisition
DEG	ENaC/Degenerin channels
DMSO	Dimethyl Sulfoxide
ENaC	The Epithelial Sodium Channel
EDTA	Ethylenediaminetetraacetic acid
ER	Endoplasmic reticulum
FBS	Fetal Bovine Serum
FADH2	Flavin adenine dinucleotide
FSK	Forskolin
GABA	Gamma-aminobutyric Acid
GCG	Pre-proglucagon gene

GCGR	Glucagon receptor
GIP	Gastric Inhibitory Polypeptide or Glucose-dependent Insulinotropic Polypeptide
GLIB	Glibenclamide
GLP-1	Glucagon-Like Peptide 1
GLP-1R	GLP-1 receptor
GPCR	G protein-coupled Receptor
GSIS	Glucose-Stimulated Insulin Secretion
GSK3	Glycogen synthase kinase 3
GO	Gene Ontology
HCD	Higher energy Collisional Dissociation
HCN channels	Hyperpolarization-activated Cyclic Nucleotide–gated channels
H&E stain	Hematoxylin and Eosin Stain
HVA	High Voltage-Activated
HRP	Horseradish Peroxidase
i.p.	Intraperitoneal Injection
IBMX	3-isobutyl-1-methylxanthine
IDF	International Diabetes Federation
IF	Immunofluorescence
IGF	Insulin-like Growth Factor
IHC	Immunohistochemical
IP3	1,4,5-triphosphate
IPGTT	Intraperitoneal glucose tolerance test
IRR	Insulin Receptor-related Receptor
IRS	Insulin receptor substrates
ISK	Ishikawa, human endometrial epithelial cell line
K_{ATP}	ATP-sensitive potassium channels
KEGG	Kyoto Encyclopedia of Genes and Genomes
LFQ	Label-free quantitation

LVA	Low Voltage-Activated
MafA	v-maf musculoaponeurotic fibrosarcoma oncogene homolog A
MS	Mass spectrometry
mRNA	Messenger RNA
mTOR	Mammalian Target of Rapamycin
MTT	3-(4,5-Dimethyl-2-thiazolyl)-2,5-diphenyl-2H-tetrazolium Bromide
NADH	Nicotinamide Adenine Dinucleotide
NCX	Sodium-calcium exchanger
NeuroD1	Neurogenic Differentiation 1
NMDG	N-methyl-D-glucamine
OCT	Optimal Cutting Temperature
OGTT	Oral glucose tolerance test
PBS	Phosphate-Buffered Saline
PDX1	Pancreatic and Duodenal homeobox 1
PEPCK	Phosphoenolpyruvate carboxykinase
PFA	Paraformaldehyde
PI3K	Phosphatidylinositol 3-kinase
PKA	Protein Kinase A
PKC	Protein Kinase C
PLC	Phospholipase C
PP	Pancreatic Polypeptide
PS	Penicillin-Streptomycin
qPCR	Quantitative Polymerase Chain Reaction
ROI	Region of Interest
SDS	Sodium Dodecyl Sulfate
siRNA	Small Interfering RNA
SGK1	Serum and Glucocorticoid-regulated Kinase 1
SGLT	Sodium-Glucose Co-Transporter
SNAP25	Synaptosomal-Associated Protein 25

SNARE	Soluble N-ethylmaleimide-sensitive-factor Attachment protein receptor
SOCs	Stored-operated Ca^{2+} channels
SSTR2	Somatostatin Receptor subtype 2
SUR	Sulphonylurea Receptor
TBS	Tris-Buffered Saline
TBST	Tris-buffered Saline with Tween-20
TCA	Tricarboxylic Acid
TRAP	Tartrate-Resistant Acid Phosphatase
TRP	Transient Receptor Potential
VAMP2	Vesicle-Associated Membrane Protein 2
VGCC	Voltage-Gated Calcium Channel
VGSC	Voltage-Gated Sodium Channel
VRAC/SWELL1	Volume-regulated anion channel
WB	Western Blot

Chapter 1: Introduction

1.1 Glucose metabolism

Glucose plays a central role in energy metabolism in the body. Derived from the breakdown of dietary carbohydrates, lipids and proteins [1], glucose is taken up by gastrointestinal epithelium into the bloodstream, circulating into whole-body organs [2]. To be utilized in cells, glucose is first transported via membrane glucose transporters into the cytosol, where it is converted into pyruvate through a biochemical process called glycolysis [1]. Pyruvates are then used by the citric acid cycle followed with oxidative phosphorylation in the mitochondria to generate high-energy molecules such as adenosine triphosphate (ATP) and reduced nicotinamide adenine dinucleotide (NADH), flavin adenine dinucleotide (FADH2), providing energy for a variety of essential biochemical reactions in cells [3, 4]. When excessive, glucose leaves the cell via transporters and is delivered to the liver where it is converted, through a process of glycogenesis, into a polymer form, glycogen, which is then stored in the liver and skeletal muscles [5]. Glycogens are used and broken down back to glucose when the energy demand escalates, the so-called glycogenolysis [6]. Glucose can also be generated from non-carbohydrate precursors through gluconeogenesis predominantly occurring in the liver or metabolized through other pathways such as pentose phosphate pathway and fructose metabolism [7].

These critical biochemical reactions for glucose metabolism are tightly regulated to realize glucose and energy homeostasis in the body. Multiple factors from the endocrine, nervous systems and locally adjacent cells/tissues/organs are documented to contribute to such control. Dysregulation of glucose metabolism is detrimental to human health resulting in critical diseases such as diabetes.

1.1.1 Physiological regulation of glucose metabolism

In response to dynamic environmental changes, glucose is actively produced, circulated, metabolized or stored in the body to provide energy equilibrium and whole-body homeostasis. Glucose level is therefore constantly fluctuating, although the blood level of glucose is kept within a narrow range (4-7 mM) in a human body [8]. Either a low (hypoglycemia) or a high (hyperglycemia) blood glucose level, in a long term, is harmful and sometimes fatal [9]. The precise control of glucose metabolism relies on highly orchestrated multifactorial mechanisms.

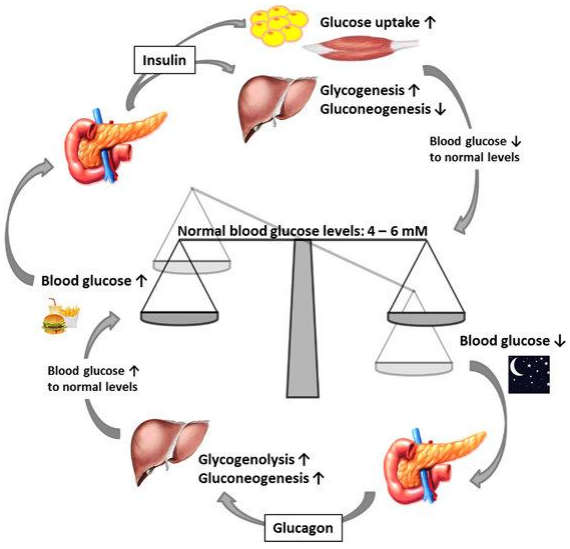

Figure 1.1 Maintenance of blood glucose levels by glucagon and insulin [10]. In

situations of low blood glucose levels, the pancreas releases glucagon, thereby increasing endogenous blood glucose levels through the process of glycogenolysis. Conversely, following a meal where exogenous blood glucose levels are elevated, the release of insulin facilitates glucose uptake into insulin-dependent muscle and adipose tissues, while also promoting glycogenesis.

Among all the regulatory factors recognized insulin is the most important peptide hormone to maintain glucose homeostasis. It is encoded by INS gene located on chromosome 11 in humans and exclusively produced in pancreatic islet β-cells [11]. The production and secretion of insulin are activated by blood glucose elevation, which is essentially involved in the regulation of glucose metabolism and will be discussed in the following sections. To exert its function, insulin binds to its receptors in plasma membranes, the insulin-like growth factor (IGF)-I receptor and the insulin receptor-related receptor (IRR) [12], which are broadly expressed in the body including skeletal muscles, adipose tissues, and the liver [13]. Once the insulin receptor is activated, it catalyzes the phosphorylation of insulin receptor substrates (IRS) which in turn activates phosphatidylinositol 3-kinase (PI3K)/protein kinase B (AKT) signaling [14]. The PI3K-Akt has multiple actions. It promotes the recruitment of glucose transporters (e.g., GLUT4) into the plasma membrane, facilitating glucose uptake into the cells [15]. Akt, by inhibiting glycogen synthase kinase 3 (GSK3), enhances the enzymatic activity of glycogen synthase and thus facilitates the production of glycogen in hepatocytes [16]. By activating mammalian target of rapamycin (mTOR), PI3K-Akt also promotes

protein synthesis, cell growth and differentiation, mobilizing energy consumption [17]. Through these pathways, insulin promotes glucose uptake, enhances glycogenesis, as well as suppresses gluconeogenesis and glycogenolysis [13], counteracting the evaluation of blood glucose. Insulin therefore serves as an anabolic hormone and plays a central role in regulating blood glucose homeostasis.

Glucagon, another peptide hormone, encoded by pre-proglucagon gene (GCG) and synthesized by the pancreatic α-cells. Glucagon is released in response to low blood glucose and serves to sustain blood glucose levels in the face of hypoglycemia or during fasting [18]. Glucagon signaling, mediated by the glucagon receptor (GCGR), presented in various tissues including the liver, brain, pancreas, kidney, intestine, and adipose tissues, plays a pivotal role in regulating glucose mobilization [19]. The binding of glucagon and GCGR activates the G protein-coupled receptor (GPCR) pathway in these cells [20]. Activation of GPCR couples to Gsα triggers increasing intracellular cyclic adenosine monophosphate (cAMP) levels through the activation of adenylate cyclase and subsequent activation of protein kinase A (PKA). PKA phosphorylates and activates glycogen phosphorylase kinase, thereby facilitating glycogenolysis and glucose production [21]. PKA activation also increased the expression and activity of phosphoenolpyruvate carboxykinase (PEPCK) stimulating gluconeogenesis while inhibiting glycolysis [22]. Additionally, PKA phosphorylates and deactivates glycogen synthase, leading to a decrease glycogen synthesis [23]. Apart from PKA pathway, the activation of GCGR also couples to Gq leading to activation of phospholipase C (PLC),

1,4,5-triphosphate (IP3) and Ca^{2+} release, which together promotes gluconeogenesis and glycogenolysis while inhibits glycogenesis and glycolysis [24]. Therefore, glucagon plays the opposite role of insulin in lowering blood glucose levels. Insulin and glucagon function within a homeostatic hormonal system as glucose 'counter-regulation', mutually influence each other in glucose metabolism [25]. High insulin levels inhibit glucagon secretion [26], while glucagon stimulates the secretion of incretin hormones that enhance insulin release in response to elevated blood glucose levels [27]. This cooperative interplay between the two hormones ensures the maintenance of a physiological balance in glucose metabolism.

Other factors including nervous system, and growth factors indirectly influence blood glucose by regulating the secretion and activity of insulin and glucagon. For example, In response to stress or exercise, adrenaline released from the adrenal gland stimulates glucagon secretion and acts on liver and muscle cells to promote glycogen breakdown, thereby working synergistically to elevate blood glucose levels [28]. The central nervous system exerts regulatory control over glucose metabolism by integrating signals from peripheral tissues, coordinating hormonal responses, and modulating neural circuits within the hypothalamus and brainstem to maintain glucose homeostasis [29]. Apart from that, growth hormone promotes the mobilization of fatty acids and enhances gluconeogenesis, increasing glucose availability. Catabolic hormones including cortisol and catecholamines promote gluconeogenesis and glycogenolysis, and reduce glucose uptake by peripheral tissues [30].

Overall, glucose metabolism is regulated by a complex interplay of various factors, contributing to the maintenance of blood glucose homeostasis. However, many aspects of the mechanisms by which hormones regulate glucose remain to be fully elucidated. Dysregulation of glucose metabolism can give rise to conditions such as hypoglycemia (low blood glucose) or hyperglycemia (high blood glucose), which are hallmark features of diabetes mellitus [31].

1.1.2 Glucose metabolic disorders

Hypoglycemia and Hyperglycemia

Hypoglycemia is typically defined by blood glucose levels below 70 mg/dL (3.9 mmol/L) [32]. It can be caused by factors such as excessive physical activity, inadequate food intake, certain medical conditions, or excessive alcohol consumption. [33]. In contrast, in hyperglycemia, the blood glucose is usually above 180 mg/dL (10 mmol/L) [34]. Contributing factors to hyperglycemia include insufficient insulin production or action, excessive carbohydrate intake, physical inactivity, stress, illness, or certain medications [9].

Long-term hypoglycemia and hyperglycemia have significant consequences and contribute to the development of serious diseases. Severe hypoglycemia causes neurological damage, cognitive impairment, and hypoglycemia unawareness [35]. For example, the brain relies heavily on a constant supply of glucose from the circulation

since it cannot synthesize glucose or store significant amounts of glycogen in astrocytes. Severe hypoglycemia commonly leads to a deprivation of brain fuel, which can result in impaired brain function and failure [36]. Prolonged hyperglycemia leads to cellular damage and dysfunction, particularly in glucose-sensitive organs and tissues such as the kidneys, eyes, and nerves. In chronic conditions like diabetes, persistent hyperglycemia can contribute to the development of long-term complications [37].

Hyperinsulinemia

Hyperinsulinemia, denoting elevated circulating insulin concentrations, exerts a substantial influence on glucose metabolism [38]. Within the context of hyperinsulinemia, surplus insulin engenders heightened cellular glucose uptake, thereby augmenting glucose utilization and inducing a decline in blood glucose levels. This effect is particularly pronounced during the postprandial phase when insulin levels surge in response to nutrient intake. Prolonged hyperinsulinemia result in elevated blood glucose levels and impaired glucose tolerance, ultimately culminating in the progression to diabetes [39].

Diabetes

Diabetes mellitus or diabetes, is a chronic, metabolic disorder characterized by prolonged elevation of blood glucose levels, commonly referred to as hyperglycemia [40]. This condition gradually gives rise to significant complications affecting various vital organs. Diabetes affects a substantial global population, with an estimated 422

million individuals affected worldwide according to International Diabetes Federation (IDF). Diabetes-related mortality results in about 1.5 million deaths annually, and there has been a persistent upward trend in its cases and prevalence [41]. The etiological classification of diabetes has gained widespread acceptance, categorizing it into two main types: type 1 and type 2 diabetes. Type 2 diabetes is the most prevalent form, accounting for over 85% of total diabetes cases [42]. Type 1 diabetes occurs at any age. It is usually considered that the major cases in type 1 diabetes are T-cell-mediated autoimmune diseases, in which β-cells are destroyed by the immune system, leading to insulin secretion and subsequent hyperglycemia [43]. However, there is a significant proportion of diabetic patients with insulin insufficiency exhibit negative results for these autoantibodies [44, 45], remaining unsolved mechanisms underlying insulin secretion in type 1 diabetes. Type 2 diabetes is characterized by high blood sugar, insulin resistance, and relative lack of insulin [46]. Lifestyle factors, dietary composition and genetics are the major causes of type 2 diabetes [47]. As a chronic metabolic disorder, type 2 diabetes exerts substantial and long-term effects on multiple organs within the body, including cardiovascular diseases, diabetic nephropathy, diabetic retinopathy, and peripheral neuropathy [48]. Type 2 diabetes arises from insufficient insulin production from β-cells in the setting of insulin resistance [49]. Insulin resistance leads to inappropriate glucose release by the liver, muscles, and fat tissue dysregulations [50]. Apart from insulin resistance, β-cell dysfunction and other factors such as fatty acid activation of β-cells, intracellular lipid metabolism, ATP production, and hypothalamic signaling contribute to the pathogenesis of type 2

diabetes [51].

Both type 1 and 2 diabetes are marked by dysregulation of insulin, a pivotal hormone in glucose metabolism. While it is generally considered that insulin deficiency leads to type 1 diabetes and insulin resistance leads to type 2 diabetes, the actual conditions become more complicated in individuals regarding blood insulin and glucose levels. Therefore, comprehending the regulation of insulin secretion in glucose metabolism assumes critical significance in the investigation of diabetes physiology and pathology. Insulin production and secretion are elusively regulated by β-cells located in the islets of Langerhans within the pancreas. The pancreas undertakes an essential role in whole-body metabolism owing to its secretion of various hormones. The following section will discuss the function of the pancreas and the mechanism underlying insulin secretion.

1.2 Insulin secretion

1.2.1 The pancreas

The pancreas, located in the abdomen and stretched from behind the stomach near the spleen in humans, serves both the digestive and endocrine systems in vertebrates [52] (Figure 1.2). As a heterocrine gland, the pancreas comprises four structurally distinct components: the exocrine pancreas, the endocrine pancreas, the blood vessels, and the extracellular space [53]. The exocrine pancreas, comprising the major volume (~95%)

of the organ, consists of pancreatic acinar cells and duct cells responsible for digestive enzymes (trypsin and amylase) production and sodium bicarbonate secretion respectively [54]. The endocrine pancreas comprises spherical structures called islets of Langerhans, which exhibit a wide range of sizes from 50 to 500 μm [55]. Although they account for only 1-2% of the total pancreatic mass [54], these islets play a crucial role in maintaining glucose homeostasis by secreting various pancreatic peptide hormones into the blood vessels. The islets comprise five major cell types: alpha cells (α-cells), beta cells (β-cells), delta cells (δ-cells), PP cells (also known as F-cells), and epsilon cells (ε-cells) [53]. These cells produce glucagon, insulin, somatostatin, pancreatic polypeptide, and ghrelin, respectively, which are secreted directly into the blood flow for further metabolism [56]. While the endocrine and exocrine functions of the pancreas are distinct, they are closely interrelated and serve important physiological roles. Williams & Goldfine [57] proposed an insulin-acinar portal system, suggesting that islet peptides regulate acinar cell function, and peptide hormones produced by islet cells contribute to the growth of acinar cells. The coordination of these hormone functions serves as the foundation for pancreatic functions and related endocrine physiology.

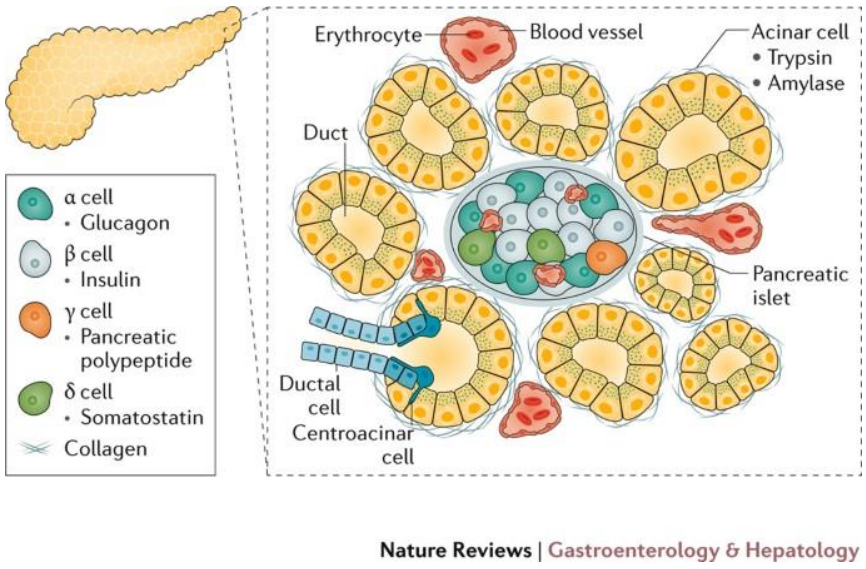

Figure 1.2 The healthy human pancreas contains both an endocrine and an exocrine compartment [52]. The endocrine pancreas consists of four primary cell types, which include β cells responsible for insulin secretion and α cells responsible for glucagon secretion. The exocrine pancreas accounts for over 95% of the pancreatic tissue and is composed of acinar cells that produce digestive enzymes like trypsin and amylase, as well as ductal cells that facilitate the transport of these enzymes to the intestine.

1.2.2 Pancreatic islet cells and glucose metabolism

The five hormone-producing cells from islets have their unique and important roles in the regulation of metabolic homeostasis. There is a difference in the distribution of islet cells in humans and rodents. Human islets are made up of 30-50% α-cells on the outer mantle and 50-60% β-cells on the inner core, while rodent islets are composed of 10-20% α-cells and 65-80% β-cells [58]. δ-cells (10%), γ-cells (1%) and ε-cells (1%) are found scattered throughout the islet (Figure 1.3). These islet cells communicate with

each other by hormone secretion, cell-cell adhesion and neural signaling.

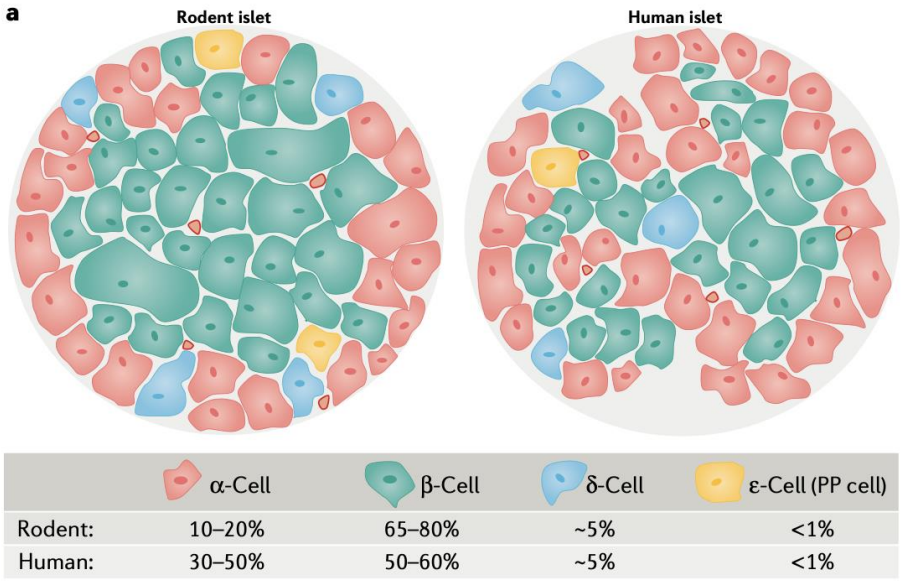

Figure 1.3 Comparison of the cellular composition of rodent and human islets [58]. Islet cellular composition is characterized by approximately 10-20% α-cells in rodents and 30-50% in humans, primarily located in the outer mantle, and 65-80% β-cells in rodents and 50-60% in humans forming the inner core.

As the most important pancreatic islet cells, β-cells are exclusively dedicated to synthesize, store, and release insulin in mammals in response to changes in plasma levels of major nutrients, particularly glucose, amino acids, and fatty acids [59]. Insulin and the partner hormones amylin and C-peptide produced by β-cells are the only way to reduce blood glucose concentrations in the body [60]. β-cells in the islet structure form a network with other endocrine cells, communicating through gap junctions and cell-to-cell adhesion [61]. Hormones or non-hormonal products of endocrine cells, such

as ATP and zinc, along with neurotransmitters, impact the function of β-cells [62]. Thus β-cells and other islet cells form a network that signals and secretes hormones together, regulating whole-body metabolism. β-cells are highly complex endocrine cells responsible for supplying insulin to maintain precise glucose levels in the body. Insulin secretion adapts to meal characteristics, target tissue sensitivity, and various stimuli such as catecholamines and thyroid hormones [63]. β-cell dysfunction is a direct feature of diabetes. In conditions such as obesity and insulin resistance, β-cells respond to increased insulin demands by increasing their mass, while the body's response declines due to decreased insulin receptor expression in liver, adipose, and muscle cells [64, 65], impairing their ability to effectively respond to circulating insulin. Chronic stimulation leads to β-cell enlargement and hyperinsulinemia [66], maintaining blood glucose levels within the normal range despite reduced insulin signaling efficacy [67]. However, prolonged metabolic demand leads to β-cell apoptosis, exhaustion, reduced function, decreased volume, and inadequate insulin secretion, ultimately resulting in the development of overt type 2 diabetes [68]. β-cells are therefore essential in the endocrine system and diabetes development.

The α-cells, located at the dorsal side of pancreatic islets, secret glucagon to increase blood glucose levels, in response to hypoglycemia, epinephrine, amino acids, other hormones, and neurotransmitters [69]. The glucagon gene (Gcg) encodes for glucagon, but during protein translation, additional hormones such as glucagon-like peptides 1 and 2 (GLP-1, GLP-2) are also produced [70, 71]. Glucagon secretion is regulated by a

combination of neuronal factors, including the sympathetic and parasympathetic nervous systems [72], as well as non-neuronal factors such as insulin [73], zinc [74], somatostatin [75], serotonin [76], 3',5'-cyclic adenosine monophosphate (cAMP) and glucose [73]. Recent studies have shown that α-cells have the potential to trans-differentiate into insulin-producing β-cells, offering a potential avenue for diabetes treatment [77]. α-cells proglucagon-derived peptides (glucagon and GLP-1) signal activates the GLP-1 receptor (GLP-1R) and GCGR on β-cells [78], leading to the enhancement of insulin secretion in response to glucose stimulation, enabling paracrine actions within the islets that likely promote β-cell growth and survival, thereby maintaining β-cell mass [79]. These findings shed light on the potential therapeutic implications of glucagon, GLP-1 and the dynamic interplay between α- and β-cells in type 2 diabetes.

Delta cells (δ-cells or D cells) produce somatostatin, which acts locally within the islets as a paracrine inhibitor of insulin and glucagon secretion [80], mediated by somatostatin receptors coupled to inhibitory G proteins, suppressing electrical activity and exocytosis in α-cells and β-cells [81]. Pancreatic polypeptide cells (PP cells), also known as gamma cells (γ-cells) or F cells, synthesize and release pancreatic polypeptide (PP) to regulate plasma glucose levels by influencing insulin secretion, intestinal functionality, and gut functions [82], with stimulation from high-protein meals, fasting, physical activity, and acute hypoglycemia, and suppression by somatostatin and glucose [83]. Epsilon cells (ε-cells) produce ghrelin, the "hunger hormone" [84], which

regulates appetite and influences neuroendocrine pathways related to growth hormone release [85], insulin sensitivity, and metabolic regulation [86].

Overall, pancreatic islet cells work together through hormone secretion and intercellular interaction to maintain glucose homeostasis. Among them, β-cells receive significant attention due to their central role in regulating blood glucose levels and their potential role for diabetes control. Studying β-cell function and the mechanisms underlying insulin action is crucial for revolutionizing glucose homeostasis and maintaining metabolic homeostasis.

1.2.3 Insulin production and synthesis

Insulin (*INS*) is composed of 51 amino acids in humans. Rodents have two functional insulin genes: Ins2, which is the homolog of most mammalian genes, and Ins1, a retroposed copy that includes the promoter sequence but lacks an intron [87]. Insulin synthesis encompasses the transcription of the INS into preproinsulin mRNA, subsequent translation and processing of preproinsulin into proinsulin within the endoplasmic reticulum, transportation to the Golgi apparatus for packaging into insulin granules, proteolytic cleavage of proinsulin to yield mature insulin, and finally, the exocytosis of insulin granules culminating in its release into the bloodstream for regulation of glucose metabolism [88, 89]. Transcription factors, including but not limited to pancreatic and duodenal homeobox 1 (PDX1), neurogenic differentiation 1

(NeuroD1), and v-maf musculoaponeurotic fibrosarcoma oncogene homolog A (MafA) control transcriptional process of the INS and the development and function of β-cells [90]. PDX1 is involved in pancreatic development and β-cell maturation and survival [91]. NeuroD1 regulates insulin exocytosis and various stages of endocrine differentiation [92]. MafA enhances insulin gene transcription [93, 94], while also regulating genes for insulin vesicle fusion such as syntaxin 1A, synaptosomal-associated protein 25 (SNAP25), and vesicle-associated membrane protein 2 (VAMP2) [95]. These transcription factors along with other regulatory factors, work in a coordinated manner to control the expression of insulin and maintain proper β-cell function.

1.2.4 Glucose-stimulated insulin secretion

Insulin secretion from pancreatic islet β-cells is prominently activated by a post-prandial increase in glucose concentrations, a process known as glucose-stimulated insulin secretion (GSIS) (Figure 1.4). GSIS is initiated by the uptake of glucose into the β-cell through glucose transporters, such as GLUT1 in humans and GLUT2 in rodents. Then the glucose is phosphorylated to glucose 6-phosphate by the enzyme glucokinase. This is followed by oxidation through the tricarboxylic acid (TCA) cycle, leading to the generation of ATP [96]. The increased ATP/ADP ratio triggers the closure of ATP-sensitive K^+ channels (K_{ATP}), resulting in membrane depolarization [97]. This depolarization leads to the initiation of an action potential, the opening of voltage-gated

calcium channels (VGCC), and subsequent influx of Ca^{2+} [98]. The elevated intracellular Ca^{2+} concentration serves as a crucial signal for insulin granule exocytosis and the subsequent secretion of insulin from β-cells [58].

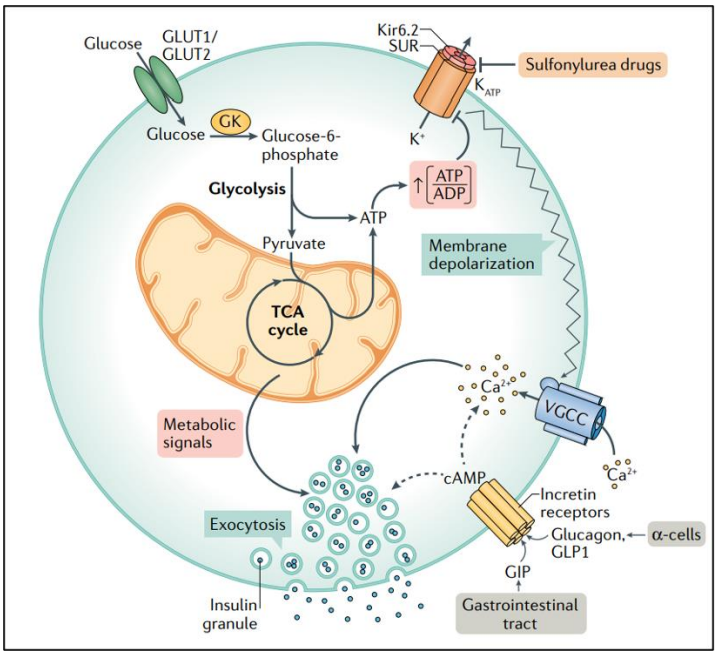

Figure 1.4 Glucose-stimulated insulin secretion is mediated by a triggering pathway and amplification pathways [58]. Glucose uptake into β-cells is facilitated by GLUT1 transporters in humans and GLUT2 transporters in rodents. Glucokinase (GK) controls the entry of glucose into the glycolytic pathway, where it is subsequently metabolized via the tricarboxylic acid (TCA) cycle, leading to the generation of ATP. This increase in the ATP to ADP ratio results in the closure of K_{ATP} channels, leading to membrane depolarization. Subsequently, voltage-gated calcium channels (VGCC) are opened, leading to an influx of calcium ions into the cytoplasm. The rise in intracellular calcium levels then triggers the exocytosis of insulin granules, thereby initiating the secretion of insulin. Multiple metabolic signaling mechanisms (cAMP, GIP, GLP1) contribute to the amplification of insulin secretion.

1.2.5 Biphasic insulin-granule exocytosis

Insulin secretion from β-cells is restricted, with approximately 5% of the stored insulin being immediately released [99]. The majority of insulin granules require additional modifications to become readily releasable, resulting in a limited proportion of insulin being released even under maximal stimulation [100]. GSIS is recognized to exhibit a biphasic response, an early transient phase, and a secondary sustained phase [101]. The initial phase, referred to as first-phase insulin secretion, involves the fusion of a small pool of readily releasable granules, attributed to the release of pre-synthesized insulin stores [102], followed by a return to the baseline level over 10-15 minutes in humans. [103]. Subsequently, the second-phase insulin secretion is specifically triggered by nutrients [104], primarily driven by the release of newly synthesized insulin (insulin biosynthesis) [105]. This phase involves the mobilization of intracellular granules to t-SNARE (trans-SNARE, soluble N-ethylmaleimide-sensitive-factor attachment protein receptor) sites at the plasma membrane, facilitating the distal docking and fusion steps of insulin exocytosis, lasting for several hours [58]. Quantitatively, second-phase insulin secretion is critical, with a rate of 5-40 granules per cell per minute over an extended period, compared to the first phase involving approximately 1% of granules [106]. The mechanism underlying biphasic insulin release is intricate and involves the interplay of various factors, including the cytoskeleton, small GTPases, and SNARE proteins within pancreatic islets [101]. In type 2 diabetes, both the first and second phases of insulin secretion are impaired, indicating β-cell dysfunction [107].

1.2.6 Ion channels in insulin secretion

Pancreatic β-cells exhibit a diverse array of ion channels, which are distributed across the cell membrane as well as subcellular organelles. Ion channels, including those involved in the flow of Ca^{2+}, K^+, Na^+, and Cl^-, play a pivotal role in the regulation of insulin secretion by controlling the electrical activity necessary for depolarization and exocytosis of insulin-containing vesicles in pancreatic β-cells, thereby contributing to the coordinated and metabolically sensitive regulation of insulin secretion in response to glucose levels [108].

1.2.6.1 K_{ATP} channels

The K_{ATP} channel in β-cells, consisting of four Kir6.2 subunits and four sulphonylurea receptor (SUR) subunits is responsible for K^+ efflux, establishing the resting membrane potential and low excitability. K_{ATP} channels are the primary ion channels responsible for β-cell excitability. ATP binds to Kir6.2 subunits of K_{ATP} channels, leading to the inhibition of ATP-sensitive K^+ conductance, and induces depolarization of the plasma membrane [109]. Heterozygous mutations in KCNJ11, encoding the Kir6.2 subunit of the K_{ATP} channel, have been identified as the underlying cause of both permanent neonatal diabetes and transient neonatal diabetes in humans [110]. Given the significance of K_{ATP} in GSIS, K_{ATP} channels are considered a crucial therapeutic target for managing type 2 diabetes and insulin resistance [111], with sulfonylureas like tolbutamide and glibenclamide reducing K_{ATP} channels activity by binding to SUR

subunits [112]. Although the K_{ATP} -dependent pathway is crucial for the activation of GSIS, under the condition that the K_{ATP} channel is neutralized by pharmacology tools such as diazoxide, insulin secretion is also in response to glucose [58]. It indicates that there still are K_{ATP}-independent GSIS pathways in β-cells.

1.2.6.2 Ca^{2+} channels

Ca^{2+} channels are the most utilized ion channels in the regulation of pancreatic β-cell function. VGCCs facilitate Ca^{2+} entry and trigger insulin exocytosis, and Ca^{2+} pumps, exchangers and endoplasmic reticulum (ER) Ca^{2+} are responsible for Ca^{2+} efflux and restoration [113]. The biphasic pattern of GSIS is partially attributed to time-dependent changes in electrical activity and cytosolic Ca^{2+} levels [114]. This concept is supported by experimental evidence demonstrating that the use of a 1 mM Ca^{2+}-buffer BAPTA preserves the first-phase insulin secretion but eliminates the second-phase insulin secretion [115]. β-cells are equipped with high voltage-activated (HVA) channels: L-type, R-type, P/Q-type, N-type, and low voltage-activated (LVA) channels T-type VGCCs in the plasma membrane which are contributed to GSIS [116, 117]. Mouse β-cells express Cav1.2 and Cav1.3 L-type calcium channels [118], with Cav1.2 playing a primary role in maintaining glucose-induced action potential firing, Ca^{2+} oscillations, and insulin secretion [119, 120], while Cav1.3 knockout leads to upregulated Cav1.2 expression and decreased basal insulin secretion [118]. Cav2.3 R-type VGCCs in mouse β-cells contribute to second-phase insulin secretion [121] and their knockout leads to impaired glucose tolerance, reduced insulin secretion, and hyperglycemia[118].

P/Q-type VGCCs are activated when other channels are blocked in β-cells [119]; T-type VGCCs are present in rat and human β-cells but not in mouse β-cells [122] and play a crucial role in glucagon regulation in α-cells of mice and guinea pigs [123].

In β-cells, the upregulation of cytosolic Ca^{2+} levels facilitates the transportation of Ca^{2+}-SERCA complexes into the ER, while Ca^{2+} release from the ER occurs via IP_3R or RyR channels [124]. Upon depletion of the ER Ca^{2+} stores, stored-operated Ca^{2+} channels (SOCs) [125] present on the plasma membrane are activated, enabling the influx of additional Ca^{2+} into the cells, thereby replenishing the ER Ca^{2+} pool. Transient receptor potential (TRP) channels (TRPC (canonical), TRPV (vanilloid), and TRPM (melastatin)) also play a role in store-dependent Ca^{2+} influx for insulin secretion [96], with TRPC channels influencing store-dependent Ca^{2+} influx [126, 127], TRPV channels activated by glucose, temperature, or certain endogenous ligands to regulate insulin release [128], and TRPM channels involved in membrane potential and Ca^{2+} signaling regulation in β-cells [129].

1.2.6.3 Na^+ channels

Sodium (Na^+) channels serve as pivotal mediators of the characteristic, rapid activating, and inactivating inward current, contributing to the swift upstroke of the sodium spike. These channels play a vital role in initiating the depolarization phase of action potentials in excitable cells [130]. β-cells as the excitable cells are equipped with TTX-sensitive Na^+ channels, with Voltage-gated sodium channels (VGSCs) being the primary subtype,

consisting of α-subunits (Nav1.1-Nav1.9/SCN1A-SCN5A, SCN8A, SCN11A) and β-subunits (beta1–4/SCN1B-SCN4B), are involved in glucose-induced electrical activity and insulin secretion in β-cells [131]. Mouse β-cells express Nav1.7 and Nav1.3, while Nav1.6 is minimally expressed. In human β-cells, Nav1.6, Nav1.7, Nav1.3, and Nav1.2 are present. Na^+ channels in pancreatic β-cells work in cooperation with Ca^{2+} channels, mitochondrial Ca^{2+} uniporter (MCU), mitochondrial sodium-calcium exchanger (NCLX) [132], and sodium-calcium exchanger (NCX) [133] together to contribute to insulin secretion. The activation of Na^+ current in mouse β-cells requires the de-inactivation of Na^+ channels, which can only be achieved by applying highly negative holding potentials [134]. Many studies highlighted the positive role of TTX-sensitive Na^+ channels in β-cells, as TTX effectively blocks sodium current at negative prepotentials in mouse islets, but TTX is without effect on GSIS under physiological conditions [135].

The understanding of Na^+ channels in pancreatic islet cells is currently limited, remained many unidentified Na^+ channels. Experimental data validating specific electrical activities resulting from Na^+ and other channel interactions are lacking. Further research is necessary to comprehensively understand these mechanisms.

1.2.6.4 Cl^- channels

The widely accepted consensus model of insulin secretion, which focuses on K_{ATP} channels, overlooks the role of anionic mechanisms that have been known for decades

in modulating β-cell electrical activity and insulin release. Some chloride channels were found to be expressed in β-cells, including the volume-regulated anion channel (VRAC/SWELL1), the cystic fibrosis transmembrane conductance regulator (CFTR). VRAC activity is proposed to induce insulin secretion in β-cells by facilitating a depolarizing efflux of Cl^- in response to glucose-induced cell swelling [136].

Our previous studies have demonstrated the functional expression of another Cl^- channel, called CFTR in β-cells (Figure 1.5) [45]. CFTR is a cAMP/PKA-dependent Cl^- channel that is gated by intracellular ATP. Suppression of CFTR expression in β-cells, or in CFTR mutant (DF508) mice, results in the elimination of GSIS associated electrical activities, Ca^{2+} oscillation thus insulin secretion [45]. CFTR is also implicated in regulating exocytosis [137], insulin processing [138], and granular acidification [139] in β-cells. Meanwhile, in pancreatic α-cell, activated CFTR potentiates K_{ATP} channel activity, resulting in Vm hyperpolarization, inhibition of Ca^{2+} influx, and suppressing glucagon secretion [140]. This interesting paradoxical function of CFTR provides a new intrinsic mechanism to pancreatic α- and β-cells.

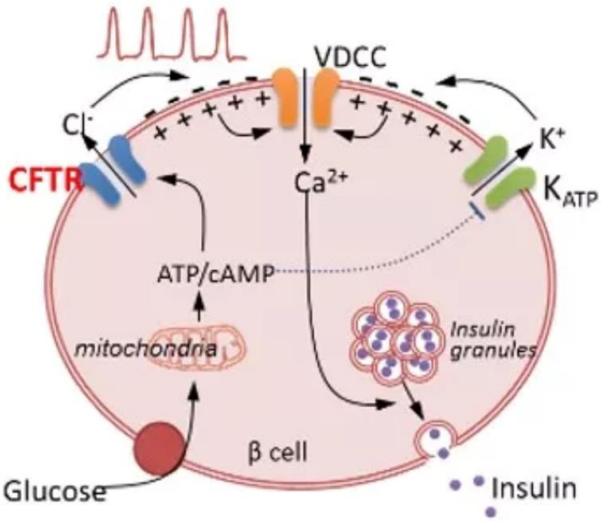

Figure 1.5 CFTR contributes to β-cell insulin secretion. The basal open state of CFTR facilitates Cl^- efflux, thereby contributing to the maintenance of the resting membrane potential at a slightly less hyperpolarized level compared to what would be determined solely by K_{ATP} channels [45].

1.2.7 Other factors in control of insulin secretion

GSIS in β-cells is augmented by the influence of amino acids, fatty acids, and hormones synthesized in α-cells and the gastrointestinal tract. The incretin effect, as the amplification of insulin secretion also plays a role in promoting insulin secretion. The discovery of GIP as the first intestinally derived peptide to stimulate insulin secretion established its role as an incretin peptide [141]. Later, the identification of GLP-1 as another incretin hormone positioned GIP and GLP-1 as sister peptides in the regulation of glucose homeostasis for the past 30 years [142].

The regulation of insulin secretion is also influenced by the surrounding islet cells and

the hormonal secretions they produce (Figure 1.6). Nutrient ingestion results in elevated circulating levels of glucose, amino acids, and incretin hormones (GIP and GLP1), thus stimulating GIPR and GLP1R activation and enhancing insulin secretion through a cAMP-dependent mechanism [58, 143].

cAMP pathway in β-cells

Upon binding to their respective GPCRs, these incretin hormones interact to activate of adenylyl cyclase with the Gs subunit, while G_i signaling inhibits cAMP generation [144]. This enzymatic activation results in the production of cAMP from ATP. Within β-cells, cAMP functions as a critical intracellular signaling molecule that enhances insulin secretion in response to the initial triggering signal. It is synthesized by adenylyl cyclases (ACs) and degraded by phosphodiesterases (PDEs) [145]. Adenylate cyclases (ADCYs) can be classified into five groups based on structure and regulation. Group I (ADCY1, 3, 8) is stimulated by G_s and Ca^{2+}, inhibited by G_i. Group II (ADCY2, 4, 7) is stimulated by G_s, not responsive to Ca^{2+} and G_i. Group III (ADCY5, 6) is stimulated by G_s, inhibited by Ca^{2+} and G_i. Group IV (ADCY9) is only stimulated by G_s, not responsive to forskolin. Group V (ADCY10) is a structurally distinct protein regulated by Ca^{2+} and bicarbonate, not GPCRs [146]. In addition to the effects mediated by GPCR agonists, glucose stimulation has been found to promote oscillatory elevations in cAMP levels. This glucose-induced elevation in cAMP involves a Ca^{2+}-dependent mechanism that activates specific ACs (AC1, AC3, AC8), primarily at lower glucose concentrations [147]. cAMP acts as a facilitator by promoting both the influx of Ca^{2+} through VGCC

and the mobilization of Ca^{2+} from intracellular stores. Afterwards, cAMP-activated PKA/ Epac2A signaling contributes meaningfully to trafficking of insulin granules and facilitates their fusion with the plasma membrane [148]. It is worth noting that the cAMP-activated signaling is essential for both first and second-phase insulin secretion. Studies have shown that the knockout of Epac2 in mouse islets diminishes the first phase of cAMP-potentiated insulin granule exocytosis [149, 150]. Additionally, suppression of glucose-induced cAMP formation with AC inhibitors impairs the second phase of insulin secretion [151]. These findings highlight the significance of cAMP signaling in regulating the initiation and maintenance of insulin granule exocytosis.

Recent studies have shown that a PKA isoform containing the regulatory subunit Riα (PKA-Riα) can act independently of the canonical cAMP signaling pathway [152]. The role of PKA in glucose homeostasis was investigated *in vivo* using a genetic mouse model. Disinhibition of PKA activity in Prkar1a KO mice improves glucose tolerance and enhances insulin secretion [153]. Prkar1a/Epac2A double KO mice studies demonstrated a reduction in GSIS, indicating that Epac2A expression is both permissive and necessary for the maximum effect of GLP-1R stimulation on insulin secretion [154]. Chronic hyperglycemia disrupts cAMP signaling in pancreatic islets through HIF1 activation, inducing PKIB, an inhibitor of PKA catalytic activity, and impairing islet function. Disruption of the PKIB gene improves islet function in obesity, highlighting the interplay between nutrient and hormonal pathways in pancreatic islet dysfunction [155]. Therefore, in addition to classical GSIS, other factors especially cAMP pathway

are highly involved in insulin secretion and regulate β-cell function.

In summary, the molecular mechanisms underlying GSIS, multiple ion channels and incretin hormonesn, cAMP signaling in pancreatic β-cells are essential and interconnected for insulin secretion. Many aspects of these mechanisms remain poorly understood and necessitate further investigation to unravel their complexities and resolve unanswered questions.

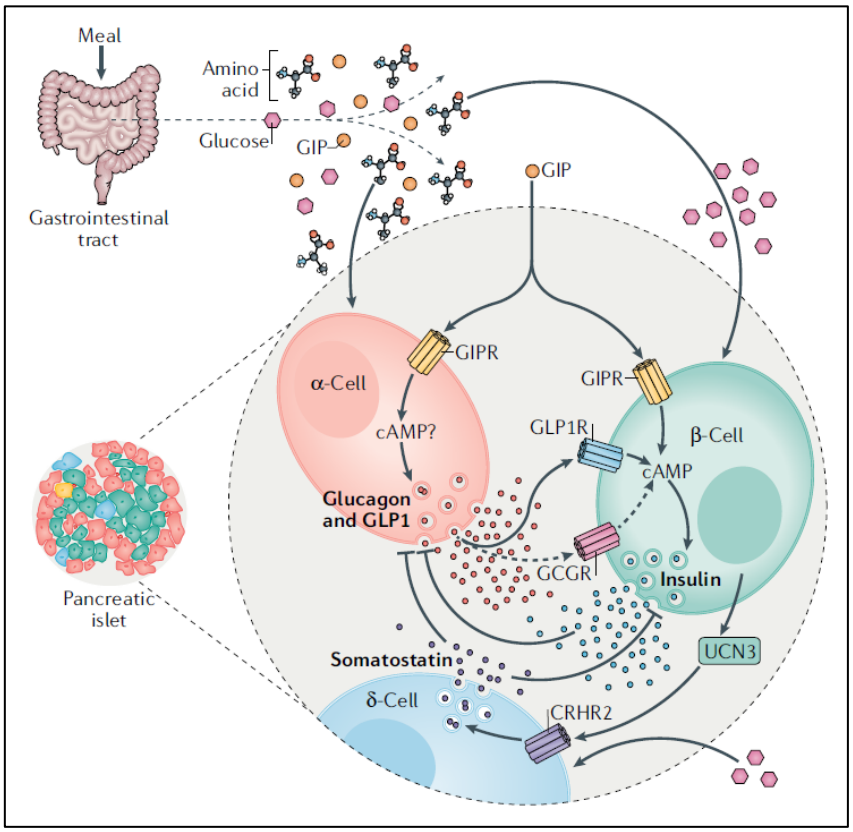

Figure 1.6 Other hormones in control of insulin secretion. Nutrient ingestion increases glucose, amino acids, and incretin hormones. GIP and GLP1 enhance insulin secretion in β-cells through cAMP-dependent mechanisms. GIP also stimulates glucagon secretion in α-cells. GLP1 and glucagon regulate insulin secretion by increasing cAMP levels in β-cells. UCN3 from β-cells inhibits β-cell secretory activity

by stimulating somatostatin secretion from δ-cells [58].

1.3 The epithelial sodium channel

The epithelial sodium channel (ENaC), a non-neuron Na^+ channel, also referred to as the amiloride-sensitive sodium channel, is a voltage-independent mechanosensitive ion channel with a specific permeability for Na^+ [156]. ENaC is predominantly localized to the apical membrane of polarized epithelial cells in specific tissues, including the kidney (particularly in the collecting tubule), lung, skin, male and female reproductive tracts, and colon [157]. ENaC is crucial for maintaining electrolyte balance and fluid homeostasis in these respective physiological systems.

1.3.1 ENaC structure and function

ENaC forms a heterotrimeric structure comprising three homologous subunits, namely α, β, and γ, which are encoded by the genes SCNN1A, SCNN1B, SCNN1G, respectively [158] (Figure 1.7). In humans, SCNN1A is located on chromosome 12p [159], while SCNN1B and SCNN1G are adjacent on chromosome 16p [160]. In mice, Scnn1a is found on chromosome 6, and Scnn1b and Scnn1g share synteny with human chromosome 16 on chromosome 7 [161]. *In vitro* experiments have demonstrated that the three subunits of ENaC can exist in different stoichiometric ratios. ENaC channel activity is critically dependent on the presence of the α subunit, while the β and γ subunits play essential roles in facilitating optimal channel expression and activity at

the cell surface [158]. The subunit α can independently form a functional channel, whereas the subunits β and γ rely on the presence of ENaCα for the attainment of complete channel functionality [162]. The ENaC subunits belong to the ENaC/Degenerin channels (DEG) superfamily, which also includes acid-sensing ion channels (ASICs) [163]. The DEG/ENaC/ASICs family of ion channels plays vital roles in sensing mechanical stimuli, maintaining salt homeostasis, and responding to acidification within the nervous system [164].

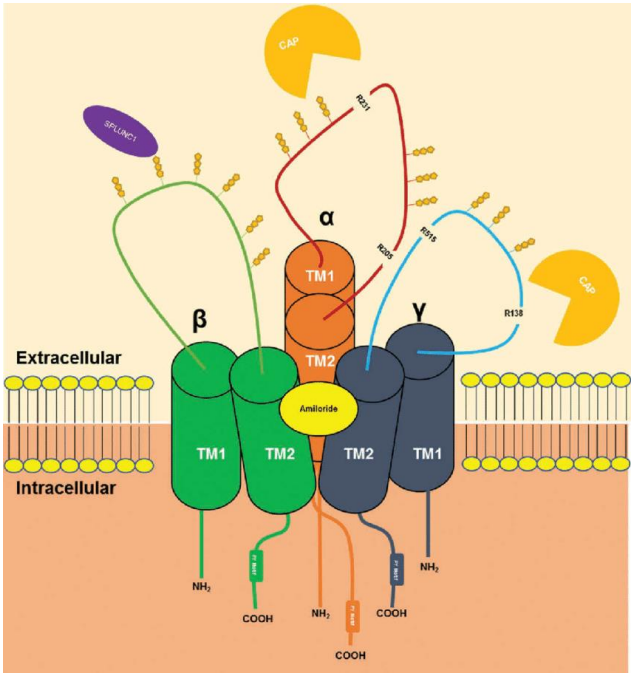

Figure 1.7 Structural features of the epithelial Na^+ channel (ENaC) [165]**.** ENaC is composed of a heterotrimeric structure comprising α, β, and γ subunits. Each subunit possesses two membrane-spanning domains, along with intracellular N- and C-termini.

The principal physiological function of ENaC is to serve as a mediator for the active translocation of Na^+ from the lumen into the epithelial cell across the apical membrane

[166]. The subsequent efflux of Na^+ ions through the Na^+/K^+ ATPase located on the basolateral membrane leads to the reabsorption of water into the bloodstream [167]. The activity of ENaC is subject to modulation by the renin-angiotensin-aldosterone system as well as a diverse range of extracellular factors, encompassing Na^+, Cl^-, protons, shear stress, and proteases [168] (Figure 1.8).

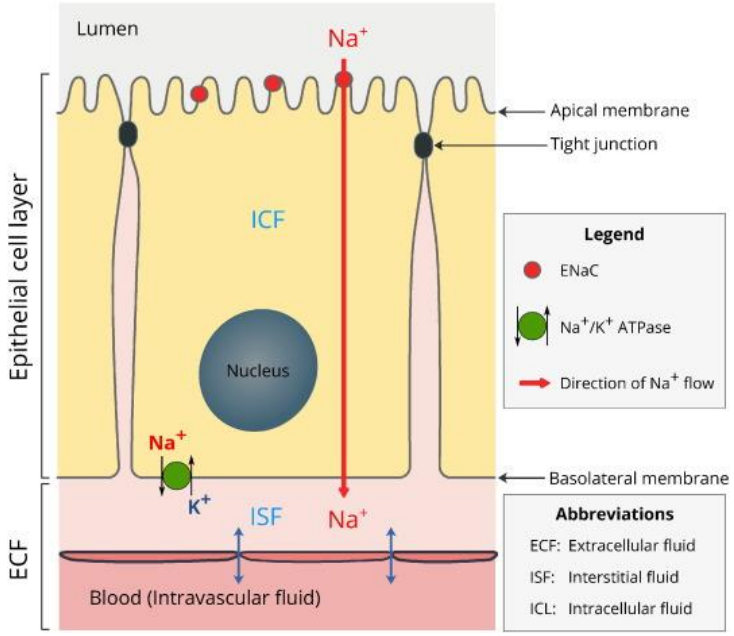

Figure 1.8 Location and function of ENaC in epithelia [156]. ENaC, predominantly found in tight or high-resistance epithelia, serves as a constitutively active channel that facilitates the movement of Na^+ ions from the lumen into the epithelial cell through the apical cell membrane. Subsequently, the absorbed Na^+ ions are transported out of the cell and into the interstitial fluid by the Na^+/K^+ ATPase located on the basolateral membrane.

1.3.2 Mutation of ENaC

ENaC mutations can lead to various diseases that are associated with impaired sodium regulation and fluid balance. Neonate mice lacking the alpha subunit of ENaC (ENaCα(-/-)) exhibited respiratory distress and succumbed to mortality within 40 hours of birth due to an inability to effectively clear liquid from their lungs [169]. Mice lacking either ENaC β or γ subunits exhibit a survival time limited to 48 hours or 36 hours post-birth, respectively, due to premature renal dysfunction. This manifestation is characterized by a multi-system pseudohypoaldosteronism (PHA) phenotype [170-172]. ENaC mutations in humans are infrequent, yet they have been identified as causative factors for certain diseases. Loss-of-function mutations in ENaC (the S562P missense mutation in ENaCα, p.Glu217fs and p.Tyr306fs mutations produced shortened ENaCβ and the K106_S108delinsN mutation in ENaCγ [173, 174]) within the kidney cause hyponatremia and severe dehydration in individuals with multi-system pseudohypoaldosteronism (PHA) [175]. Gain-of-function mutations in ENaC (truncation of the β or γ subunits [174]) within the kidney lead to excessive reabsorption of sodium and increased potassium excretion, resulting in hypertension and hypokalemia which collectively define a genetic disorder—Liddle's syndrome [176]. Mutations in ENaC subunits also result in increased sodium reabsorption in the kidneys, leading to salt-sensitive hypertension, where blood pressure elevates in response to high salt intake [177]. In the respiratory tract, upregulated ENaC expression on fetal lung epithelial cells facilitates active Na^+ transport, aiding in the clearance of fetal fluid before birth [178]. While reduced ENaC expression impairs the clearance of lung fluid,

potentially resulting in respiratory distress, particularly in pre-term infants [179]. These findings highlight the importance of ENaC genes in epithelia. However, it is worth noting that there are still numerous emerging functions of ENaC in various other physiological conditions.

1.3.3 Physiological roles of ENaC in epithelial cells and beyond

ENaC functions in the control of sodium balance. In the kidney, plasmin is identified as the primary serine protease in the nephrotic urine, and activation of ENaC by plasmin may empower Na retention in nephrotic syndrome [180], providing the potential mechanism for diseases with proteinuria. Interestingly, ENaC and multiple regulators of ENaC participate in circadian oscillations of sodium excretion in the urine [181], which indicates the importance of ENaC in the transepithelial sodium reabsorption for the circadian clock.

Apart from as a mediator for Na^+ resorptions, ENaC plays an essential role in cell signaling transduction. Our research group previously has demonstrated that ENaC functions in the female reproductive system. In mouse endometrial epithelial cells, activation of ENaC by trypsin induces cell membrane depolarization, facilitating the opening of voltage-sensitive Ca^{2+} channels and activating Ca^{2+}/cAMP sensitive transcription factor CREB, upregulating COX-2 expression, and ultimately resulting in the production of PGE_2, which is required for stromal decidualization and implantation [182]. Later, Sun et al. revealed that ENaC-dependent activation of the transcription

factor CREB in mouse and human endometrial epithelial cells represses miR-101a and miR-199a-3p, which regulate COX-2 expression post-transcriptionally [183]. Moreover, the activation of ENaC by terms signals or preterm risk triggers a pro-inflammatory response in endometrial epithelial cells by shifting labor-associated inflammatory cytokines profile, resulting in uterine contractility from quiescent to a contractile state for labor at term and preterm [184]. These studies have provided a novel and expanded role of ENaC that extends beyond its traditional function in electrolyte and fluid transport, demonstrating its crucial involvement in the regulation of signaling pathways.

1.3.4 Protein-protein interaction of ENaC

1.3.4.1 ENaC and CFTR

ENaC and CFTR, which are responsible for Na^+ absorption and Cl^- secretion, respectively, often demonstrate functional interplay in multiple organ systems characterized by the abundance of epithelial cells [185]. In individuals with cystic fibrosis (CF), a genetic disorder caused by the mutation of CFTR, there is an elevated Na^+ absorption in the airways, likely due to enhanced ENaC activity, excessive proteolytic cleavage of ENaC, and abnormal ENaC activation by cAMP [186]. These mechanisms lead to a depletion of airway surface liquid (ASL) volume [187]. Clinical trials evaluating the efficacy of amiloride, a selective ENaC blocker, and its more potent analogue, benzamil, as CF treatment drugs, have not shown success [188, 189]. Studies

have demonstrated that in the female reproductive system, the uterine expression of CFTR and ENaC undergoes cyclic changes in response to hormonal fluctuations during the estrus cycle in mice [190], with CFTR upregulated during estrus and ENaC upregulated during diestrus, enabling dominant uterine secretion during estrus and uterine absorption during diestrus to support reproductive processes [191].

Interestingly, recently we have investigated a phasic regulation of CFTR functional expression by ENaC in endometrial epithelial cells, with low-degree ENaC deficiency stimulating CFTR expression while high-degree deficiency either restoring or inhibits CFTR expression. Intracellular Ca^{2+}-modulated sAC-driven cAMP production positively regulates CFTR under low-degree deficiency, while negative regulation may occur at post-transcriptional stages under high-degree deficiency [192] (Figure 1.9). The interaction between ENaC and CFTR is important for understanding epithelial homeostasis, but many aspects of this interaction are still not fully understood. While CFTR's role in β-cell excitability and insulin secretion is known, the potential involvement of ENaC in β-cells is an intriguing question that requires further exploration.

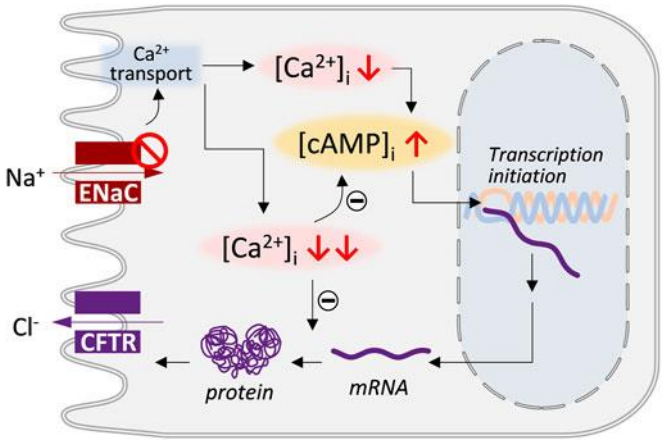

Figure 1.9 Biphasic regulatory action of ENaC on CFTR expression [192]. The deficiency of ENaC results in a decrease in $[Ca^{2+}]_i$. This reduction in $[Ca^{2+}]_i$ has the potential to elevate $[cAMP]_i$ and initiate the transcription of the CFTR. However, if ENaC inhibition is intensified, leading to a substantial decrease in $[Ca^{2+}]_i$, it may impact the stability of CFTR mRNA or protein, ultimately resulting in the downregulation of CFTR expression.

1.3.4.2 Other proteins

ENaC is also regulated by other factors. Aldosterone activates SGK1, which phosphorylates ENaC subunits, particularly the α subunit, and promotes their insertion into the apical membrane, regulating sodium transport and maintaining electrolyte homeostasis [193]. Dysregulation of this interaction can lead to hypertension and other sodium handling disorders [194]. Serine proteases such as trypsin, furin, and plasminogen can activate ENaC by cleaving inhibitory tracts in the finger domains of the α and γ subunits, resulting in channel opening. These proteases increase the open probability of ENaC and decrease the close time of the channel [195].

1.3.5 ENaC, hypertension, and diabetes

1.3.5.1 ENaC and hypertension

ENaC plays a crucial role in the regulation of body fluid volume and the maintenance of Na^+ homeostasis, which has implications for blood pressure control. Dysregulation of ENaC function is associated with various forms of hypertension, including salt-sensitive hypertension and obesity-related hypertension. The proper functioning of ENaC is essential for maintaining blood pressure within the normal range [196]. A direct inhibitor of ENaC—amiloride is a diuretic by enhancing urine flow, thereby reducing water content and aiding in the lowering of blood pressure [197]. Clinically, Amiloride is not employed as a single drug therapy for hypertension but is often administered in conjunction with a thiazide diuretic [198]. Although clinical evidence supports the use of amiloride in managing hypertensive patients who demonstrate resistance to conventional treatments, its utilization for hypertension remains limited due to the apprehension of hyperkalemia [199].

Many diabetes patients are accompanied by hypertension due to the uncontrolled high blood glucose levels traveling through the body [200]. According to data from the Centers for Disease Control and Prevention (CDC) and the National Health and Nutritional Examination Survey (NHANES) database, a substantial 73.6% of individuals aged 18 years or older with diabetes exhibit comorbid hypertension. The co-occurrence of hypertension and diabetes is not merely coincidental; it is frequently observed in patients with type 2 diabetes due to a cluster of metabolic abnormalities

known as the cardiometabolic or cardiorenal metabolic syndrome [201]. Diuretics typically form third-line therapy and if blood pressure targets are not achieved with loop and thiazide-like diuretics, potassium-sparing diuretics such as amiloride can be considered. Consequently, there is a need to investigate the role of amiloride and ENaC in the management of diabetes, as they may hold potential therapeutic implications.

1.3.5.2 Sodium environment in β-cells

Elevated dietary sodium intake is a widely acknowledged risk factor associated with the development of hypertension [202]. A comprehensive meta-analysis has demonstrated a significant reduction in elevated blood pressure through the implementation of dietary sodium restriction [203]. This finding holds relevance in the context of individuals with diabetes, as hypertension often coexists in this population as we discussed before. According to a report conducted in an adult Finnish population, high sodium intake was identified as a predictor for the risk of developing type 2 diabetes [204]. A study from Korea revealed a correlation between dietary sodium intake and diabetes. The findings suggest that a high salt intake contributes to the development of obesity and metabolic syndromes, including diabetes [202]. Although this could be attributed to the impaired mechanism of sodium intake that regulates glucose homeostasis through PPAR/SGLT pathway, as observed in individuals with diabetes [202, 205], the relationship between sodium diet and diabetes remains unclear.

The association between excessive sodium consumption and insulin sensitivity has

been a topic of controversy. Teki et al. demonstrated that excessive NaCl intake along with a high-fat diet in C57 BL/6J mice exacerbates glucose intolerance by impairing insulin secretion due to diminished expansion of β-cell mass in the pancreas [206]. However, in normal SD rats, a two-week salt loading resulted in a slight but significant elevation in blood pressure, while body weight and food intake remained unchanged [207]. The role of sodium intake and sodium environment remains controversial and inadequately studied, highlighting the significance of investigating novel mechanisms linking glucose levels to the sodium environment in understanding β-cell function, diabetes, and its related comorbidities.

1.4 Hypothesis and Objectives

In summary, the regulation of glucose metabolism and insulin secretion is crucial for maintaining endocrine homeostasis, disruptions of which lead to metabolic disorders such as diabetes. Insulin is exclusively secreted from pancreatic islet β-cells and it is secreted under blood glucose level elevation. Glucose-stimulated insulin secretion and cAMP-amplificated insulin secretion are the principal mechanisms of insulin regulation, a process regulated by multiple factors and ion channels; nevertheless, the precise mechanisms governing this complex cellular event remain largely elusive. ENaC, an epithelial sodium ion channel, is responsible for mediating sodium and water absorption in the body. It has been reported that excessive dietary Na^+ intake was linked to the risk of developing diabetes, but the exact mechanisms by which the Na^+ environment and possible Na^+ channel genes regulate insulin secretion remain unknown. Our previous

studies demonstrated that CFTR, an epithelial chloride channel, contributes to β-cell excitability and insulin secretion. In epithelial cells, CFTR is known to interact closely with ENaC. ENaC is also involved in Ca^{2+} mobilization and signaling transduction in other cells. However, whether and how ENaC plays a role in β-cells has never been studied.

Hence, we hypothesize that **ENaC is expressed in pancreatic islet β-cells and plays a role in insulin secretion, thereby contributing to the regulation of glucose metabolism.**

To test the hypothesis, we aim to

1) Profile the functional expression of ENaC and its correlation with insulin secretion in pancreatic islet β-cells;

2) Investigate the mechanisms underlying ENaC-mediated insulin secretion;

3) Elucidate the effects of ENaC on insulin secretion and glucose metabolism *in vivo*.

Chapter 2: Materials and Methods

2.1 Human database analysis

Human protein atlas https://www.proteinatlas.org/ was used for analysis of the expression of ENaC in human pancreas tissues. Previously published datasets from whole-genome gene expression microarrays in cadaver pancreas tissues (http://www.ncbi.nlm.nih.gov/geo, accession number: GSE20966) was analyzed for research on the differential expression of ENaC or other genes on diabetic or non-diabetic individuals.

2.2 Animals

2.2.1 Wild-type mice and rats

C57BL/6 wild-type mice or Sprague Dawley rats were purchased from Centralized Animal Facilities (CAF) at The Hong Kong Polytechnic University. All animals were housed in a controlled animal facility (CAF) and subjected to experimental procedures that were approved by the Animal Subjects Ethics Sub-committee at Hong Kong Polytechnic University (19-20/41-BME-R-GRF).

2.2.2 β-cell-specific *Scnn1a*-knockout mice

The recombinant enzyme system (Cre-loxP) based transgenetic conditional knockout (cKO) mice (genetic background: CS7BL/6JGpt) were used to construct the pancreatic islet β-cell ENaCα (*Scnn1a*) conditional knockout mouse model. β-cell-specific Scnn1a-knockout mice (*Ins2*-Cre^{+}.*Scnn1a*$^{fl/fl}$) were generated by mating mice

expressing the Cre recombinase gene under the rat insulin 2 gene promoter (*Ins2*-Cre^{+}) (Strain #003573, The Jackson Laboratory) with Scnn1a (*Scnn1a*$^{fl/+}$) mice (GemPharmtech, Jiangsu, China) to obtain *Ins2*-Cre^{+}. *Scnn1a*$^{fl/+}$ mice, which were then crossed to get *Ins2*-Cre^{+}. *Scnn1a*$^{fl/fl}$ knockout (cKO) mice (Figure 2.1). In brief, CRISPR/Cas9 techniques were employed to insert the loxP sequence (ATAACTTCGTATAGC ATACATTATACGAAGTTAT) into the upstream and downstream regions of intron of exon 2 in the Scnn1a gene (ENSMUST00000081440.13). The RIP-Cre transgene consists of three key components: a 668 bp fragment of the rat insulin II promoter, nuclear-localized Cre recombinase, and a 2.1 kbp fragment derived from the human growth hormone gene. These transgenic mice, carrying the RIP-Cre transgene, serve as a valuable Cre-lox tool for targeted deletion of Scnn1a floxed sequences specifically in pancreatic β-cells. Mice were genotyped using the following primers (table 2.1) using Phire Tissue Direct PCR Master Mix (#F170L, Thermofisher) with the following cycling conditions: 98 ℃, 5 min; 98 ℃, 5 s, 65 ℃, 5 s, Inc-0.5℃/Cyc, 68 ℃, 20 s (10 cycles); 98 ℃, 5 s, 60 ℃, 5 s, 72 ℃, 20 s (30 cycles); 72 ℃, 1 min; 4 ℃, 1 min. Reactions were separated on 2% agarose gels yielding a ≈ 300 bp band. The following band sizes were observed for Ins2-Cre^{+}: ≈ 324 bp and ≈100 bp, Ins2-Cre^{-}: 324 bp. The same sample was used for flox mice (table 2.1) using the same polymerase as Cre with the following cycling conditions: 98 ℃, 5 min; 98 ℃, 5 s, 65 ℃, 5 s, Inc-0.5℃/Cyc, 72 ℃, 20 s (20 cycles); 98 ℃, 5 s, 55 ℃, 5 s, 72 ℃, 20 s (20 cycles); 72 ℃, 5 min; 4 ℃, 1 min. The following band sizes were observed for *Scnn1a*$^{fl/fl}$: ≈ 450 bP, *Scnn1a*$^{fl/+}$: ≈ 450 bp and 350 bp.

Ins2-Cre^{+} mice were used as controls (Cre-Ctrl). The mice with Cre positive and Scnn1a$^{fl/fl}$ genotype were selected as homozygous ENaCα-knockout mice and the mice with Cre positive and Scnn1a$^{fl/+}$ genotypes were regarded as heterozygotes.

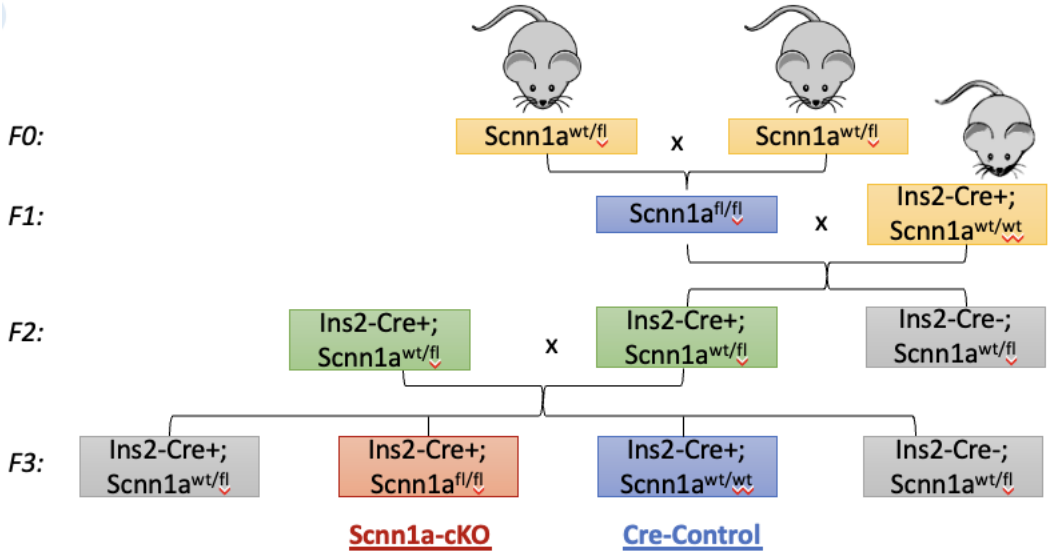

Figure 2.1 Schematic flow diagram of cKO (*Ins2*-Cre^{+}. *Scnn1a*$^{fl/fl}$) and Cre-Ctrl (*Ins2*-Cre^{+}. *Scnn1a*$^{wt/wt}$) mice.

Table 2.1 Primers for genotyping

Primer name	Forward 5'-3'	Reverse 5'-3'
Scnn1a-5wt-t	TCCTCGGAAGAGCATCACATG	CCAGATGAAGTTCCTACCTTTGC
Scnn1a-3wt-t	TATGTGTGTAACCCAGGTCCTTG	TTGAGGTAATGGTAGGCAGTGC
Ins2-Cre	ACTCCAAGTGGAGGCTGAGA	TCCTTCCACAAACCCATAGC
Internal positive control	CTAGGCCACAGAATTGAAAGATCT	GTAGGTGGAAATTCTAGCATCATCC

2.3 Cell culture

RINm5F cells purchased from ATCC were cultured in RPMI 1640 (11875093, Thermofisher) containing 10% fetal bovine serum (FBS, 10270106, Gibco, South American (CE)), 1% L-glutamine (25030081, Gibco), 1% penicillin-streptomycin (15140122, Gibco) in 5% CO_2 incubators at 37 ℃. To validate the glucose responsiveness of the RINm5F cells utilized in this study, insulin-releasing responses were assessed by adding glucose to the culture media after a 2 or 24-hour incubation in glucose-free 1640 medium (11879020, Gibco).

2.4 Islet isolation

The following solutions were prepared for islet isolation [208]:

Table 2.2 Solutions for mouse islet isolation

Solution	**Composition**
Solution 1	Ice-cold HBSS solution (14170120, ThermoFisher) containing 1 mM $CaCl_2$ (BP510-250, Fisher Bioreagents)
Solution 2	1 mg ml^{-1} Type XI collagenase (C7657, Sigma, USA) dissolved in ice-cold HBSS solution
Solution 3	RPMI 1640 (11875093, Thermofisher) containing 10% fetal bovine serum (FBS, 10270106, Gibco, South American (CE)), 20 mM L-glutamine (25030081, Gibco), 1% penicillin-streptomycin (15140122, Gibco).

a) Surgical operation

The mice were euthanized using CO_2 inhalation followed by cervical dislocation. An incision was made around the upper abdomen to expose the liver and intestines. The

ampulla was located, and surgical clamps were used to block the bile pathway to the duodenum on the duodenum wall.

b) Pancreas perfusion and removal (Figure 2.2)

Firstly, a 5 ml syringe mounted with a 30 G 1/2-G needle was used to take 3 ml of Solution 2. Under a microscope, the needle was inserted into the common bile duct through the joint site of the hepatic duct and the cystic duct, reaching the middle of the common bile duct. The pancreas was distended by slowly injecting 3 ml of Solution 2 and then removed and placed in a 50 ml tube containing 2 ml of Solution 2.

c) Pancreas digestion

The tube containing pancreas tissues was incubated in a water bath at 37.5 ℃ for 15 min, with brief manual shaking two to three times during the incubation. After incubation, the pancreas was disrupted by shaking the tube manually until the tissue suspension became homogeneous. The digestion was terminated by placing the tube on ice and adding 25 ml of Solution 1. The tube was centrifuged at 290 g for 30 s at 4 ℃, and the supernatant was discarded. The pellet was resuspended with 20 ml of Solution 1, followed by another centrifugation at 290 g for 30 s at 4 ℃ and the supernatant was discarded again.

d) Islet purification

The above resulting pellet was resuspended with 15 ml of Solution 1 and poured onto

a pre-wetted 70 μm cell strainer. The tube was washed with 20 ml of Solution 1 twice by being poured onto the strainer. The strainer was then inverted over a new petri dish, and the captured islets were rinsed into the 150 mm petri dish (SPL-10090, SPL) with 15 ml of Solution 3. The isolated islets were hand-picked using a pipette under an inverted microscope (P-DSL32, Nikon) and then cultured a 5% CO_2 incubator at 37 ℃ individually in culture dishes for insulin measurement or seeded on the glass-bottom dishes for Ca^{2+} measurement. To get isolated islet cell, islets were incubated in an enzyme-free cell dissociation solution (Millipore, Cat. S-004-B) for 5 minutes. Subsequently, the islets were dispersed into single cells to perform patch clamp experiments.

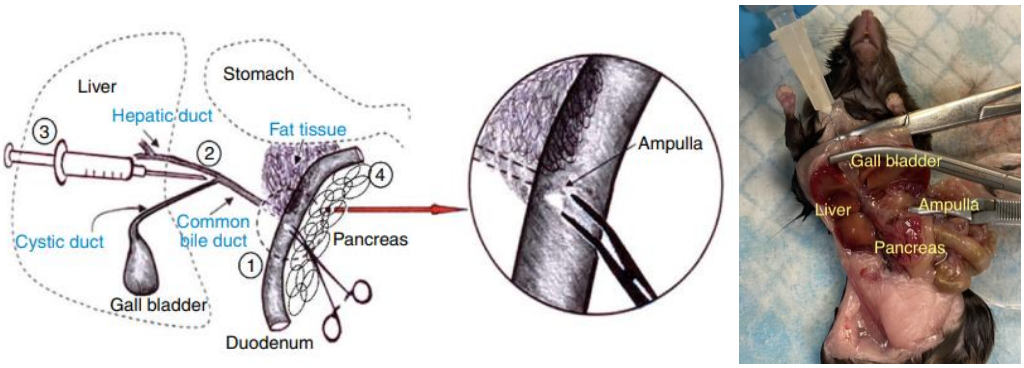

Figure 2.2 Workflow of mouse pancreas perfusion and extraction. (1) Identification and clamping of the ampulla using curved hemostatic forceps. The ampulla, situated near the fat tissue margin on the duodenum wall, is depicted in the figure insert. This step can be performed without the assistance of a microscope [208]. (2) Insert the needle into the common bile duct via the junction of the hepatic duct and cystic duct. (3) Gradual administration of the first half of the solution, followed by an increase in

injection speed. (4) Isolation of the distended pancreas, beginning from the duodenum while being cautious to avoid the accumulation of adipose tissue clusters.

2.5 RNA interference for ENaC knockdown

RINm5F cells were seeded in 12 or 24-well plates and grown until 60 to 70% cell density in RPMI 1640 culture medium. Various small interfering RNAs (siRNAs, 100 nmol per 35-mm^2 dish, Table 2.3) were transfected using DharmaFECT 1 transfection reagent (2 μL per 35-mm^2 dish, T-2001-01, HORIZONDISCOVERY) in the OptiMEM medium (100 μL per 35-mm^2 dish, #31985062, Thermofisher Scientific) plus antibiotic-free RPMI 1640 medium (900 μL per 35-mm^2 dish), following the manufacturer's instruction. After overnight incubation, the medium was replaced with the growth medium. Cells were collected 48 or 72 h after transfection for other experiments. For glucose challenge in the insulin ELISA experiment, cells and culture medium were collected 48 h post-transfection plus 24 h fasting period, using glucose-free RPMI 1640 medium (11879020, ThermoFisher). Double RNA interference transfection with the same protocol was performed after 24 h and maintained for another 24 h for later measurements.

Table 2.3 Sequences of siRNAs

Small interference RNA	Catalog	Sequence
siGENOME Non-Targeting siRNA Pool #2	D-001206-14-05	UAAGGCUAUGAAGAGAUAC, AUGUAUUGGCCUGUAUUAG, AUGAACGUGAAUUGCUCAA,

		UGGUUUACAUGUCGACUAA.
siGENOME Rat Scnn1a (25122) siRNA-SMARTpool	M-091898-01-0005	GAGCUGAACUAUAAAACUA, GAAAUUACGGCGACUGUAC, CAACAUUGACCUAGACCUU, GCGAUGUCCCGGUCAAGAA.
siGENOME Rat Adcy6 (25289) siRNA-SMARTpool	M-100104-01-0005	GAACAUGGGUCCGGUUGUA, GGUAACGGGUGUAAAUGUG, GGAGGGUAGCGCUCAAAUA, UCUAAGGCAUUCCGACAGA.
siGENOME Rat Adcy8 (29241) siRNA-SMARTpool	M-091166-01-0005	GAGAACAUGCUUCGCAAUA, GGAUUAACGAGACCUAUUU, GAACUGCCAUUCGACAACA, UUGCAGAUGUCAAAGGAUU.

2.6 ENaC overexpression

RINm5F cells were seeded in 12-well plate and grown until 60 to 70% cell density in RPMI 1640 culture medium. DNA plasmids (2 μg per 35-mm^2 dish) were transfected using Lipofectamine 2000 transfection reagent (6 μL per 35-mm^2 dish, #11668027, Thermofisher Scientific) in the OptiMEM medium (100 μL per 35-mm^2 dish, #31985062, Thermofisher Scientific) plus antibiotic-free RPMI 1640 medium (900 μl per 35-mm^2 dish), following the manufacturer's instruction. Cells were collected 48 or 72 h after transfection for other experiments. For glucose challenge in the insulin ELISA experiment, cells and culture medium were collected 48 h post-transfection plus

24 h fasting period, using glucose-free RPMI 1640 medium (11879020, ThermoFisher). h-alpha-ENaC Sequences (83430, Addgene, USA) was used to overexpress ENaCα and null sequence pcDNA3.1 (V790-20, Addgene, USA) as the vector.

2.7 RNA extraction and Quantitative PCR (qPCR)

Tissues were ground into powders using homogenization in liquid nitrogen. Subsequently, the powdered tissues were transferred into RNAase-free microtubes (Axygen, MCT-175-C) containing 500 μL of TRIzol (Invitrogen, 15596018). For adherent cultured cells, 500 μL of TRIzol was directly added into the culture dish to induce cell lysis by pipetting the solution up and down. Subsequently, the lysates were collected using RNase-free microtubes.

All steps involved in RNA extraction were conducted following the manufacturer's instructions. Firstly, 100 μL of chloroform was added to each tube containing 500 μL of TRIzol, which was vigorously vortexed for 15 s. Subsequent centrifugation at 1300 rpm for 10 min at 4 ℃ facilitated phase separation, allowing for careful aspiration of the RNA-containing top aqueous phase, which was then transferred to RNase-free microtubes. For RNA precipitation, the aqueous phase containing the RNA was combined with 40 μL of isopropanol and incubated at -20 ℃ for 30 min. Following another centrifugation at 1300 rpm for 10 min at 4℃, the resulting RNA pellets were obtained. The supernatant was removed, and the pellets were washed with 75% ethanol. Afterward, the pellets were dissolved in DEPC-treated water following centrifugation.

The concentration and purity of the extracted RNA were assessed using a NanoDrop spectrophotometer (Thermo Fisher Scientific, ND-ONE-W). Subsequently, 1 μg of total RNA was reverse-transcribed into complementary DNA (cDNA) using the High-Capacity cDNA Reverse Transcription kit (Thermo Fisher Scientific, 4368814) in accordance with the manufacturer's instructions. After reverse transcription, 0.1 μg of cDNA from each sample was subjected to amplification in a 10 μL reaction system. The reaction mixture included SYBR Green Premix Ex TaqTM Mix (Takara, RR420A) and the corresponding primers (see Table 2.4). The amplification was carried out using the Bio-Rad real-time PCR system (Bio-Rad, CFX96). All target genes with sequences from 5' to 3' were shown in Table 2.4.

Table 2.4 List of primers for qPCR

Gene name	**Forward (5'-3')**	**Reverse (5'-3')**
Scnn1a	CCCAAGGGAGTTGAGTTCTG	AGGCGCCCTGCAGTTTAT
Scnn1b	GCAGGAACTGAGACTTCTATTG	GATGGAATAGGTCGTGTTGTAG
Scnn1g	ACCACCTCCCAGATACAATA	GAAAGACAGAGCAAGGATAGG
Adcy1	AGGGCAAGGGAGAGATGCTA	AGGGCAAGGGAGAGATGCTA
Adcy2	TCTCATTGCCAGTGGTCGTC	TCGGGCACTATAAACCAAAGTA
Adcy3	CGGGGTTCCCAACTGTTGAA	CTTTGGGGAAGCTACAGGCA
Adcy4	GCTTAACACAAAGCAGGCAGG	GATACTGTTGGCTCAGGCTGT
Adcy5	GAATCCACTGCTCGCCTTGA	GTACAGTTCATCATTGCGCCG

Adcy6	TACTGTTGACCTTCCACGCC	GGCGGAAGCTATGTCGGTTA
Adcy7	ATGACGTGTGGTCCCATGAC	TCCAGGTGATTCAGTGTCGC
Adcy8	CCAACCCTACGCAACTCCTT	ATGCCCTTGAGAGGGTCCAT
Adcy9	AGGTCTGAACTTCCCTCTGGA	ACCTTTCCCGAACAGGTCAG
Adcy10	CAGACCCCCTTCCTGTTCTC	CTGTTCTCCAAGACGGAGGAAA
Gapdh	GATGCTGGTGCTGAGTATGTCGTG	TGCATTGCTGACAATCTTGAGGG

2.8 Western blot

For cell or tissue lysis, RIPA buffer was used. The RIPA buffer composition consisted of 50 mM Tris-Cl (pH 7.5), 150 mM NaCl, 1% NP-40, 0.5% DOC, and 0.1% SDS. Additionally, 1% protease inhibitor cocktails (#11873580001, Roche) were added to the RIPA buffer. The lysing process was performed on ice for a duration of 30 min. The lysates were centrifuged at 13000 rmp for 30 min at 4 ℃ and the supernatant was collected for western blot after testing the protein concentration by Pierce BCA assay kit (#23225, Thermofisher Scientific). The protein lysates (35 to 50 μg of total protein) were denatured in LDS sample buffer (Thermo Fisher Scientific, NP0007) plus 4% β-mercaptoethanol (Acros, 125472500) with heating at 70 ℃ for 10 min to detect ENaCα, or boiling at 95 ℃ for 10 min or incubated at room temperature for other antibodies. After denaturation, proteins were separated by SDS-polyacrylamide gel electrophoresis and subsequently transferred to equilibrated nitrocellulose (NC) membrane in the transferring buffer (57.66 mM Tris, 191.8 mM glycine, 0.1% SDS, 20% methanol) at a constant voltage of 25 mV and a limited current of 1.0 A for 60 min at room temperature. After transferring the proteins onto the membrane, the total protein on the membrane

was analyzed prior to blocking. The blocking step was carried out by incubating the membrane in 5% skim milk in TBS buffer (20 mM Tris, 150 mM NaCl) for a minimum of 30 min. The membrane was incubated with the primary antibodies in 5% non-fat milk in TBS at 4 ℃ overnight. Primary antibodies against ENaCα (1:1000, anti-rabbit, StressMarq, SPC403), ENaCα (1:1000, anti-mouse, StressMarq, SMC242D), β-Tubulin (1:1000, Thermofisher Scientific, PA5-16863) and actin (1:2000, Sigma Aldrich, MAB1501R) were used. On the following day, the NC membrane was washed with TBST buffer (0.05% Tween 20 in TBS) 5 times (10 min each), and incubated with horseradish peroxidase (HRP)-conjugated antibodies at room temperature for 1 h. The membrane was washed with TBST buffer as before and visualized by ECL substrates (Bio-Rad, 170-5060) by ChemiDoc MP Imaging System (Bio-Rad). HRP-conjugated secondary antibodies were goat anti-rabbit IgG (1:2000, Bio-Rad, 12004159) and goat anti-mouse IgG (1:2000, Bio-Rad, 12004159). Image J software was used for the densitometry of western blots.

2.9 Patch-clamp

RINm5F and single islet cells were cultured on 35 mm culture dishes for 1-2 days before patch-clamp recording. Borosilicate glass-made patch pipettes (BF150-86-7.5, Sutter Instrument Co., USA) were pulled with a micropipette puller (P-1000, Sutter Instrument Co., USA) to a resistance of 5–7 MΩ before filled with a pipette solution (in mM): KCl 138, NaCl 10, $MgCl_2$ 1 and HEPES 10 with D-manitol compensated for osm 290 (pH 7.4). Membrane potentials of cells were recorded with a patch-clamp

amplifier (Multiclamp700B, Axon Instruments) and a data acquisition system (DigiData1550B, Axon Instruments). Cells were bathed in a solution (Margo-Ringer solution) containing (in mM): NaCl 130, KCl 5, $MgCl_2$ 1, $CaCl_2$ 2.5, Glucose 10, HEPES 20 (pH 7.4). Once the whole-cell giga seal was established, the membrane potential of the cells was measured using current clamp step recording. In this recording, currents ranging from 0 to 500 pA were injected into the cells with an increment of 50 pA and a duration of 0.8 ms.

2.10 Intracellular Ca^{2+} imaging

Cells seeded on the glass-bottom dishes (Invitrogen, 150680) were washed with the bath solution twice as used in patch-clamp or Margo-Ringer glucose-free solution containing (mM): NaCl 130, KCl 5, $MgCl_2$ 1, $CaCl_2$ 2.5, Hepes 20 with D-manitol compensated for osm 285 (pH 7.4), incubated with Fura-2 (2.5 μM, Invitrogen, F1200) and Pluronic F-127 (1.25 μM, Invitrogen, P3000MP) in the bath solution at 37 ℃ for 30 min and equilibrated at room temperature for 10 min. After equilibrium, the coverslip was mounted on to a mini chamber with 1 ml bath solution in a fluorescence microscope (Eclipse Ti2, Nikon, Tokyo, Japan) for intracellular Ca^{2+} measurement. Fluorescence was alternatively excited by dual-wavelength 340 and 380 nm with an interval of 3 s, and the emitted fluorescent lights were collected at 510 nm.

2.11 Intracellular cAMP imaging

The plasmid pCAG-G-Flamp1 (#188567, Addgene) was employed as a green biosensor

for real-time cAMP measurement. In brief, a reverse transfection method was utilized to introduce 3 μg of the plasmid into a cell suspension following the Lipofectamine 2000 protocol. Subsequently, the transfected cells were seeded onto glass-bottom dishes for 24 h or 48 h before imaging measurements. The glass was transferred to a mini chamber containing 1 ml bath solution as used in patch-clamp and then mounted on to a fluorescence microscope (Eclipse Ti, Nikon, Tokyo, Japan) and green fluorescence (495/520 nm excitation/emission) with an interval of 3 s was monitored at room temperature for intracellular cAMP measurement.

To record cAMP imaging and patch clamp experiment concurrently, cells exhibiting green fluorescence (495/520 nm excitation/emission) were selected for patching using different sodium concentration pipette solutions: 10 mM Na^+ pipette solution (KCl 128, NaCl 10, CsCl 10, MgATP 2 and HEPES 10 with D-manitol compensated for osm 290 (pH 7.4)), 15 mM Na^+ pipette solution (KCl 128, NaCl 15, CsCl 5, MgATP 2 and HEPES 10 with D-manitol compensated for osm 290 (pH 7.4)), 20 mM Na^+ pipette solution (KCl 128, NaCl 20, MgATP 2 and HEPES 10 with D-manitol compensated for osm 290 (pH 7.4)). The patch-clamp and cAMP signals were simultaneously recorded in real-time.

2.12 Intracellular Na^+ imaging

Intracellular Na^+ concentration was measured with the Na^+-sensitive fluorescent dye sodium-binding benzofuran isophthalate (SBFI, Invitrogen, S1264). While the

selectivity of SBFI for Na^+ is not as high as that of calcium indicators like fura-2, it still demonstrates adequacy in detecting physiological levels of Na^+ even when other monovalent cations are present. SBFI exhibits a dissociation constant (Kd) of 3.8 mM for Na^+ when K^+ is absent, and 11.3 mM when Na^+ and K^+ are present at a combined concentration of 135 mM. This indicates that SBFI has approximately 18-fold higher selectivity for Na^+ compared to K^+. The cells cultured onto the glass were loaded by incubation in Margo-Ringer solution that contained 5–10 μM SBFI-AM and 0.01% Pluronic F-127 at room temperature for ~40 min. Dye-loaded cells were then kept in Margo-Ringer solution for at least 30 min before use. Fluorescence was alternatively excited by dual-wavelength 340 and 380 nm with an interval of 3 s, and the emitted fluorescent lights were collected at 510 nm.

2.13 cAMP ELISA

Intracellular cAMP concentration was measured using Direct cAMP ELISA Kit (Enzo Life Sciences, Cat. No. ADI-900-066). Cells were seeded in a 12-well plate and grown until 60 to 70% cell density in RPMI 1640 culture medium. Before the cell lysate, cells were incubated with serum-free, antibiotic-free medium overnight. Subsequently, each well was lysed with 200 μL of 0.1M HCl at room temperature for 10 min, and collect the supernatants by centrifuging the cell lysates at 1000 g for 5 min. A portion of the supernatants was used to determine protein concentration for normalization in each sample with Pierce BCA assay kit (#23225, Thermofisher Scientific). Another portion of the supernatants was used for cAMP measurement and treated with acetylating

reagent (10 μL for every 200 μL sample) to enhance assay sensitivity. Sample wells, cAMP standard wells and other reference wells were loaded and processed according to the assay layout sheet and product manual. The optical density (OD) of each well was measured at 405 nm using a Ledetect 96 Absorbance Plate Reader (Labexim Products). The mean OD of the substrate blank was subtracted from all measurements to eliminate background signal. Concentration of cAMP in each sample was calculated with a four-parameter logistic curve fitting program and normalized to protein content.

2.14 Insulin ELISA

RINm5F cells were grown on 12 or 24-well plates and transfected with siRNA or DNA plasmid for 48 h. The cells were fasted from glucose for 24 h and the islets were fasted from glucose for 2 h in glucose-free RPMI 1640 medium before adding RPMI 1640 medium containing 10mM glucose. Islets of similar size (about 100 mm diameter) were used for insulin ELISA measurement. Culture media were collected 10, 30 and 60 min after the glucose challenge. For whole-cell insulin ELISA measurement, RINm5F cells after knockdown or drug inhibition were lysed with RIPA buffer. Insulin in the culture media or RIPA buffer was measured by Wide Range Rat Insulin ELISA kit (33100, ImmunoDiagnostics, Hong Kong) following the manual of the manufacturer and normalized to protein content. Protein content was determined using the Pierce™ BCA protein assay kit (23225, Thermo Fisher Scientific). Insulin in blood serum was measured by IMD Ultra-sensitive mouse Insulin ELISA kit (32380, ImmunoDiagnostics, Hong Kong) following the manufacturer's manual.

2.15 ATP assay

RINm5F cells were cultured on a 96-well plate until reaching a cell density of approximately 60 to 70%. Subsequently, they were transfected with siRNAs or plasmids to induce knockdown or overexpression of ENaC, respectively, for a duration of 48 h. Alternatively, the cells were subjected to drug treatment for 30 min prior to the ATP assay. Intracellular ATP levels were quantified in cell lysates using a Luminescent ATP Detection Assay Kit according to the manufacturer's instructions (Abcam, Cambridge, UK, Cat# ab113849).

2.16 Hematoxylin and eosin (H&E) staining

Mouse pancreas tissues were collected by whole-body perfusion fixation. Briefly, the mouse reached a surgical plane of anesthesia before the experiment. Then, surgical treatment was performed to expose the heart of the mouse. A total of 50 mL of phosphate-buffered saline (PBS, pH = 7.4) solution followed by 30 mL of 4% paraformaldehyde (PFA, Solarbio, P1110) were injected into the mouse's circulatory system via the heart and allowed to flow out, effectively perfusing the entire body of the mouse. Following the perfusion fixation, the pancreas tissues were carefully harvested from the mouse and fixed by immersion PFA overnight at 4 ℃ before they were embedded in paraffin. The tissues were dehydrated by a gradient increase of ethanol concentration from 70% to 100%, xylene, and then embedded in paraffin (Table 2.5). The tissues were cut into 5 μm sections by microtone (Leica RM2235) and stained with H&E following the protocols in Table 2.6.

Table 2.5 Protocol of dehydration and paraffin embedding

Step	**Reagent**	**Time**
1	50% - 60% - 70% -80% - 90% - 95% - 95% ethanol 100% - 100% ethanol	30 min for each 20 min for each
2	The mixture of xylene and ethanol (1:1)	5 min
3	Xylene - Xylene	2 min for each
4	Paraffin - Paraffin	50 min for each

Table 2.6 Protocol of hematoxylin and eosin (H&E) staining for pancreas paraffin section

Step	Reagent	Time
1.Deparaffinization	Xylene - Xylene	5 min for each
2.Rehydration	100% - 90% - 70% ethanol ddH_2O	3 min for each 2 min
3. Nuclei staining	Harris modified hematoxylin solution (sigma, HHS32)	1 min
4. Removal of excessive hematoxylin	ddH_2O	1 min
5. Decoloration (removal of background hematoxylin)	Acid alcohol (1% HCl in 75% ethanol)	1 sec
6. Removal of Acid alcohol	ddH_2O	1 min
7. Bluing of hematoxylin	Scott's tap water (20 g/L $MgSO_4 \cdot 7H_2O$ + 2 g/L $NaHCO_3$)	3 min
8. Removal of Scott's tap water	ddH_2O	1 min
9. Counterstaining with Eosin Y	0.5% (w/v) eosin Y (sigma, 230251) in 95% (v/v) ethanol w/ 0.05% (v/v) acetic acid	2 min

10. Dehydration	ddH_2O 70% - 80% - 90% - ethanol 100% - 100% ethanol	1min 5 sec for each 3 min for each
11. Clearance of ethanol	Xylene Xylene	3 min 5 min
12. Slide mounting	Neutral resin (solarbio, G8590)	Dry overnight

2.17 Immunofluorescence

Pancreas tissues were collected by whole-body perfusion fixation. The procedure of immunofluorescence staining for the section was followed by table 2.7. After three times washed in PBS, pancreas tissues were cryoprotected in 30% sucrose in PBS at 4 ℃ for 24 h, mounted in optimal cutting temperature (OCT) embedding media (Tissue-Tek, 4583, Sakura), and cryo-sectioned into 5 μm sections. Slices were rehydrated in PBS for 5 min and microwaved in Tris-EDTA buffer (Tris Base 10 mM, EDTA 1 mM, pH = 9.0) for 20 min to retrieve antigens. After cooled down to room temperature and treated with 1% SDS in PBS for 4 min, sections were blocked with 1% bovine serum albumin in PBS for 15 min, incubated with primary antibody ENaCα (1:100, PA1920A, Thermo), ENaCα (1:100, anti-rabbit, StressMarq, SPC403), ENaCα (1:100, anti-mouse, StressMarq, SMC242D), insulin (1:200, ab7842, abcam) overnight at 4 ℃ and subsequently fluorochrome-conjugated secondary antibody (Invitrogen) for 1 h at room temperature. DAPI (H-1800-10, Vector Labo retories) was used to stain cell nuclei. Images were acquired with a fluorescence microscope (Eclipse Ti2, Nikon, Tokyo, Japan), and a confocal microscopy (TCS SP8 MP Multiphoton/Confocal Microscope, Leica, Germany).

Table 2.7 Protocol of immunofluorescence for pancreas OCT section

Step	Reagent	Time
1. Retrieve antigen	PBS 10mM 95 ℃ Tris-EDTA buffer, pH= 9.0	5 min 20 min
2. Permeabilization	1% SDS in PBS	4 min
3. Wash	PBS	5 min, 3 times
4. Blocking	1% BSA in PBS	20 min
5. Primary antibody	Diluted in blocking solution Washed by High-salt PBS (18 g NaCl in 1xPBS) PBS	4 ℃ overnight 5 min, 2 times 5 min
6. Second antibody	Diluted in blocking solution Washed by High-salt PBS PBS	1 h at RT 5 min, 2 times 5 min
7. Counter stain with DAPI	VECTASHIELD Vibrance Antifade Mounting Medium (H-1800)	1 min
8. Mount	Nail polish	Dry overnight

2.18 Immunohistochemistry

Pancreas paraffin sections were used for immunohistochemical staining (Table 2.8). Antibodies against ENaCα (1:100, anti-rabbit, StressMarq, SPC403), ENaCα (1:100, anti-mouse, StressMarq, SMC242D), insulin (1:200, ab7842, Abcam) were used to incubate sections. Following incubation with HRP-labeled secondary antibodies specific to the species of the primary antibodies, diluted at a ratio of 1:500 (v/v), the samples were further incubated for 1 hour at room temperature. The subsequent detection of HRP signals was accomplished using the DAB Substrate Kit (Abcam, ab64238).

Table 2.8 Protocol of immunohistochemistry for pancreas paraffin section

Step	Reagent	Time
1.Deparaffinization	Xylene - Xylene	5 min for each
2.Rehydration	100% - 90% - 70% ethanol ddH_2O ddH_2O	3 min for each 2 min
3. Quench	3% H_2O_2 in methanol 100 uL each slide PBS	20 min 5 min
4. Retrieve antigen	10 mM 95 ℃ Tris-EDTA buffer, pH = 9.0 PBS	20 min 5 min, 3 times
5. Blocking	1% BSA in PBS	20 min
6. Primary antibody	Diluted in blocking solution Washed by PBS	4 ℃ overnight 5 min, 3 times
7. Second antibody	Diluted in blocking solution Washed by PBS	1 h at RT 5 min, 3 times
8.Develop color	DAB kit (Abcam, ab64238) PBS	10 min 5 min
9. Counter stain with hematoxylin	Harris modified hematoxylin solution ddH_2O Acid alcohol (1% HCl in 75% ethanol) ddH_2O Scott's tap water (20 g/L $MgSO_4 \cdot 7H_2O$ + 2 g/L $NaHCO_3$) ddH_2O	2 min 2 min 1 sec 1 min 1 min 3 min
10. Dehydration	ddH_2O 70% - 80% - 90% - ethanol 100% - 100% ethanol Xylene Xylene	1 min 5 sec for each 3 min for each 3 min 5 min
11.Mounting	Neutral resin (solarbio, G8590)	Dry overnight

2.19 Mass spectrometry

RINm5F cells were subjected to siRNA-mediated knockdown of ENaCα in a 6-well plate for 48 h. Subsequently, the cells were processed for further analysis using the EasyPepTM Mini MS Sample Prep Kit (Thermo Fisher Scientific, A40006) according to the manufacturer's instructions. This involved steps such as lysis, reduction/alkylation, digestion, and clean-up to generate peptides for subsequent mass spectrometry (MS) analysis. The resulting peptides were dried using a vacuum centrifuge at 4 ℃ and reconstituted in 50 µL of 0.1% trifluoroacetic acid (TFA) for MS analysis.

Liquid chromatography-tandem mass spectrometry (LC-MS/MS) (Orbitrap™ IQ-X™ Tribrid™ Mass Spectrometer, FSN05-10001) was performed using an Agilent 1260 LC chromatograph coupled to an Agilent 6460 mass spectrometer equipped with an electron spray ionization interface and a heated nebulizer. Peptides were separated over a 120-min gradient from 2% to 28% buffer B, where buffer B consisted of 0.1% formic acid in 80% acetonitrile and 20% water. The liquid phase gradients were programmed as follows: 2% buffer B for 10 min, 6% buffer B for 12 min, 20% buffer B for 82 min, 30% buffer B for 92 min, 90% buffer B for 100 min, 90% buffer B for 105 min, 2% buffer B for 105 min, and finally 2% buffer B for 120 min.

An inline mass spectrometric analysis was performed using a hybrid quadrupole-Orbitrap instrument (Q Exactive Plus, Thermo Fisher Scientific). The analysis

employed a data-dependent acquisition (DDA) approach, where the most abundant precursor ions from the survey scan were dynamically selected for higher energy collisional dissociation (HCD) fragmentation. In the first full-scan MS analysis, the following parameters were set: scan range of 400-1500 m/z, Orbitrap resolution of 60,000, automatic gain control (AGC) target of 4.0e5, and a maximum injection time of 20 ms. In the second scan mode, HCD-MS/MS was performed using the following parameters: isolation width of 1.6 m/z, HCD fragmentation with a normalized collision energy of 30%, Orbitrap resolution of 7,500, AGC target of 5.0e4, and a maximum injection time of 30 ms. Only precursors with charge states ranging from 2 to 7 were subjected to MS2. Monoisotopic precursor selection and dynamic exclusion (40 s duration, 10 ppm mass tolerance) were enabled.

Analysis of mass spectrum

The raw data obtained from the LC-MS/MS analysis were processed using Proteome Discoverer 2.5 software (ThermoFisher Scientific, USA). The search was conducted against the UniProtKB protein database for Rattus norvegicus, which contained 47942 entries. For data analysis, the following search parameters were used: trypsin was selected as the protease, allowing for a maximum of two missed cleavages. Carbamidomethyl cysteine was specified as a fixed modification, while acetylation of protein N-termini and oxidation of methionine were included as variable modifications. Peptides with a minimum length of 6 amino acids were considered. The mass tolerances for precursor ions and fragment ions were set at 10 ppm and 0.02 Da, respectively. A

global false discovery rate (FDR) threshold of 1% was applied to peptide and protein identification, ensuring a high level of confidence in the results. Proteins identified by at least one unique peptide were selected for further analysis.

To determine protein abundances, the label-free quantitation (LFQ) algorithm was employed to calculate protein abundances to identify differentially expressed proteins between siNC and siENaCα RINm5F cells. The protein abundance was calculated as the sum of the peptide group abundances associated with that particular protein. This approach allows for the relative quantification of proteins based on the intensity of their corresponding peptides. To integrate the results from two repeated experiments, proteins with an abundance ratio p-value less than 0.05 were selected from twice all detected proteins. Subsequently, KEGG (Kyoto Encyclopedia of Genes and Genomes) enrichment analysis was conducted using KOBAS software to map these proteins to the signaling pathway database, thereby identifying the significant changes resulting from ENaCα knockdown in the two experimental sets.

2.20 Glucose tolerance test (GTT)

Mice were deprived of food overnight before an intraperitoneal injection or oral gavage of glucose (IPGTT or OGTT, 2 g kg^{-1} body weight) was made on each mouse. Blood samples (3 μL each) were collected via the tail at specific time points: 0, 10, 30, 60, and 120 minutes after the glucose injection. The levels of glucose in the collected blood were immediately determined using glucose test strips (Bayer HealthCare LLC).

2.21 Blood collection

The animal was securely placed in an appropriate restraint device to expose the entire tail, following which the tail was immobilized using the non-dominant hand while the lateral tail vein was visualized. A needle with the bevel up or a 4 mm lancet tip was used to puncture the vessel at a shallow angle, starting from the distal end of the tail. Blood samples were collected using a pipette or a collection tube until the desired volume was obtained (3 μL for glucometer, 10 μL for insulin/glucagon ELISA). Manual pressure was applied to achieve hemostasis and stop bleeding. To alleviate pain during the recovery period, analgesics were administered to the animals. The blood sample was used for insulin levels measurement by an insulin ELISA kit (32380, ImmunoDiagnostics, Hong Kong).

2.22 Insulin tolerance test

Mice were deprived of food for 4 h before an i.p. intraperitoneal human normal insulin (0.75 IU/ kg body weight) was made on each mouse. Blood was collected via the tail 0, 15, 30, 60 and 90 min after the insulin injection. Plasma glucose was determined by glucose test strip (Bayer HealthCare LLC).

2.23 Islet number quantification

Age-matched Cre-Ctrl and cKO mice were sacrificed on the same day. Standardized surgical procedures and islet isolation protocols, employing identical solutions, were employed for both groups of mice. Whole pancreas tissues were collected from each

mouse in the respective groups. The isolated islets were meticulously hand-picked using a pipette under an inverted microscope (P-DSL32, Nikon) in a blinded manner to minimize observer bias. Subsequently, the quantification of islet numbers was performed.

2.24 Statistics

The data are presented as mean ± standard error of the mean (s.e.m). To compare two groups, a two-tailed unpaired Student's t-test was employed. For comparisons involving two independent categorical variables, a two-way analysis of variance (ANOVA) was used. Statistical significance was defined as p-values below 0.05. All graphs were generated, and statistical analyses were performed using GraphPad Prism 10.

Chapter 3: ENaC functional expression in β-cell in negative correlation with insulin secretion

3.1 Introduction

Insulin is exclusively secreted from pancreatic islet β-cells and plays a crucial role in maintaining the homeostasis of glucose metabolism in the body [31]. Insulin secretion in response to glucose elevation is a complex process, which involves a series of sequential cellular events in β-cells including activation or inactivation of different ion channels resulting in action potentials [113], Ca^{2+} influxes, and insulin-containing vesicle exocytosis. Na^{+} channels, a key player in generating action potentials in neurons [209], are less studied in β-cells, and their involvement in insulin secretion remains obscure [108]. Previously, our research team demonstrated that CFTR (cystic fibrosis transmembrane conductance regulator), a Cl^{-} channel predominantly expressed in epithelial cells, is expressed in β-cells to critically regulate the excitability and insulin secretion function [210]. In epithelial cells, CFTR is known to interact with the epithelial sodium channel (ENaC) [192], which is a voltage-independent Na^{+} channel encoded by SCNN1A, B and G genes in humans and primarily responsible for Na^{+} absorption across the epithelium [156]. Although a previous study showed ENaC expression in β-cells, whether and how exactly ENaC regulates insulin secretion remains largely unclear.

The studies described in this chapter were carried out to determine 1) the expression of

ENaC in pancreatic islet β-cells, and 2) whether ENaC function in β-cells is required for insulin secretion. Human databases were analyzed. Mouse pancreatic tissues, isolated mouse pancreatic islets and islet cells, as well as RINm5F cells, a rat β-cell line, were used, where the mRNA, protein expression as well as Na^+-transporting activities of ENaC were examined in combination with pharmaceutical drugs that inhibit ENaC, siRNA based knockdown assays as well as overexpression of ENaC. Key cellular events leading to insulin secretion including membrane depolarization, Ca^{2+} dynamics as well as insulin secretion levels were examined.

3.2 Results

3.2.1 ENaC is expressed in the human pancreas

In an available human database https://www.proteinatlas.org/, single-cell RNA sequencing revealed SCNN1A mRNA expression in human pancreatic endocrine cells, although the expression level was relatively low compared to that in exocrine cells in the pancreas (Figure 3.1 A). Additionally, an analysis was conducted on a previously published dataset (GSE20966) from pancreatic β-cell whole gene expression (mRNA level by GeneChip Human X3P Array) profiles obtained from cadaver pancreases using the laser capture microdissection technique. The dataset included samples from 10 control (non-diabetic) subjects and 10 individuals diagnosed with Type-2 diabetes (T2D). The results revealed a significant upregulation of ENaCα expression in both female and male subjects with Type-2 diabetes compared to the control group, though

no significant differences were observed in the expression levels of ENaCβ and ENaCγ between the control and diabetic subjects (Figure 3.1 B). These findings provide insights into the expression of ENaC in the human pancreas and suggest a potential involvement of ENaC in β-cell pathology and diabetes in humans.

3.2.2 ENaC is expressed in rodent pancreatic islet cells

Immunofluorescence staining for ENaCα in mouse pancreatic tissues showed ENaCα expression in islets, in both insulin-expressing and non-expressing islet cells, with a more notable emphasis on islet insulin-positive cells (β-cells) (Figure 3.2 A). In a commonly used rat pancreatic β-cell line, RINm5F, mRNA levels of ENaCα, β, and γ subunits were detected, the sequences of which were confirmed to align with rat *Scnn1a*, *Scnn1b* and *Scnn1g* genes respectively. As a positive control, rat kidney tissue was used to validate the expression of these subunits. (Figure 3.2 B). Western blotting with an antibody against rat ENaCα showed a band of about 85 kDa in RINm5F cells and rat kidney tissues, suggesting protein expression of ENaCα in β-cells, though both mRNA and protein expression level in RINm5F cells was relatively low compared to that in rat kidney tissues (Figure 3.2 C).

3.2.3 ENaC mediates glucose-independent Na^+ entry in pancreatic β-cells

ENaC, as a sodium channel, plays a major role in mediating Na^+ influx into the cells.

We also measured intracellular Na^+ levels ($[Na^+]_i$) using a Na^+-sensitive fluorescent dye, the sodium-binding benzofuran isophthalate (SBFI). Real-time $[Na^+]_i$ measurement revealed that in both RINm5F (Figure 3.3 A) and primary mouse islet cells (Figure 3.3 B), the addition of amiloride (1 to 10 μM), a selective blocker of ENaC, immediately lowered $[Na^+]_i$ by about 20-30%, in either the presence or absence of glucose in the bath (Margo-Ringer solution). These findings suggest that there is a continuous influx of sodium ions via ENaC into β-cells, independent of the glucose concentration in the extracellular environment.

3.2.4 ENaC deficiency induces membrane depolarization in pancreatic β-cells

We further studied whether the detected ENaC expression and activity would be significant to β-cell functions. Considering the importance of electrical activity and Ca^{2+} mobilization in the insulin secretion process, we first conducted patch-clamp to monitor membrane potential changes in β-cells. In the presence of glucose (10 mM) in the bath, the cells exhibited an averaged membrane potential of -40.9 ± 5.2 mV, and a few electrical spikes, suggesting a relatively subdued electrical activity. Unexpectedly, upon the addition of amiloride (10 μM) or benzamil (1 μM, another selective blocker of ENaC) in the bath, a gradual membrane depolarization was observed within a time frame of 5 to 10 min followed by robust electrical pulses in RINm5F cells or isolated mouse islet β-cells (Figure 3.4 A-B) indicating a significant increase in electrical activity.

3.2.5 ENaC deficiency enhances Ca^{2+} oscillation in pancreatic β-cells

The same condition was used for Ca^{2+} imaging by Fura-2 in RINm5F cells, which consistently showed that amiloride (1-10 μM) evoked Ca^{2+} spikes (Fig 3.5 A-B). To facilitate the analysis of Ca^{2+} response, we classified the observed oscillations into three patterns: blank, small, and large Ca^{2+} spikes (see methods). Subsequent analysis involved calculating the frequency of Ca^{2+} spikes before and after the treatment of amiloride or DMSO as the vehicle control revealed that blocking ENaC by amiloride significantly facilitated Ca^{2+} spikes in the cells (Figure 3.5 C). Moreover, similar Ca^{2+} responses to amiloride were detected in isolated islets from C57BL/6 wild-type mouse pancreas. In the presence of glucose, the islet has dramatic and synergistic Ca^{2+} oscillations with small spikes. Amiloride (1 or 10 μM) accelerated the whole period of Ca^{2+} dynamics and the instantaneous oscillations sustained the peak Ca^{2+} response and facilitated Ca^{2+} oscillation frequency obviously, along with large spikes as compared to non-treated cells (Figure 3.6 A-B). These results consistently revealed the unexpected role of inhibiting ENaC in triggering membrane depolarization and Ca^{2+} mobilization in β-cells.

3.2.6 ENaC deficiency promotes insulin secretion in pancreatic β-cells

We next investigated the role of ENaC in glucose-induced insulin secretion in β-cells. In line with the above results, treatment with amiloride (1-10 μM) for 30 min indeed promoted insulin secretion from RINm5F cells in either the absence or presence of glucose (Figure 3.7 A). To confirm this, RINm5F cells were treated with siRNA against

ENaCα (siENaCα), the rate-limiting subunit of ENaC, which achieved about 80% knockdown of ENaCα mRNA and protein expression (Figure 3.7 B-C). The insulin amount secreted from the cells in 1 h, both in the presence and absence of glucose, exhibited a significant increase of 130.2 ± 20.1%-fold in the siENaCα-treated cells compared to that in cells treated with non-silencing control siRNAs (siNC) (Figure 3.7 D).

3.2.7 ENaC overexpression attenuates insulin secretion in pancreatic β-cells

Overexpression of plasmids containing human ENaCα gene (phENaCα) was also performed in RINm5F cells, which caused a small but statistically significant reduction in insulin secretion compared to control cells (pNC) after 1 h glucose challenge. However, no significant difference was observed in insulin secretion at 10, 30, and 45 minutes of glucose challenge (Figure 3.8 A-C). Collectively, these results provide compelling evidence suggesting ENaC to be inversely correlated with insulin secretion in β-cells.

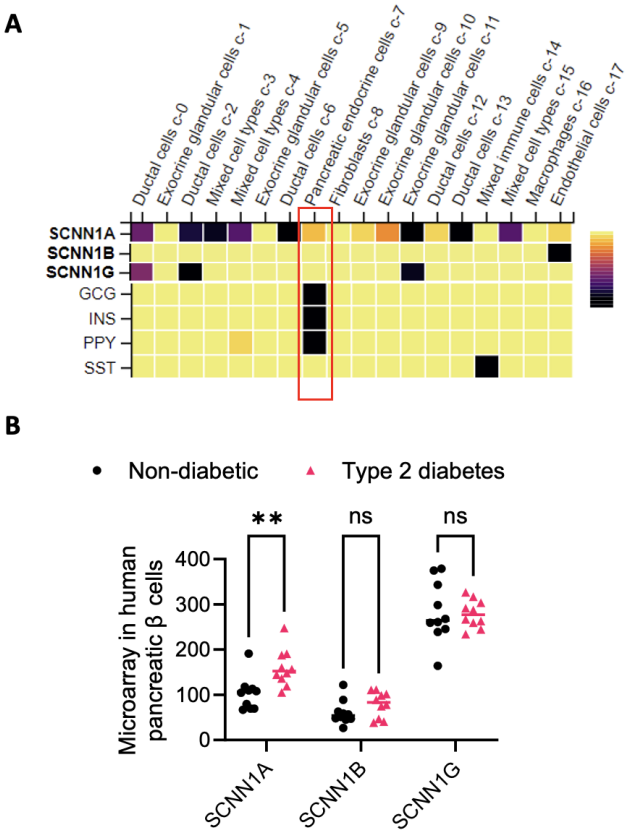

Figure 3.1 Expression of ENaC in human pancreas. (A) RNA expression analysis of pancreatic single cell type clusters using the single-cell RNA sequencing (scRNA-seq) database (https://www.proteinatlas.org/). The ENaCα subunit gene (SCNN1A) expression in the pancreas is visualized by a bar chart. (B) Comparative analysis of ENaC gene (*SCNN1A, SCNN1B*, *SCNN1G*) mRNA expression in the pancreas tissues collected from human non-diabetic (ND) and Type-2 diabetic (T2D) cadaver pancreas subjects. The microarray data were retrieved from a human database (Accession number: GSE20966). $n = 20$. ns $P > 0.05$, ** $p < 0.01$. Unpaired *t*-tests. Data are mean ± s.e.m.

A

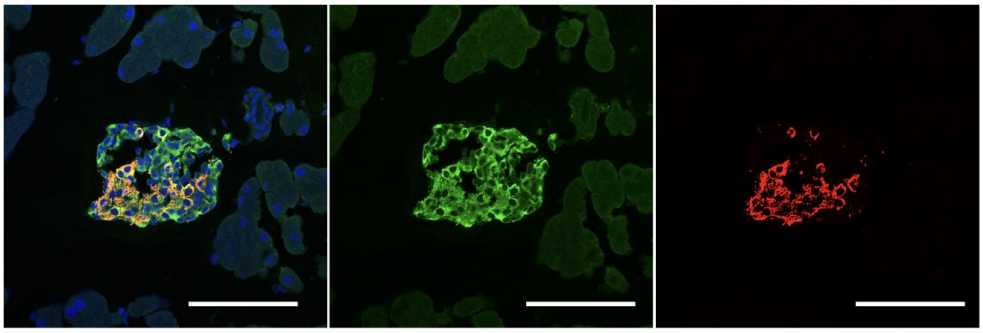

B

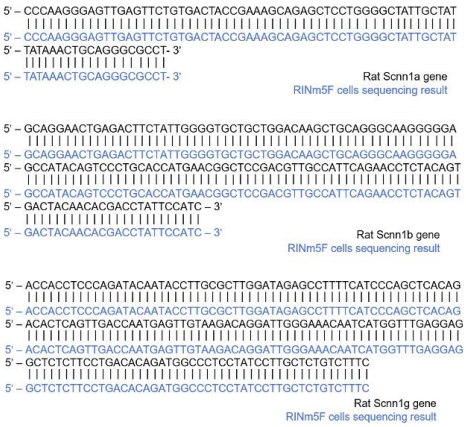

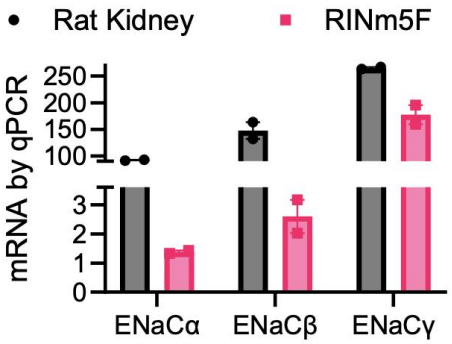

Cell	ENaCα	ENaCβ	ENaCγ	GAPDH
RINm5F	29.40	28.15	22.20	15.87
Rat kidney	23.29	22.79	21.77	15.85

C

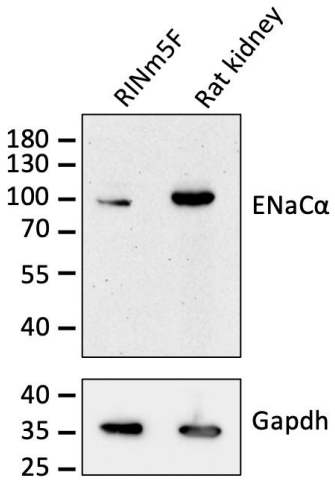

Figure 3.2 Expression of ENaC in rodent pancreas. (A) Confocal images for Immunofluorescence of ENaCα (green) and insulin (purple) in mouse pancreatic tissues. Scale bars, 100 μm. (B) mRNA expression by qPCR of ENaC α, β and γ in a rat β-cell line, RINm5F, the sequence of which was validated by DNA sequencing to match rat Scnn1a, Scnn1b, Scnn1g genes. The rat kidney serves as the positive control. Cycle of threshold (Ct) value are listed in the table. (C) Protein expression by western blot for ENaCα in RINm5F cells and rat kidney, Gapdh was used as loading control.

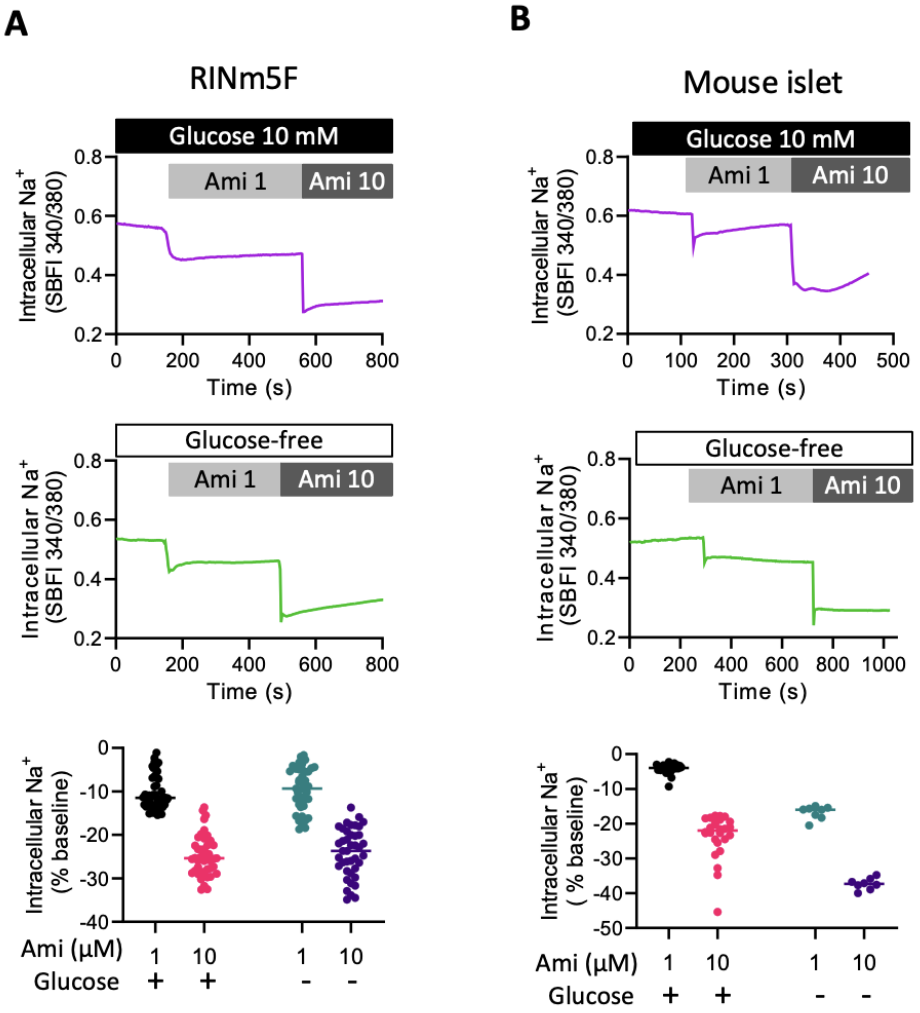

Figure 3.3 Channel function of ENaC in β-cells. Representative time-course tracing and corresponding quantification of intracellular Na^+ change by Na^+ sensitive dye SBFI in RINm5F cell (A) or isolated mouse islets (B) treated with a selective inhibitor of ENaC, amiloride (Ami, 1 or 10 μM) in the presence or absence of glucose. The experiment was repeated three times. Each dot means a cell.

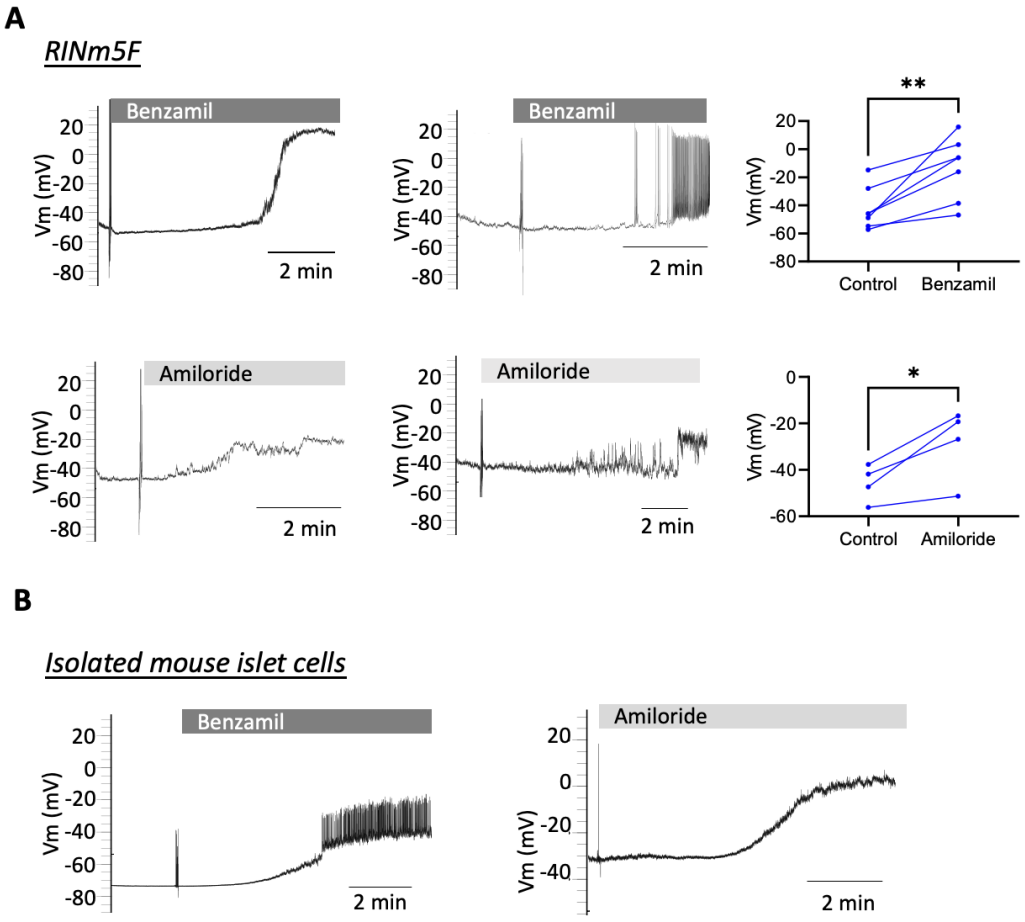

Figure 3.4 Effect of ENaC inhibition on membrane potential in β-cells. Current-clamp whole-cell recording of membrane potential changes by patch-clamp in RINm5F cells (A) or isolated mouse islet cells in response to another ENaC inhibitor benzamil (1 μM) or Ami (10 μM). n = 4-6. * $p < 0.05$, ** $p < 0.01$. Paired t-test. Data are mean ± s.e.m.

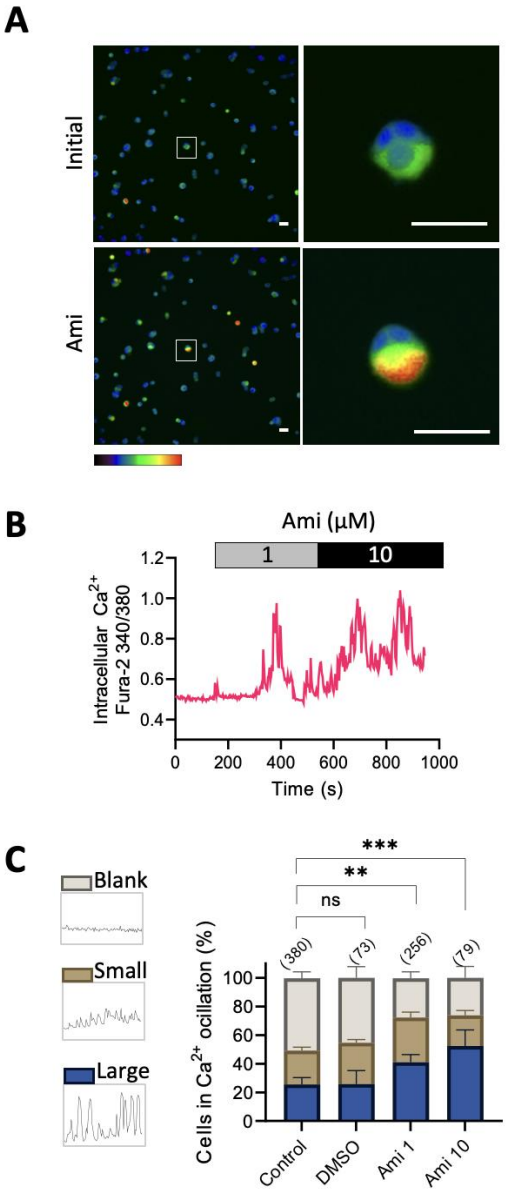

Figure 3.5 Effect of ENaC inhibition on Ca^{2+} oscillations in RINm5F cells. Representative fluorescence images (A) and time-course traces (B) of intracellular Ca^{2+} measurement using Fura-2 in RINm5F cells in response to Ami (1-10 μM). DMSO treatment was used as the negative control. Pseudo-colors from purple to red indicate Fura-2 intensity from low to high. Scale bars, 100 μm. (C) Calculation of Ca^{2+} responses

in A-B based on three types of Ca^{2+} oscillations defined by the change ratio of Ca^{2+} spikes using Fura2 340/380 fluorescence: blank/no response (≤ 0.05), a small slow rise (≥ 0.05 & ≤ 0.15), and at least one spike (≥ 0.15). The experiment was repeated over 3 times. ** $p < 0.01$, *** $p < 0.001$. Pearson's chi-square test.

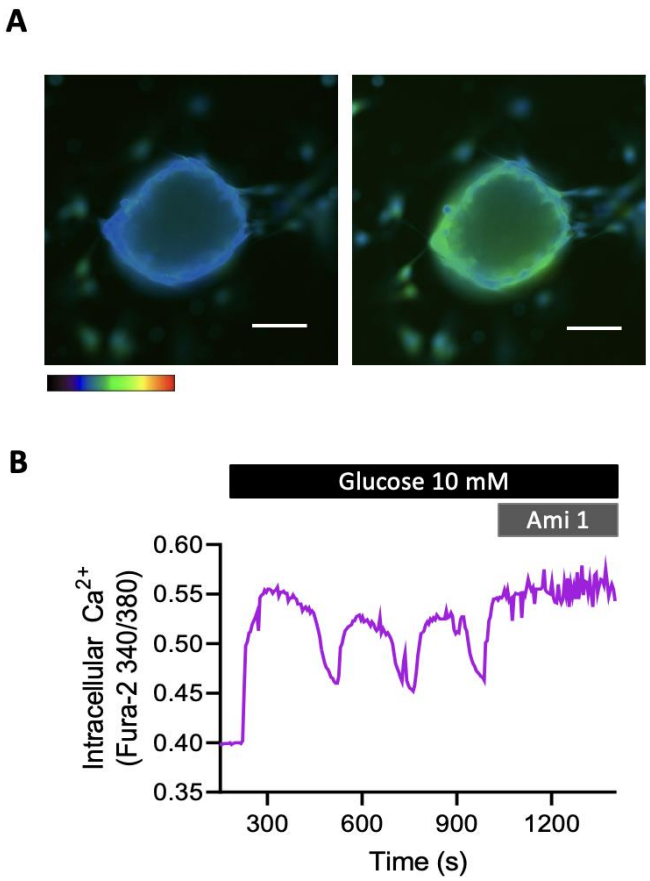

Figure 3.6 Effect of ENaC inhibition on Ca^{2+} oscillations in isolated mouse islets. Representative fluorescence images (A) and time-course traces (B) of intracellular Ca^{2+} measurement using Fura-2 in isolated mouse islets in response to Ami (1-10 μM). The experiment was repeated three times. Scale bars are 100 μm.

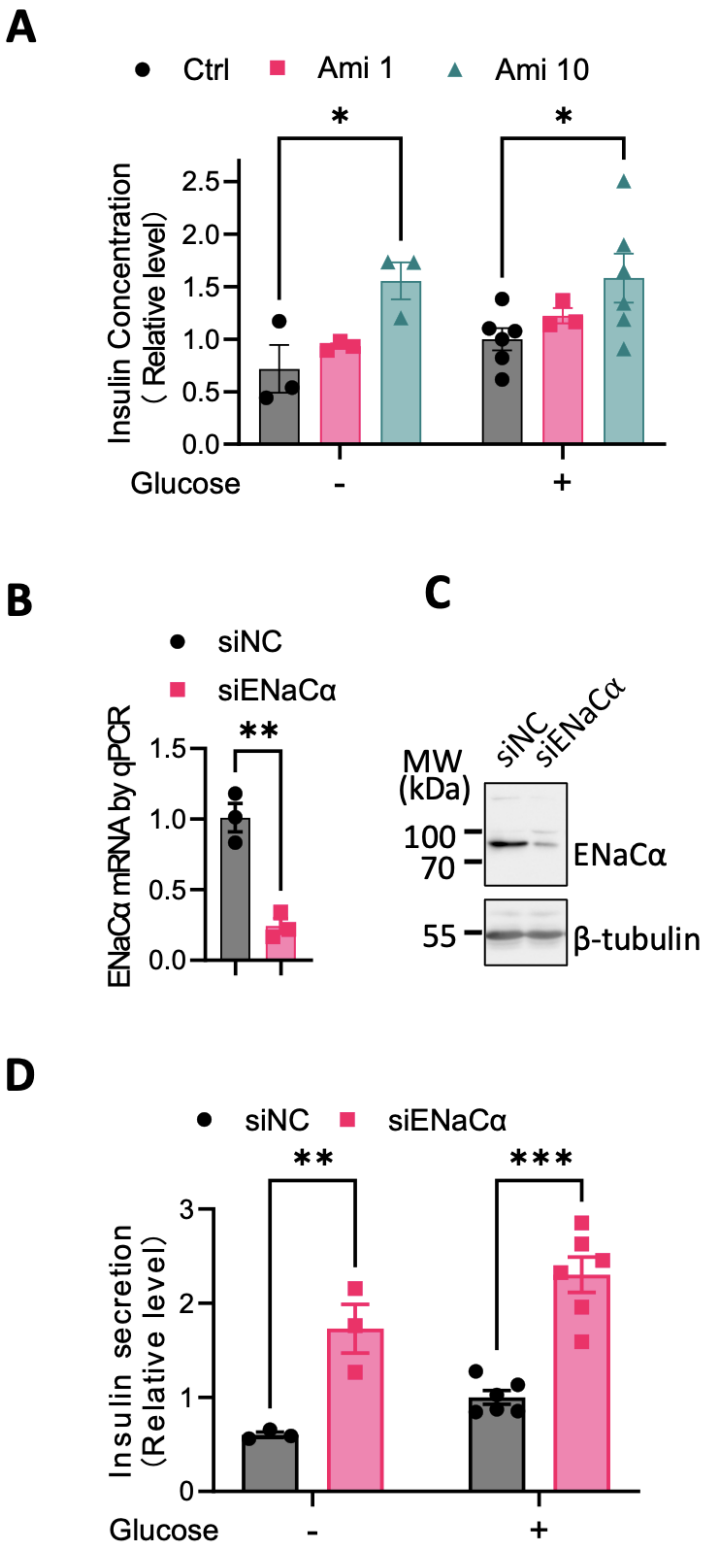
A
Ctrl
Ami 1
Ami 10
*
*
Insulin Concentration
(Relative level)
2.5
2.0
1.5
1.0
0.5
0.0
Glucose
-
+
B
siNC
siENaCα
**
ENaCα mRNA by qPCR
1.5
1.0
0.5
0.0
C
siNC
siENaCα
MW
(kDa)
100
70
ENaCα
55
β-tubulin
D
siNC
siENaCα
**
***
Insulin secretion
(Relative level)
3
2
1
0
Glucose
-
+

Figure 3.7 Effect of ENaC knockdown on insulin secretion. (A) ELISA measurement of inusulin secretion from RINm5F cells treated with Ami (1-10 μM) for 30 min before and after glucose (10 mM) challenge, DMSO was used as the control. The relative insulin levels were normalized by whole-cell protein concentration. n = 3-6 biologically independent samples per group. * $p < 0.05$. One-way analysis of variance. (B-C) qPCR (B) and western blot (C) for ENaCα expression in RINm5F cells treated with siRNAs against ENaCα (siENaCα) or negative control siRNAs (siNC) for 48 h and 72 h respectively. n = 3 biologically independent samples per group. ** $p < 0.01$ by unpaired t-test. (D) ELISA measurement of insulin secretion within 1 h in response to glucose from RINm5F cells after transfected with siNC/siENaCα for 72h. n = 3-6 biologically independent samples per group. ** $p < 0.01$, *** $p < 0.001$. One-way analysis of variance.

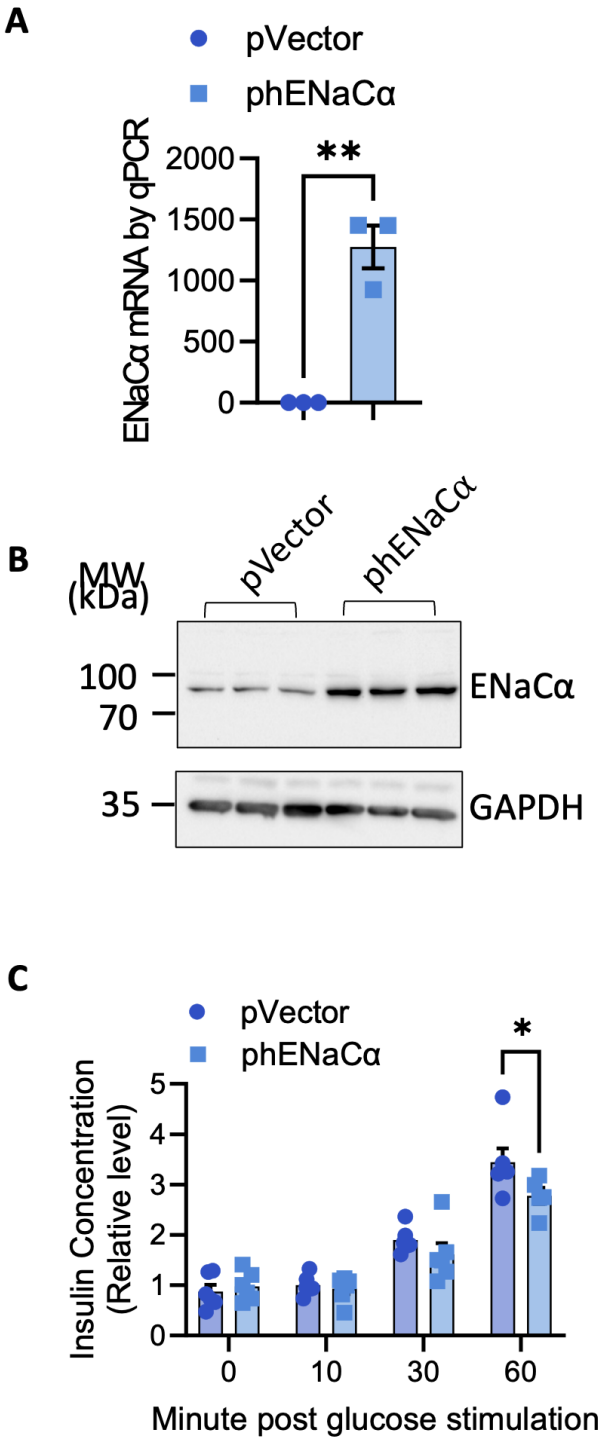

Figure 3.8 Effect of ENaC overexpression on insulin secretion. (A-B) qPCR (A) and western blot (B) for ENaCα expression in RINm5F cells treated with human ENaCα plasmid (ph ENaCα) or negative control (pNC) for 48 h and 72 h respectively. *n* = 3

biologically independent samples per group. ** $p < 0.01$ by unpaired *t*-tests. (C) ELISA measurement of insulin secretion within 1 h in response to glucose (10 mM) from RINm5F cells after transfected with phENaCα or pNC for 72 h. n = 3-6 biologically independent samples per group. The experiment was repeated twice. * $p < 0.05$. One-way analysis of variance.

3.3 Discussion

Taken together, results obtained above have confirmed ENaC functional expression in pancreatic islet β-cells, which is also revealed to be inversely correlated with insulin secretion. It therefore suggests ENaC to play a role in suppressing insulin secretion in the β-cells.

Several lines of evidence collected presently support the **direct expression and channel activity of ENaC in β-cells**. First, mRNA expression of all three subunits of ENaC was detected in RINm5F cells with the sequences confirmed. Second, protein expression of ENaCα was detected in RINm5F cells as well as in insulin-expressing islet cells in mouse pancreatic tissue sections. Moreover, human databases especially a single-cell RNAseq study showed mRNA expression of SCNN1A in human pancreatic endocrine cells. It should be noted that protein expression of ENaCβ and ENaCγ was not detectable in RINm5F cells by western blot, nor the mRNA of ENaCβ and ENaCγ found in human pancreatic endocrine cells by RNAseq. These negative results, although possibly due to detection/technical limitations, might also suggest very low expression of ENaCβ and ENaCγ in β-cells. However, importantly, amiloride-sensitive Na^+ influxes were observed in RINm5F cells and isolated mouse islets, indicating ENaC channel activities in β-cells. Since ENaCα is the most important subunit for ENaC and know to conduct Na^+ by itself [211], the detected ENaC activities in β-cells is likely to be mainly attributed by ENaCα. In addition, it is interesting to note that in immunostaining experiments, ENaCα was also found in non-insulin expressing islet

cells. In Na^+ measurements in isolated mouse islets (containing both β-cells and non-β islet cells), the amiloride-sensitive Na^+ change was found to be greater in absence of glucose than that in the presence of glucose. Since α cells are more active at a low glucose condition, it is possible that ENaC may play a role in α cells, which should be further investigated in future.

Unexpectedly, ENaC, a Na^+ channel, was found to **suppress but not promote the excitability of β-cells for insulin secretion**. Supporting data include that 1) amiloride or benzamil evoked membrane depolarization and/or Ca^{2+} increases in RINm5F cells, isolated mouse islets or islet cells; 2) insulin secretion from RINm5F cells was promoted by amiloride or ENaCα knockdown, while inhibited by overexpression of ENaCα. Previously, TTX-sensitive voltage-dependent Na^+ channels such as Nav1.7 (Scn9a) and Nav1.3 (Scn3a) were demonstrated to play a positive regulatory role in insulin secretion in β-cells by facilitating the upstroke of the action potential [134]. However, in an early study on mouse β-cells [212], it was found that the TTX-sensitive Na^+ channels were inactivated at quite negative membrane potentials starting from -80 mV, suggesting a limited role of these Na^+ channels in generating action potentials for insulin secretion. Therefore, it appears that Na^+ or Na^+ channels in β-cells, different from those in neurons, may have distinctive physiological roles. Further investigations are needed to understand how exactly Na^+ channels regulate insulin secretion; whether malfunction of Na^+ channels is related to β-cell dysfunction. It is worth to note the upregulation of SCNN1A in type 2 diabetes patients as revealed by the microarray

database, which might suggest a possible involvement of ENaC alteration in relation with β-cell dysfunction. Thus, the discovery of ENaC activities in β-cells might be of physiological significance.

There are a couple of interesting features of ENaC observed in β-cells. First, ENaC's role in β-cells seems to be **independent of environmental glucose**. Amiloride elicited intracellular Na^+ decreases in RINm5F cells to a similar extent with or without glucose in the bath. Consistently, amiloride or ENaC knockdown promoted insulin secretion in either presence or absence of glucose. Despite documented ENaC gating regulatory factors [213-216], ENaC is believed to be constantly open, contributing to the basal currents across epithelial tissues [217]. The presently observed insensitivity to glucose of ENaC in β-cells might suggest that ENaC is constantly open in β-cells too, providing continuous Na^+ influx to regulate the basal level of insulin secretion, which could be important to either condition with or without glucose.

The second feature is that β-cells did not respond to ENaC inhibition immediately. Amiloride/benzamil elicited a slow and gradually increased membrane depolarization. Ca^{2+} responses were also gradually increased in response to amiloride. 30 min incubation with amiloride elevated the insulin level, which was not seen at 10-15min (data not show). It is thus **a delayed response**. It is possible that the inhibition of ENaC blocking Na^+ entry may induce a membrane hyperpolarization first, which may be counteracted by certain mechanisms and eventually overridden to transit into

depolarization. Of note, glucose-induced insulin secretion (GSIS) is considered to be biphasic, consisting of an acute first phase with a spike of about 10 minutes, followed by the second phase, a sustained plateau lasting for 2-3 hours [218]. The delayed response to ENaC inhibition may suggest ENaC to be important to the secondary phase of GSIS. The molecular mechanisms responsible for the biphasic response of β-cells in insulin secretion remain unresolved. A proposed possible mechanism is that factors like GLP-1 and cAMP-releasing agents enhance the release of insulin granules at the second phase [219]. Whether ENaC interacts with these signaling pathways to regulate the second phase awaits further investigation.

In summary, the results of this Chapter have revealed a role of ENaC in β-cells in suppressing insulin secretion. However, questions remain. How does ENaC exert such a suppressing role? What are the underlying molecular mechanisms? Is such a suppressing effect really of physiological significance? Would insulin and glucose homeostasis be altered in vivo when ENaC malfunction occurs? The following Chapters will experimentally address these questions.

Chapter 4: Mechanisms underlying ENaC-mediated suppression of insulin secretion

4.1 Introduction

The previous Chapter demonstrated a role of ENaC in pancreatic islet β-cells to suppress insulin secretion. However, the underlying mechanisms remained unknown. As introduced in Chapter 1, insulin secretion is a multifactorial event. Glucose stimulated insulin secretion in β-cells involves sequentially glucose uptake, ATP elevation, closure of ATP-sensitive K^+ channels (K_{ATP}), membrane depolarization, opening of voltage-gated Ca^{2+} channels (VGCCs) and thus Ca^{2+} influx to trigger the exocytosis of insulin granules [114]. Recently, insulin secretion is also revealed to be amplified by cAMP-mediated pathways, resulting from the activation of adenylyl cyclase (AC)-activating G-protein-coupled receptors in β-cells by paracrine/endocrine factors such as islet α cell-secreted glucagon and gastrointestinal-derived glucagon-like peptide-1 and glucose-dependent insulinotropic polypeptide [220, 221].

In this Chapter, we explored possible actions of ENaC on the key steps of insulin secretion. We measured intracellular ATP level in RINm5F cells with or without ENaC inhibitor/knockdown. In monitoring intracellular Ca^{2+} dynamics in RINm5F cells, we tested possible interplay between ENaC and K_{ATP}, VGCC and other Ca^{2+} channels. Given the known interaction between ENaC and CFTR, we also tested if CFTR mediates the action of ENaC in suppressing insulin secretion. We also did unbiased

analysis through proteomic analysis of RINm5F cells with or without ENaCα knockdown by mass-spectrometry. Given the mass-spectrometry results indicating alteration of cAMP pathway by ENaC knockdown, particular effort was made to understand whether and how ENaC regulates cAMP. Intracellular cAMP level in RINm5F cells was examined by ELISA as well as in a real-time manner by imaging with a fluorescent cAMP indicator. The involvement of ACs was examined. Strategies such as pharmaceutical inhibition of ACs, knockdown of ACs as well as blockage of cAMP degradation were used. In understanding if Na^+ itself modulates cAMP production, we combined the measurement of intracellular cAMP level with patch-clamp, where intracellular Na^+ concentration of the patched cells was artificially manipulated and its effect on cAMP was investigated.

4.2 Results

4.2.1 ENaC influences multiple factors related to insulin secretion in β-cells

To understand why this Na^+ channel could be inversely correlated with insulin secretion in β-cells, we examined several factors that could be involved. ENaC knockdown or inhibition by amiloride (10 μM, 30 min) did not alter the whole-cell amount of insulin in RINm5F cells (Figure 4.1 A). These results exclude the possibility of ENaC affecting insulin production/synthesis and suggest ENaC only participates in insulin secretion process. The ATP levels in the cells were not affected by ENaC inhibitors but a little bit increased with ENaC knockdown (Figure 4.1 B-C). To investigate the role of K_{ATP}

channels, the promotion of Ca^{2+} oscillations induced by ENaC inhibition with amiloride was further enhanced in the presence of the K_{ATP} inhibitor glibenclamide (GLIB). However, when GLIB was administered before amiloride treatment, there was no significant difference in the enhanced Ca^{2+} oscillation, suggesting that the involvement of K_{ATP} and ENaC in insulin secretion occurs through independent pathways (Fig 4.2 A-C). Apart from that, the amiloride-evoked Ca^{2+} spikes were abolished by Ca^{2+} removal from the bath solution or pretreatment of the cells with Ca^{2+} channel blockers, nifedipine (20 μM), ruthenium red (100 μM) (Figure 4.2 D-G). Amiloride's effect in potentiating insulin secretion was partially reversed by pretreatment with a CFTR inhibitor, Inh172 (10 μM), and abolished by nifedipine (20 μM), ruthenium red (100 μM) (Figure 4.2 H). Due to a depolarization but not hyperpolarization occurring under ENaC inhibition, we propose that HCN (hyperpolarization-activated cyclic nucleotide–gated) channels may be involved in the mechanism. Under the effect of HCN inhibitor zatebradine (10 μM) for 30 min, ENaC knockdown-promoted insulin secretion was attenuated in the presence of glucose. These results indicate that ENaC influences multiple factors in the progression of insulin secretion.

4.2.2 ENaC knockdown alters signaling network in β-cells

To gain further insight into the signaling pathways involved in ENaC-regulated insulin secretion, proteomic analysis was performed using mass spectrometry (MS) on RINm5F cells treated with ENaCα knockdown. Two separate mass spectrometry experiments were conducted with the detection of a total of 3165 and 2734 effective

proteins, respectively. KEGG enrichment analysis of the protein profile showed that SNARE interactions and vesicular transport pathways, which are essentially involved in insulin granule exocytosis, were significantly upregulated in cells with ENaCα knockdown in comparison to those of the control cells (Figure 4.3 A). Of note, the expression levels of Ins1 and Pdx1, genes involved in insulin production, decreased rather than increased in response to ENaC knockdown. These data therefore indicated that multiple factors known to be critically involved in insulin secretion process in β-cells (e.g., Ca^{2+} channels, CFTR, SNARE proteins, granule exocytosis) were influenced by ENaC, suggesting ENaC's action site possibly at a step upstream to these factors.

Interestingly, the proteomic analysis also showed that proteins related to cAMP-mediated pathways were significantly upregulated in cells with ENaCα knockdown (Figure 4.3 B). Notably, the proteins Prkr1b and Prkr1a displayed the highest upregulation consistently across the two mass spectrometry experiments, with fold changes exceeding 2-fold. Other cAMP-related factors such as Adcy9, Arpp19, and Prkacb also demonstrated significant upregulation in response to ENaC knockdown in β-cells. These findings suggest a potential involvement of cAMP signaling pathways in ENaC-regulated insulin secretion. We therefore went on to test the possible effect of ENaC on cAMP in β-cells.

4.2.3 ENaC deficiency increases intracellular cAMP levels in β-cells

To obtain a comprehensive understanding of cAMP signaling pathways involved in

ENaC-regulated insulin secretion, we first performed ELISA measurement of cAMP, which showed that RINm5F cells treated with amiloride (10 μM, 30 min) or siENaCα for 48 h, had significantly higher levels of intracellular cAMP in comparison with their control cells respectively (Figure 4.4 A). In addition, we used a cAMP sensor, G-Flamp1 [222], to monitor intracellular cAMP changes in real-time in response to ENaC inhibition by amiloride in RINm5F cells. Within 10 min after the addition of amiloride or benzamil (1 μM) onto the cells, a slow and gradual increase in G-Flamp1 intensity in the cells was observed (Figure 4.4 B-C), indicating cAMP elevation. The average increase in G-Flamp1 intensity at 10 min post amiloride was 18.1 ± 1.5 %, significantly higher than the controls by DMSO treatment (3.0 ± 0.8 %). cAMP synthesis enzyme adenylyl cyclases activator forskolin (FSK, 1 μM) or inhibitor DDA (2',5'-dideoxyadenosine, 10 μM) were added after ENaC inhibitors treatment to serve as positive and negative controls.

4.2.4 ENaC-mediated Na^+ entry inhibits cAMP activity in β-cells

We then asked how blocking the Na^+ channel could result in cAMP elevation and whether the Na^+ ions entered through ENaC play a role in regulating cAMP. We next performed G-Flamp1-based cAMP imaging combined with simultaneous patch-clamp recording. Using patch-clamp, we manipulated pipette/intracellular Na^+ concentrations ($[Na^+]_i$) (see methods) (Figure 4.5 A). Results interestingly showed that when $[Na^+]_i$ was controlled at 10 mM, the patched cells responded to forskolin (a potent activator of adenylyl cyclase, 1-10 μM) in increasing G-Flamp1 intensity/cAMP level with the

responding time and amplitude almost identical to the non-patched cells. However, when $[Na^+]_i$ was increased to 20 mM, the patched cells were almost irresponsive to forskolin (1-10 μM) in G-Flamp1 imaging, which was substantially impaired compared to the non-patched cells. At the same time, patch-clamp recording of membrane potential changes consistently indicated that the cells responded to forskolin with $[Na^+]_i$ at 10 mM, but not at 20 mM (Figure 4.5 B-C). In addition, to test whether the inhibition of cAMP by Na^+ entry is mediated by ENaC, we conducted overexpression of ENaCα or ENaCα/β/γ in RINm5F cells, followed by transfection with G-Flamp1. Results showed that overexpression of ENaC significantly abolished the cAMP response to DDA in RINm5F cells when compared to the vehicle group. It therefore revealed an inhibitory effect of increased $[Na^+]_i$ on adenylyl cyclase-dependent cAMP synthesis.

4.2.5 ENaC modulates insulin secretion through adenylyl cyclase and cAMP

We then investigated whether adenylyl cyclase-dependent cAMP synthesis indeed mediates ENaC's role in β-cells. In the presence of DDA (10 μM), a selective blocker of membrane adenylyl cyclases (mACs), the inhibition of ENaC (by benzamil/amiloride) no longer increases intracellular cAMP (Figure 4.6 A) or promotes Ca^{2+} spikes (Figure 4.6 B) or induced depolarization (Figure 4.6 C). Instead, in patch-clamp recording of membrane potentials, a hyperpolarization (-27.0 ± 9.2 mV) was shown after the addition of benzamil (1 μM), DDA (10 μM) also abolished ENaC knockdown-enhanced insulin secretion. While IBMX (100 μM), an inhibitor of phosphodiesterase (PDE) that maintains cAMP level from degradation, potentiated the

effect of ENaC knockdown in enhancing insulin secretion (Figure 4.7 A). We examined the mRNA expression of mAC genes ADCY-1 to -9 as well as the soluble adenylyl cyclase, ADCY-10, and found high expression of ADCY-6 and -8 in RINm5F cells (Figure 4.7 B). siRNAs against ADCY6 or ADCY8 were applied to knockdown these two genes (Figure 4.7 C). With either ADCY6 or ADCY8 knocked down, ENaC-modulated insulin secretion was absent (Figure 4.7 D). Together, these results demonstrated that ENaC suppresses mACs and cAMP to modulate insulin secretion.

4.2.6 The correlation of SCNN1A and ADCY in human pancreas

To investigate the potential role of ADCY and its correlation with ENaC in humans, a previously published dataset from pancreatic β-cell whole gene expression (GSE20966) was reanalyzed (Figure 4.8 A-B). In individuals with Type-2 diabetes, there was a significant upregulation of ADCY6 expression compared to control subjects. Additionally, a significant positive correlation was observed between ENaCα and ADCY6 expression levels. However, ADCY8 did not show altered expression between the two groups and did not exhibit any correlation with ENaCα. These findings suggest a potential correlation between ENaC and ADCY6 in human diabetes.

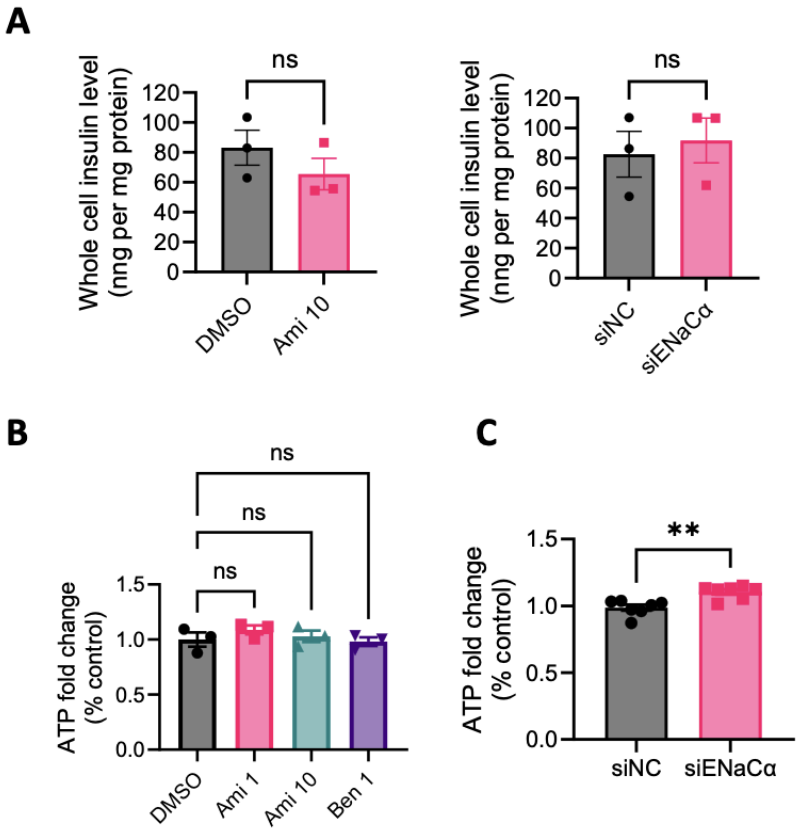

Figure 4.1 Effect of ENaC deficiency mediated insulin production and ATP levels in β-cells. (A) ELISA measurement of whole-cell insulin level extracted by RIPA from RINm5F cells. Cells were treated with DMSO/10 μM amiloride for 1 h or transfected with siNC/siENaCα for 72 h before measurement. n = 3 biologically independent samples per group. (B-C) Relative ATP production in RINm5F cells in treatment with ENaC inhibitors (B), or ENaC knockdown (C). n = 3-7 biologically independent samples per group. ns $p > 0.05$ by unpaired t-test. Data are mean ± s.e.m.

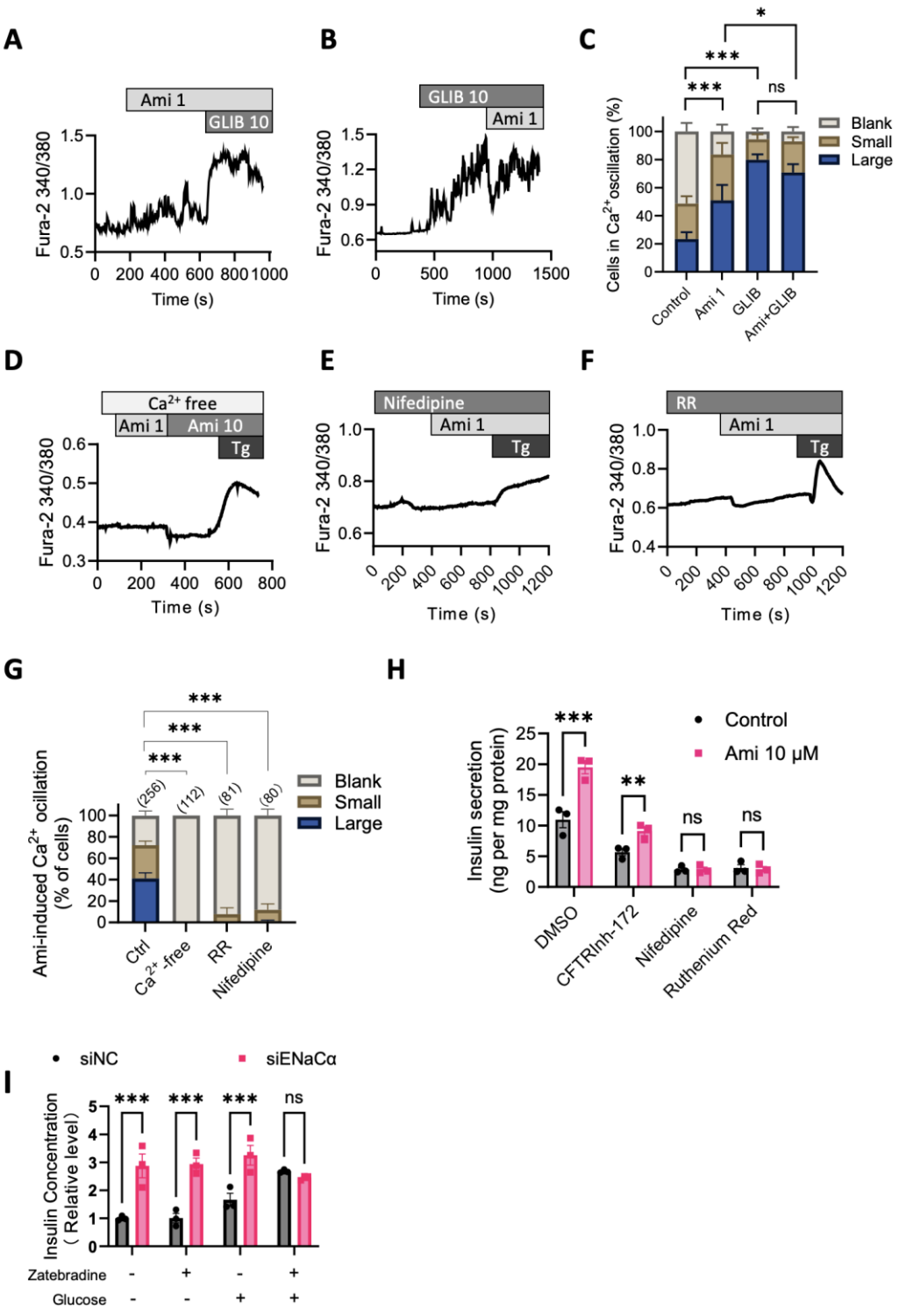

Figure 4.2 ENaC mediated multiple factors in the regulation of β-cells. (A-G) Time-course traces and corresponding quantification of intracellular Ca^{2+} oscillations induced

by Ami (1 μM) in RINm5F cells under different pretreatment conditions. Cells were pretreated with either glibenclamide (GLIB, 10 μM) (A-C), Ca^{2+}-free margo bath solution (see method), Ca^{2+} channel inhibitor nifedipine (20 μM), or ruthenium red (100 μM) (D-G). The experiment was repeated five times. * $p < 0.05$, *** $p < 0.001$. Pearson's chi-square test. Data are mean ± s.e.m. (H) ELISA measurement of glucose-stimulated insulin secretion in RINm5F cells treated with amiloride in response to CFTR inhibitor 172 (CFTRInh-172, 10 μM), nifedipine (20 μM) or ruthenium red (100 μM). $n = 3$ biologically independent samples per group. ** $p < 0.01$, *** $p < 0.001$. One-way analysis of variance. (I) ELISA measurement of insulin secretion in RINm5F cells after transfected with siENaCα or siNC for 72h in response to HCN channel inhibitor zatebradine (10 μM) in the absence or presence of glucose challenge. $n = 3$ biologically independent samples per group. *** $p < 0.001$, ns $p > 0.05$. One-way analysis of variance.

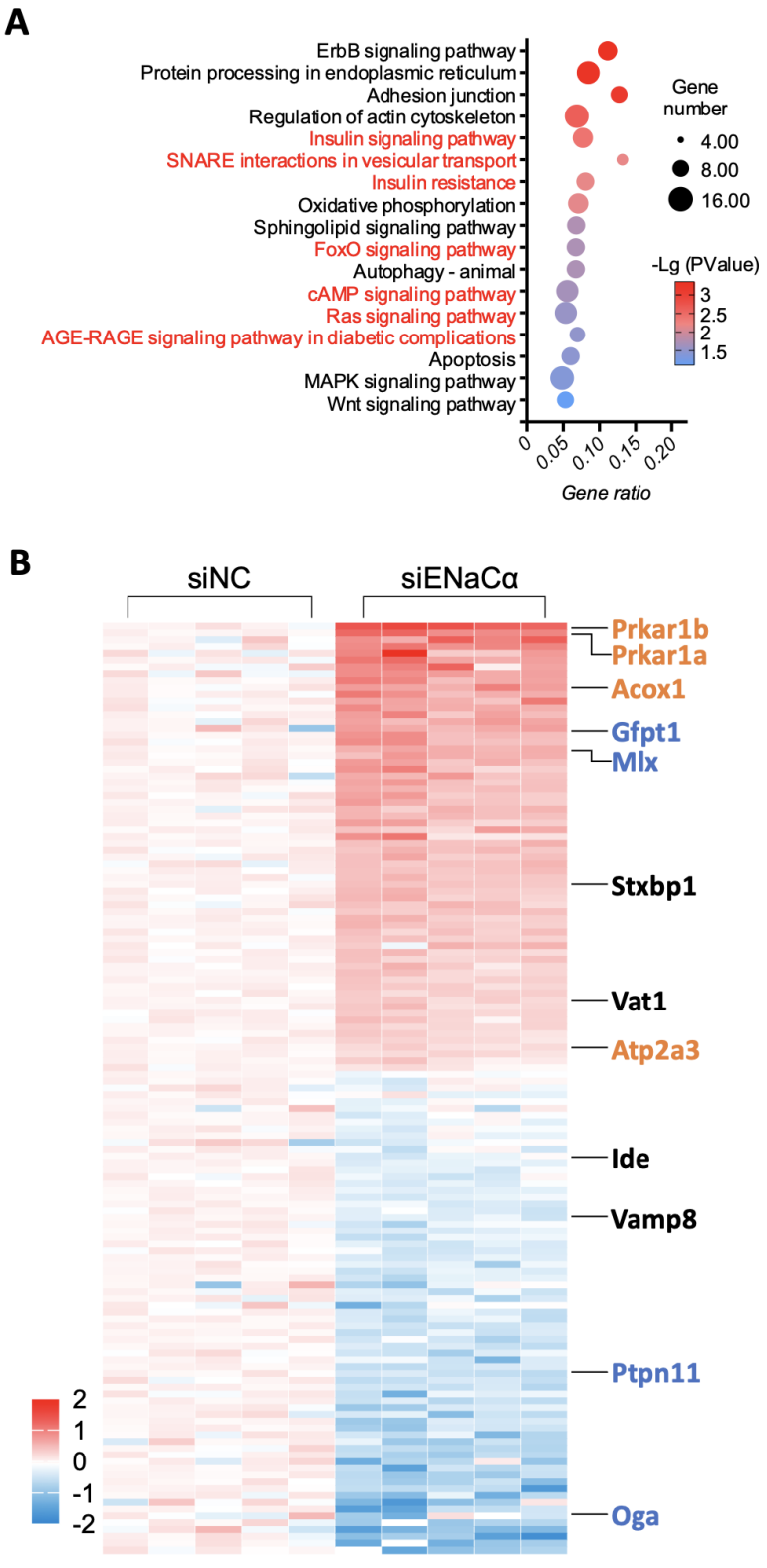

Figure 4.3 Effects of ENaCα knockdown on proteomic profile in β-cells. (A) Mass

spectrometry analysis of the proteins extracted from RINm5F cells treated with siENaCα or siNC. The experiment was repeated two times, n = 2 and 3 biologically independent samples per group respectively. (A) Pathway analysis of the proteins significantly changed after ENaCα knockdown with KEGG (Kyoto Encyclopedia of Genes and Genomes). Enrich ratio is calculated by input gene number/background gene number involved in the specific pathway. Dot size from small to large indicates the number of proteins in the specific pathway from few to many. Pseudocolor from purple to yellow represents the $-\log_{10}$ (p value) of enriched function from small to large. (B) Heatmap analysis of the overlayed significantly altered genes in twice mass spectrum. Specific genes were highlighted in related pathways. Genes labeled with orange: cAMP signaling pathway, blue: Insulin signaling pathway and insulin resistance, black: SNARE interactions in vesicular transport.

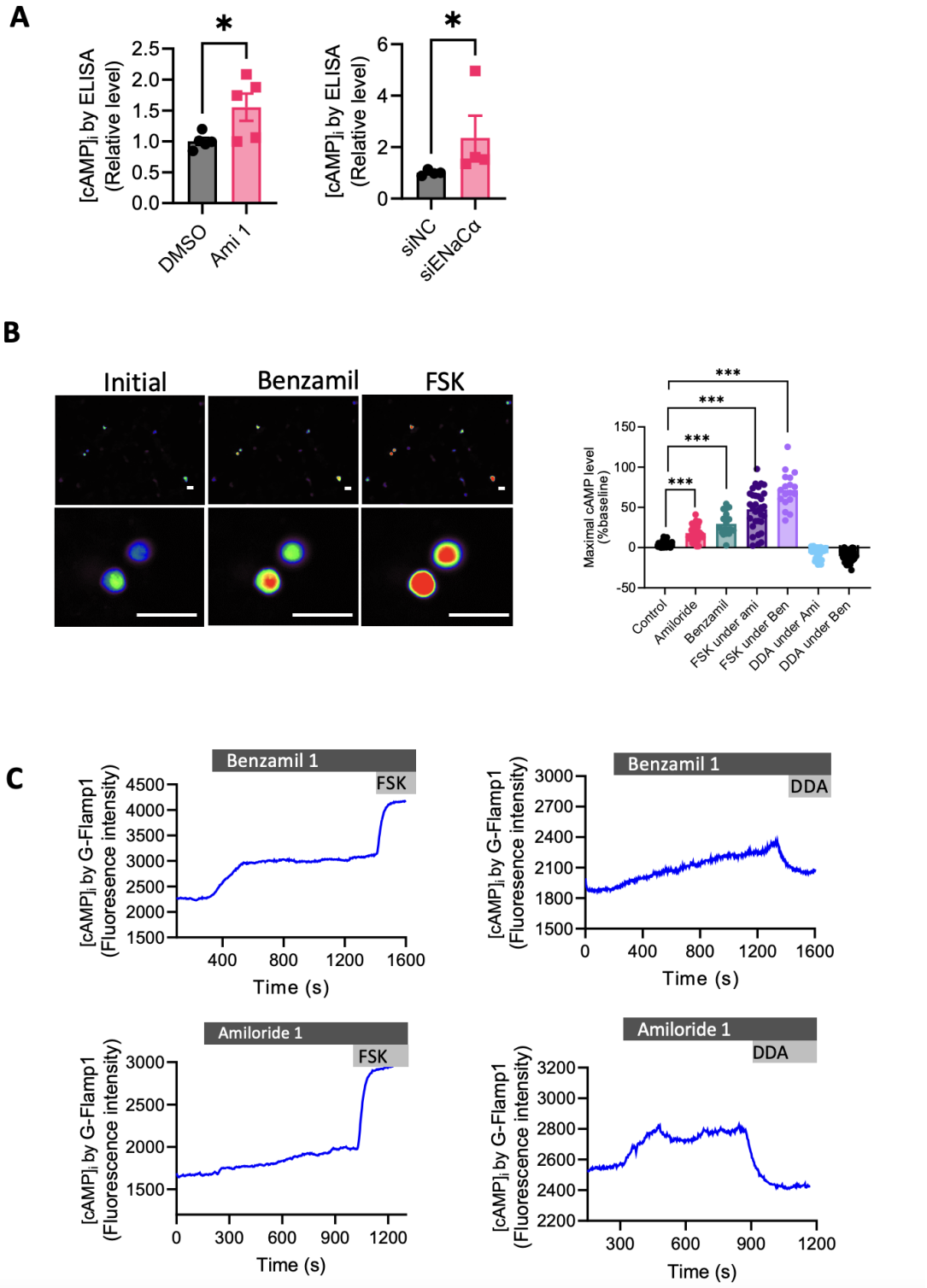

Figure 4.4 Effect of ENaC deficiency on intracellular cAMP levels in β-cells. (A) ELISA measurement of intracellular cAMP concentration in RINm5F cells treated with Ami (1 μM) or DMSO, or post-transfected with siENaCα or siNC for 72 h. n = 4-5 biologically independent samples per group. * $p < 0.05$ by unpaired t-tests. (B-C)

Representative fluorescence images (B), time-course traces (C), and corresponding quantification (B) of intracellular cAMP levels in response to ENaC inhibitors in RINm5F cells transfected with a cAMP biosensor pCAG-G-Flamp1 (G-Flamp1) for 24 h. Adenylyl cyclase (AC) agonist forskolin (FSK, 1 μM) and membrane AC inhibitor DDA (10 μM) were served as the positive and negative controls, respectively. The experiment was repeated three times. *** $p < 0.001$ by unpaired *t*-tests. Data are mean ± s.e.m. Scale bars are 100 μm.

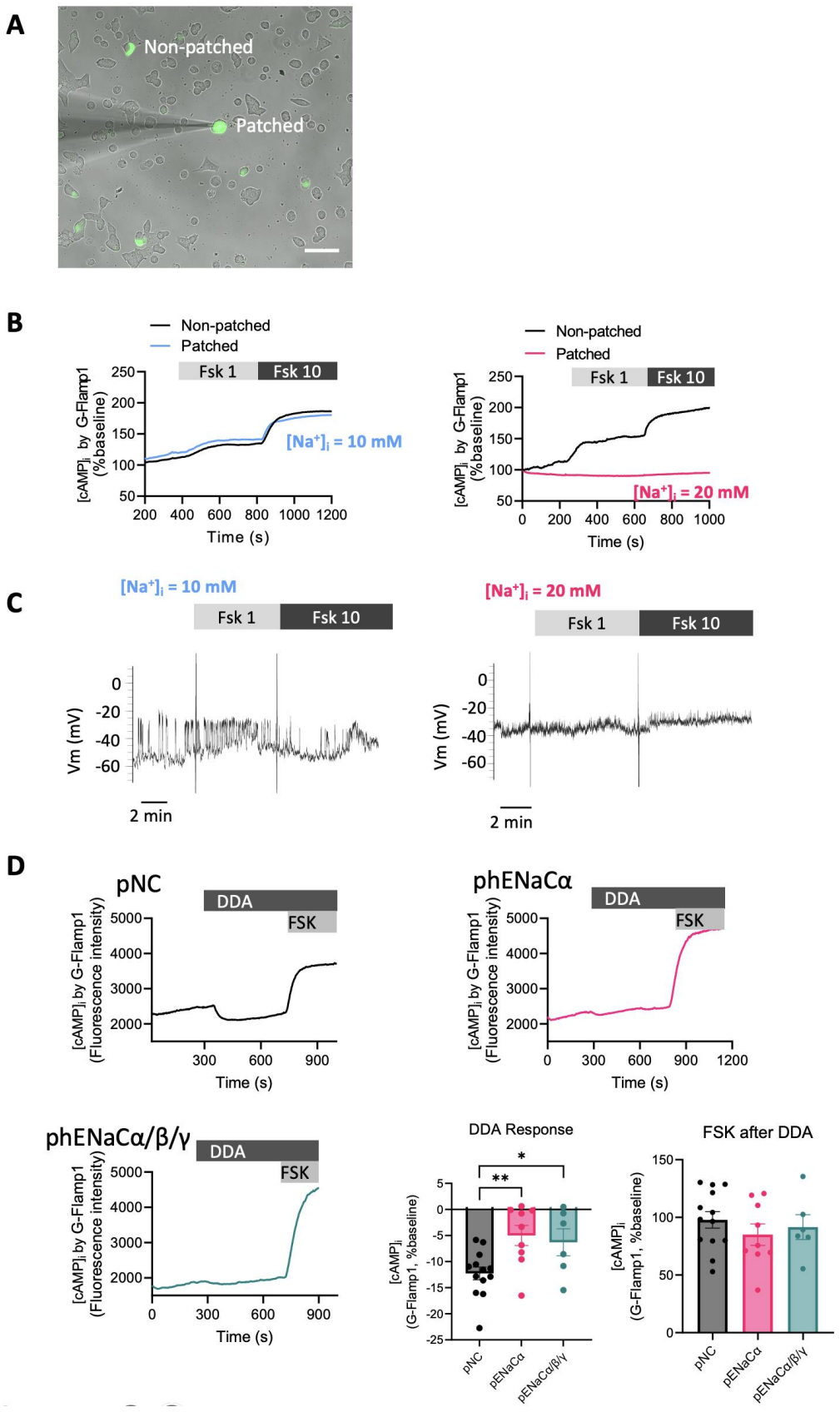

Figure 4.5 Effect of intracellular Na^+ concentration on cAMP activity in β-cells.

Simultaneous application of G-Flamp1-based cAMP imaging and current-clamp recordings treated with different pipette/intracellular Na^+ concentrations in RINm5F cells transfected with G-Flamp1 for 24 h. Representative fluorescence merged bright field image (A), time-course traces of intracellular cAMP levels (B), and whole-cell recording of membrane potential and quantifications (C) in response to FSK (1-10 μM) in patched and non-patched RINm5F cells. The experiment was repeated three times. (D) Time-course traces and corresponding quantification of cAMP imaging in response to DDA (10 μM) or FSK (1 μM). RINm5F cells were transfected with pNC, phENaCα, or phENaCα/β/γ for 48 h and subsequently transfected with G-Flamp1 for 24 h. The experiment was repeated three times. * $p < 0.05$, ** $p < 0.01$ by unpaired *t*-tests. Data are mean ± s.e.m.

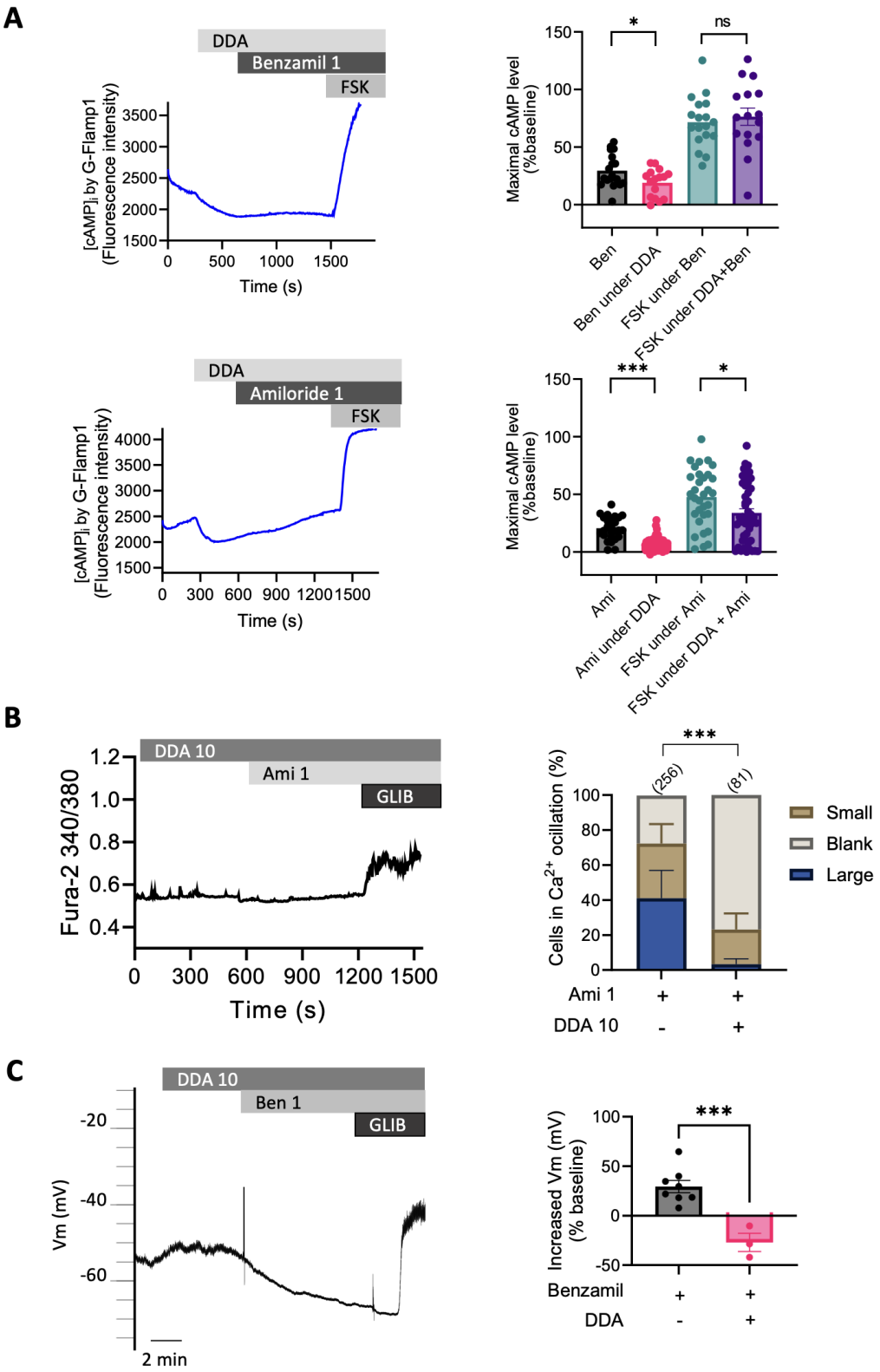

Figure 4.6 Effect of ENaC deficiency on cAMP activity in β-cells under inhibition

of mAC. (A) Time-course traces and quantification of intracellular cAMP levels by G-Flamp1 in RINm5F cells treated with benzamil or amiloride in the presence of DDA (10 μM). FSK was served as the positive control. The experiment was repeated three times. * $p < 0.05$, *** $p < 0.001$. Unpaired Student's *t*-tests. (B) Time-course traces and oscillation quantification of intracellular Ca^{2+} measurement in RINm5F cells treated with amiloride in the presence of DDA. GLIB was served as the positive control. The experiment was repeated three times. *** $p < 0.001$. Pearson's chi-square test. (C) Current-clamp whole-cell recording of membrane potential changes by patch-clamp in RINm5F cells in response to benzamil (1 μM) in the presence of DDA. GLIB was served as the positive control. The experiment was repeated three times. *** $p < 0.001$. Unpaired *t*-tests. Data are mean ± s.e.m.

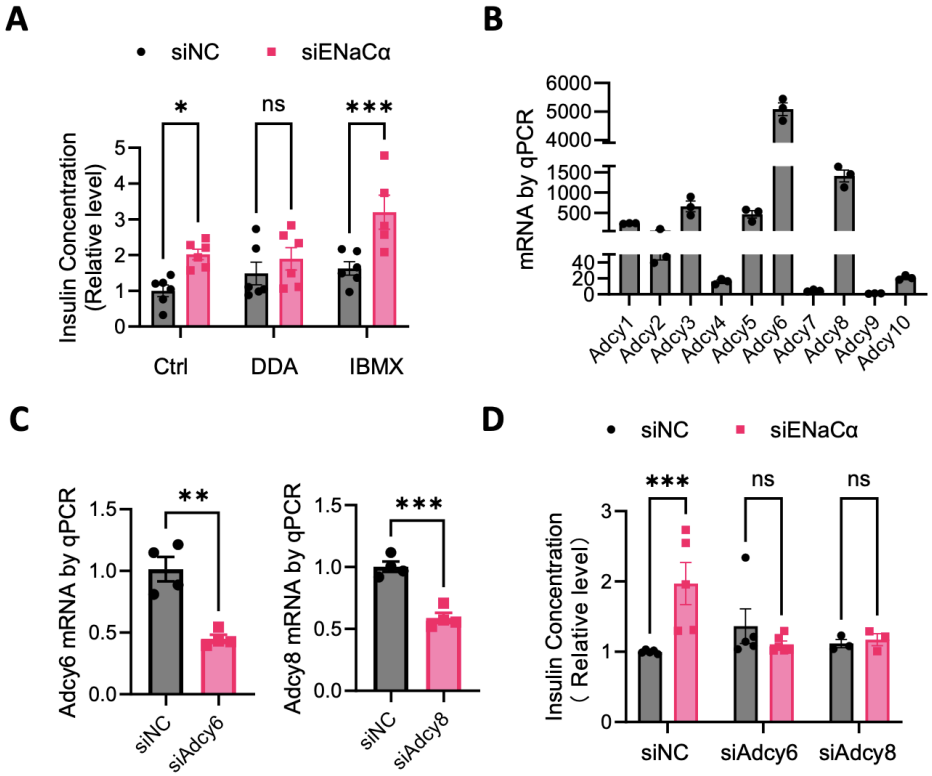

Figure 4.7 Effect of inhibition of cAMP synthesis on ENaC deficiency promoted insulin secretion. (A) ELISA measurement of glucose-stimulated insulin secretion in RINm5F cells treated with siNC/siENaCα for 72h in response to DDA, IBMX (inhibitor of phosphodiesterase, 100 μM), or DMSO as the control. n = 5-6 biologically independent samples per group. ns P >0.05, ** p < 0.01, *** p < 0.001. Two-way analysis of variance. (B) qPCR analysis of the expression of different adenylyl cyclase subunits (Adcy 1-10) in RINm5F cells. n = 3 biologically independent samples per group. (C) qPCR analysis of Adcy6/8 expression in RINm5F cells treated with siRNAs against Adcy6/8 (siAdcy6/8) or negative control siRNAs (siNC) for 48 h. n = 3 biologically independent samples per group. ** p < 0.01, *** p < 0.001. Unpaired Student's t-tests. (D) ELISA measurement of glucose-stimulated insulin secretion in RINm5F cells which were subjected to three groups: control group (treated with siNC),

double knockdown group (treated with siENaCα together with siAdcy6 or siAdcy8). *n* = 3-6 biologically independent samples per group. ns $P > 0.05$, *** $p < 0.001$. Two-way analysis of variance. Data are mean ± s.e.m.

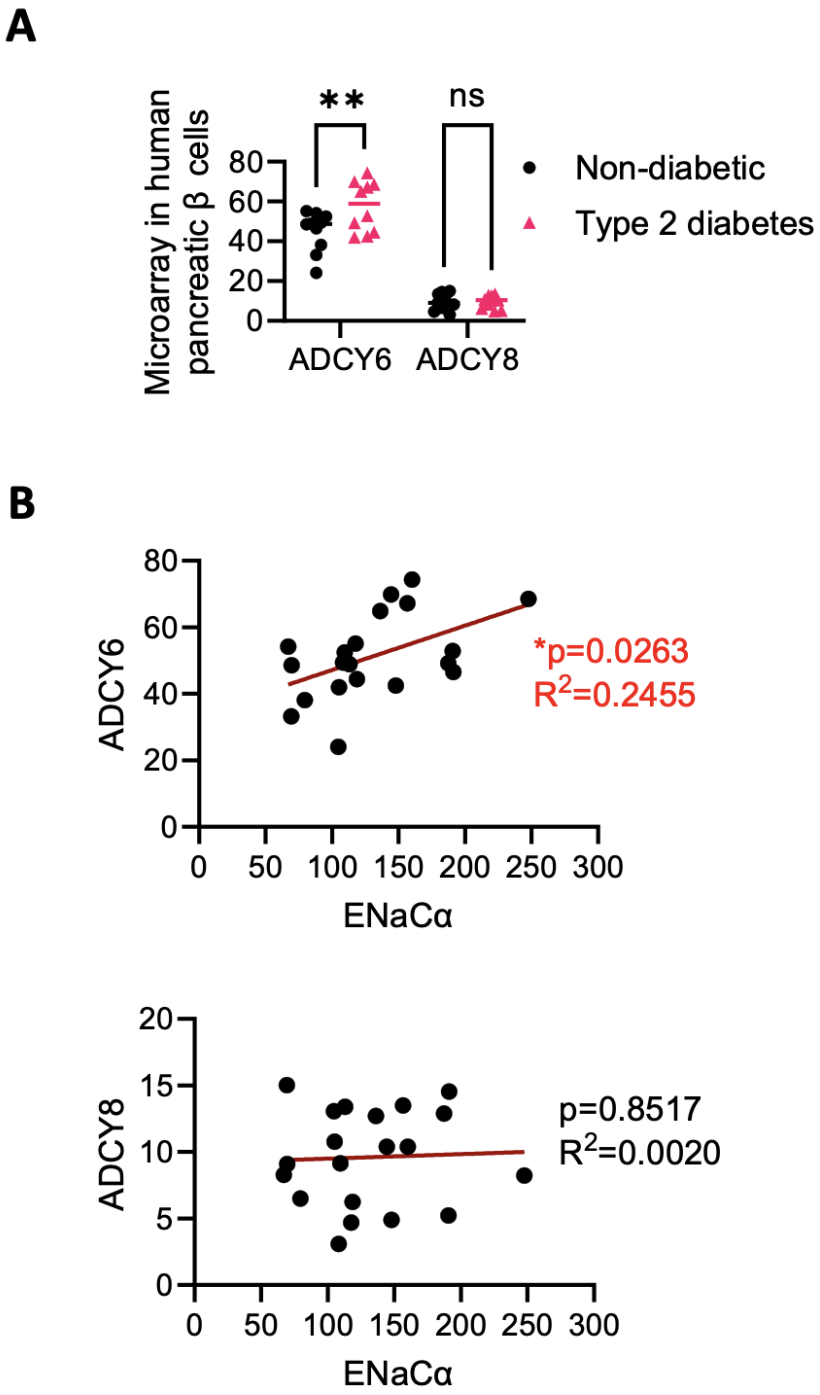

Figure 4.8 Expression of mAC in human database. (A) Comparative analysis of ADCY6 and ADCY8 mRNA expression by microarray in the pancreas tissues collected

from human non-diabetic (ND) and Type-2 diabetic (T2D) cadaver pancreas subjects from a human database (GSE20966). $n = 20$. ns $P > 0.05$, ** $p < 0.01$. Unpaired *t*-tests. Data are mean ± s.e.m. (B) Correlation analysis of gene expression between ENaCα and ADCY6, ADCY8 in ND and T2D human pancreas tissues. * $p < 0.05$. Pearson correlation test and values of R^2 and P are shown for each analysis.

4.3 Discussion

Taken together, the above results have demonstrated that ENaC-mediated Na^+ entry exerts an inhibitory effect on ACs activity and thus cAMP production which modulates multiple downstream events/factors to suppress insulin secretion in β-cells.

The suppression of cAMP by ENaC is evident. First, independent assays (i.e., ELISA, G-Flamp1 imaging and mass-spectrometry) all consistently indicated that inhibition/knockdown of ENaC induces elevation of intracellular cAMP or alters cAMP-related signaling. Second, pharmaceutical inhibition of membrane AC or knockdown AC6/AC8 abolished the effects of ENaC knockdown including membrane depolarization, Ca^{2+} increases and/or insulin secretion. cAMP serves as a crucial second messenger in the amplification of insulin secretion. By activating PKA or Epac2A, cAMP has multiple downstream action sites in β-cells. It facilitates the influx of Ca^{2+} through potentiating VGCCs and mobilizing Ca^{2+} from intracellular stores [221]. The cAMP/PKA cascade has been found to augment vesicular release at cerebellar granule cell synapses and enhance the interaction of Snapin and synaptotagmin with SNARE complexes [223, 224]. Additionally, cAMP activates CFTR, which promotes β-cell excitability and insulin secretion [45, 225]. It therefore explains the observed effect of blocking of CFTR, Ca^{2+} channels in counteracting amiloride-induced Ca^{2+} increase and/or insulin secretion.

We also made efforts to understand how ENaC suppresses cAMP in β-cells. The first

observation was that ENaC knockdown induced a small increase in intracellular ATP level. It is known that in epithelial cells, apical ENaC is functionally coupled with basolateral Na^+/K^+ ATPase to realize across-epithelial Na^+ absorption. ENaC knockdown may result in reduction in Na^+/K^+ ATPase activity and thus reduced ATP hydrolysis/consumption, leading to excessive ATP conversion into cAMP. However, the extent of ATP increase by ENaC knockdown was quite small (about 10%) and ENaC inhibitors did not produce ATP increase, suggesting extra mechanisms underlying ENaC regulation of cAMP. Indeed, our data support a major role of ENaC in inhibiting AC-driven cAMP production. ENaC may inhibit AC by mediating Na^+ entry, given that manipulation of intracellular Na^+ level in patch-clamp as high as 20 mM inhibited AC. This is consistent with an early study where AC was demonstrated in cell-free condition to be inhibited by Na^+ [226]. The present study is the first, to our best knowledge, to document Na^+ on AC activity and cAMP production in physiological conditions. Since ACs are well demonstrated to be regulated by Ca^{2+} [146], an interaction between AC proteins and Na^+ might exist as well, although further biochemical understanding of such interaction will be needed. It worth to note that cAMP was reported to either stimulate or inhibit Na^+ reabsorption in the kidney [145, 227]. Mutual regulation of each other might exist between Na^+ and cAMP. In addition, a previous study on intestinal epithelial cells revealed protein-protein interaction between AC6 and CFTR [228]. Given the known interaction between CFTR and ENaC, it is plausible that ENaC-mediated suppression of cAMP in β-cells could be attributed to a protein-protein interaction between ENaC and AC. The significant correlation between ADCY6 and

SCNN1A observed in pancreas tissues in humans may support this possible mechanism, although further investigation is needed to verify ENaC-AC interaction.

An important experiment done in this Chapter reveals that in the presence of DDA inhibiting ACs, benzamil induced a hyperpolarization instead of the depolarization observed in normal/control conditions. It experimentally proves what we proposed in Chapter 3 that ENaC contributes to a depolarization first before it suppresses insulin secretion. Therefore, the suppression through inhibition of cAMP production is delayed. We believe this delay to be of physiological significance because it allows a window period for depolarization to occur for the generation of action potentials and insulin secretion at the beginning. In this sense, ENaC contributes to a precise control of the timing and degree of such a suppression of insulin secretion.

cAMP signaling is primarily initiated by receptor agonists and is partly influenced by glucose for ATP generation. However, since the ATP concentration is potentially saturating even under low glucose conditions, glucose has a limited impact on cAMP levels [229]. The effects of glucose on cAMP content or AC activity have yielded conflicting results in studies. Considering the conclusion from Chapter 3, ENaC participates in a glucose-independent insulin secretion signaling pathway in β-cell function. Chapter 4 elucidated the rationale behind the glucose-independent pathway of insulin secretion, attributing it to the ENaC-dependent inhibition of cAMP production. This consistently suggests that ENaC suppresses insulin secretion in a way

independent on glucose. Nevertheless, recent studies have revealed, in addition to glucose, insulin secretion is regulated by incretin hormones GLP-1 and GIP binding to β-cell receptors, which are largely mediated by cAMP and subsequent activation of PKA or Epac2A [230]. Therefore, the discovery of ENaC regulation of cAMP production may also be important to understand incretin signaling for insulin secretion in β-cells.

Chapter 5: Effects of β-cell-specific knockout of ENaCα in mice

5.1 Introduction

In the previous chapters, we have demonstrated ENaC in the expression and function, as well as the mechanism underlying ENaC-regulated insulin secretion by cAMP in pancreatic islet β-cell *in vitro.* However, the role of ENaC in β-cell insulin secretion and glucose metabolism has not been studied *in vivo*. Insulin secretion and glucose metabolism are closely intertwined processes involved in maintaining blood glucose levels within a narrow range for physiological function. Disruptions in insulin secretion and glucose metabolism can lead to conditions such as hypoglycemia, hyperglycemia, and diabetes [231], characterized by abnormal blood glucose levels and disturbed blood insulin secretion levels, as well as β-cell failure [232].

In this chapter, to explore the role of ENaC-dependent insulin secretion *in vivo*, a mouse model was established and used. Due to the reported lethality of ENaCα (−/−) mouse neonates from respiratory distress [233], the conditional knockout (cKO) mouse model based on recombinant enzyme system (Cre-loxP) was generated with β-cell-specific Scnn1a-knockout. Genotyping and Na^+ measurement based on SBFI were employed to confirm its successful establishment. To evaluate various phenotypes related to glucose metabolism, oral and intraperitoneally glucose tolerance tests, insulin tolerance tests, and blood insulin secretion levels were performed in both these mice at different ages.

Pancreas tissue sections were examined using immunostaining to evaluate morphology, insulin production and downstream protein PKA of cAMP signaling. Isolated pancreatic islets were also analyzed for β-cell function in glucose-stimulated insulin secretion and islet number.

5.2 Results

5.2.1 Establishment of β-cell-specific knockout of ENaCα in mice

Given the observed effects of ENaC deficiency on β-cells *in vitro*, we next built a β-cell-specific knockout of ENaCα by crossing a β-cell-specific Cre mouse line (*Ins2*-Cre^{+}) [234] with an ENaCα gene-floxed (*Scnn1a*$^{fl/fl}$) mouse line (see method). Since the *Ins2*-Cre line was reported to have some glucose disturbance [235], we used *Ins2*-Cre^{+}. *Scnn1a*$^{wt/wt}$ mice as the control (Cre-Ctrl) to compare with the conditional knockout (cKO) mice (*Ins2*-Cre^{+}. *Scnn1a*$^{fl/fl}$). We confirmed the genotypes of the successful deletion of Scnn1a in β-cells by performing PCR using primers targeting exons2 in tissues from *Ins2*-Cre^{+}. *Scnn1a*$^{wt/wt}$, heterozygous (*Ins2*-Cre^{+}. *Scnn1a*$^{wt/fl}$), and homozygous (*Ins2*-Cre^{+}. *Scnn1a*$^{fl/fl}$) ENaCα-knockout mice (Figure 5.1 A). To assess the successful knockout of ENaCα in β-cells, intracellular Na^{+} levels were measured in primary cultured pancreatic islets obtained from Cre-Ctrl and cKO mice. The results demonstrated that the application of amiloride (1 μM) immediately and significantly reduced intracellular Na^{+} levels in islets from Cre-Ctrl mice. However, in the islets of cKO mice, intracellular Na^{+} levels showed a slow and slight decrease after

the addition of amiloride (Figure 5.1 B), indicating impaired ENaC channel function in cKO mice islets. The remaining response to amiloride in cKO islets may be attributed to other cells within the islets without ENaC knockout that are responsive to amiloride. These collectively suggest that the mouse model with a β-cell-specific knockout of ENaCα was successfully established.

5.2.2 Mice with β-cell-specific knockout of ENaCα exhibited low blood glucose level at young ages

In the two groups of mice, they did not show significant differences in body weight over different ages from 4-week-old to 28-week-old (Figure 5.2 A-B). At young ages before puberty (4- to 5-week-old), the glycemia or blood glucose levels were significantly lower in cKO than the Cre-Ctrl mice, in glucose tolerance tests using either oral (OGTT, Figure 5.3 A) or intraperitoneally injected glucose (IPGTT, Figure 5.3 B), although the difference between cKO and Cre-Ctrl mice was more obvious in OGTT than in IPGTT.

5.2.3 Mice with β-cell-specific knockout of ENaCα exhibited insulin hypersecretion at young ages

At young ages, the cKO mice exhibited drastically higher fasting blood insulin levels, 13.7 ± 6.5 folds higher than those in Cre-Ctrl (Figure 5.3 C). In response to glucose administration (i.p. 2 g kg^{-1}) after overnight fasting, the circulating insulin amount secreted at 10, 30, 60 and 120 min in cKO mice were all found significantly higher than

those in Cre-Ctrl (Figure 5.3 D), indicating insulin hypersecretion in the cKO mice. In isolated islets from two groups, the insulin amount secreted from the cells within 1 h glucose (10 mM) stimulation showed a substantial increase of 94.5 ± 3.8%-fold in the cKO mice islets compared to the Cre-Ctrl group (Figure 5.3 E). Such a phenotype is consistent with the *in vitro* observations showing that loss of ENaC leads to insulin hypersecretion.

5.2.4 Pancreas morphology in mice with β-cell-specific knockout of ENaCα

Next, we investigated the morphology of the pancreas in the two groups of mice. H&E staining analysis revealed no substantial difference in islet morphology or number in cKO mice (Figure 5.4 A). Immunohistochemical staining of insulin further demonstrated that there were no differences observed between the Cre-Ctrl and cKO groups (Figure 5.4 B), indicating that the mice with β-cell-specific knockout of ENaCα did not affects pancreas morphology or insulin production at young ages.

5.2.5 Enhanced β-cell PKA activity at young ages in mice with β-cell-specific knockout of ENaCα

To test whether such knockout of ENaC also influences cAMP pathways *in vivo*, immunofluorescence staining from Cre-Ctrl and cKO mice pancreas tissues demonstrated that PKA C-α, the active form of PKA regulated by cAMP directly, exhibited significant enrichment in pancreatic islet β-cells of cKO mice compared to Cre-Ctrl β-cells, consistent with upregulated cAMP levels observed in RINm5F cells

with ENaC deficiency (Figure 5.5 A-B). Thus far, our primary focus has been on confirming that the effect of absence of ENaCα in β-cells *in vivo* aligns with the observations made *in vitro*.

5.2.6 Phenotypes in glucose metabolism were diminished at mature ages in mice with β-cell-specific knockout of ENaCα

Interestingly, started at 8 weeks of age, which is the maturation stage of C57BL/6 mice, The cKO mice exhibited unstable glycemia levels, with some showing high glucose tolerance and others displaying low glucose tolerance compared to the Cre-ctrl mice. Assessing glucose tolerance using both OGTT (Figure 5.6 A-C) and IPGTT (Figure 5.6 D-F) tests, we found no significant variation in blood glucose levels between Cre-Ctrl and cKO mice aged 8 to 24 weeks, regardless of gender. In particular, among them, only the cKO female mice exhibited a notable increase in glycemia levels in response to glucose after the 60-minute time point in the IPGTT test, whereas no difference was observed in the OGTT test.

In order to comprehend the mechanism underlying this age-dependent disruption in glucose control, we first investigated whether the attenuation of glucose metabolism is associated with insulin resistance. The circulating glucose concentrations was observed to be decreased equally in cKO and Cre-Ctrl mice aged at 8-24 weeks after insulin administration, as determined by the insulin tolerance test (ITT) (Figure 5.7 A). Further analysis revealed that pancreas morphology was similar (Figure 5.7 B), and insulin

labeling by IHC showed no difference in insulin production between the two groups aged at 8-24 weeks (Figure 5.7 C). However, immunofluorescence staining for PKA C-α showed relatively lower signals in pancreatic islet β-cells of cKO mice compared to the Cre-Ctrl mice, indicating a little bit downregulation of PKA C-α expression in the cKO mice at mature ages.

To identify islet and β-cell function of cKO mice at mature ages, two group whole islets were isolated in the same protocol (see method 2.4). The insulin amount secreted from the islets within 1 h in response to a glucose (10 mM) challenge still exhibited a significantly increase of 41.5 ± 0.8%-fold in the cKO mouse islets compared to the Cre-Ctrl mouse islets (Figure 5.8 A). The number of whole-body islets isolated form the two groups was slightly reduced in cKO mice at mature ages (21-28 weeks old) (Figure 5.8 B), suggesting a fraction of β-cell damage after chronic absence of ENaC. Plasma glucagon levels revealed no changes along ages in the two groups, suggesting the diminished phenotype was not related to α-cells (Figure 5.8 C). Hence, these findings suggest that after mice maturation, these phenotypes were attenuated, but the islet of cKO mice consistently revealed insulin hypersecretion.

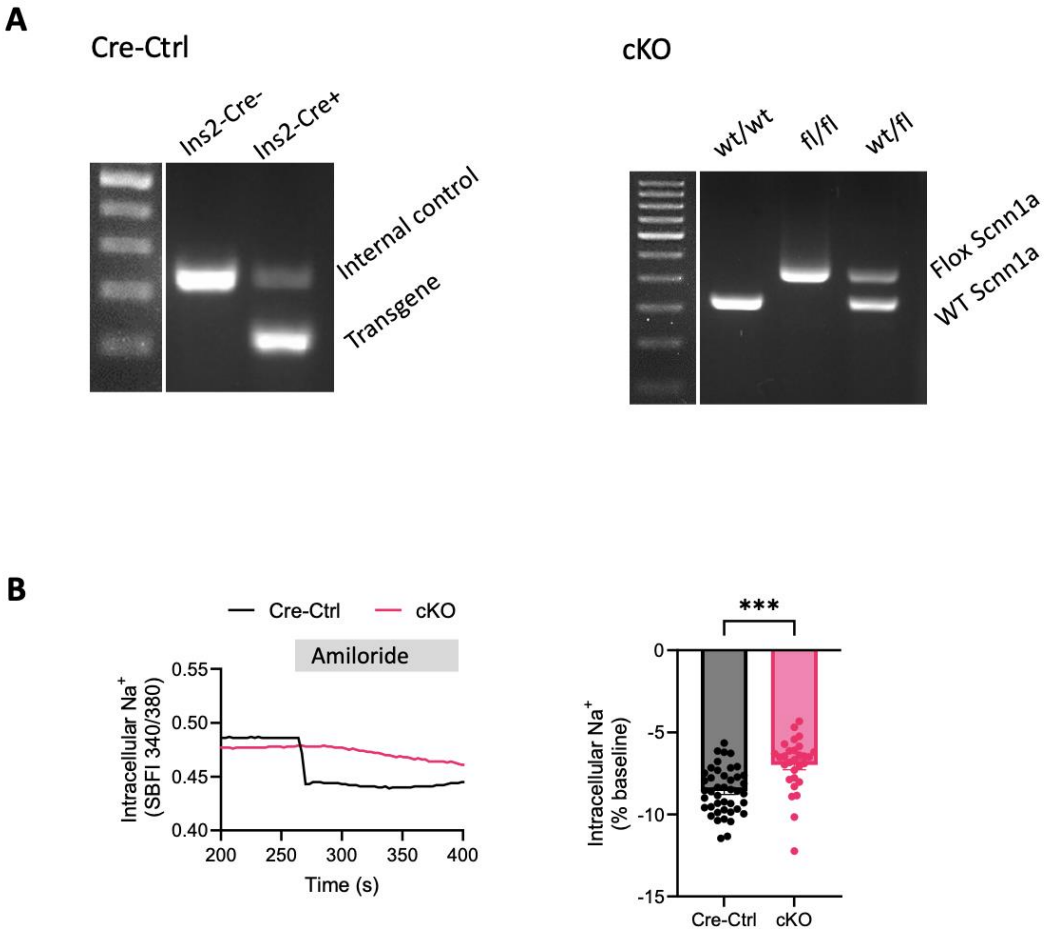

Figure 5.1 Establishment of conditional knockout of ENaCα in β-cells *in vivo*. (A) Representative images of genotyping results showing *Scnn1a*$^{wt/fl}$ (wt/fl) or *Scnn1a*$^{fl/fl}$ (fl/fl) in 5' and 3'-arm of mouse Scnn1a gene, and *Ins2*-Cre^{+} or *Ins2*-Cre^{-} (WT) in mice. (B) Representative time-course traces and corresponding quantification of Na^{+} change by Na^{+} sensitive dye SBFI in islets isolated from cKO (*Ins2*-Cre^{+}. *Scnn1a*$^{fl/fl}$) and Cre-Ctrl (*Ins2*-Cre^{+}. *Scnn1a*$^{wt/wt}$) mice in response to amiloride (1 μM). Data are mean ± s.e.m. *n* number is shown in each group. *** $p < 0.001$ by unpaired *t*-test.

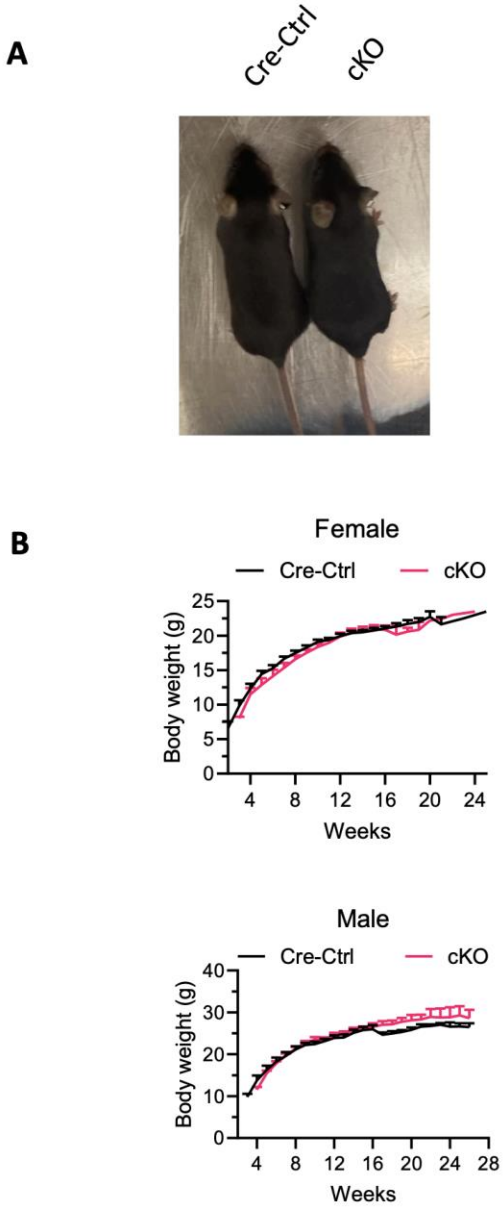

Figure 5.2 Effect of β-cell-specific knockout of ENaCα on mice body weight. Habitus (A) and body weight (B) of mice with Cre-Ctrl and cKO mice 3-25 weeks after birth.

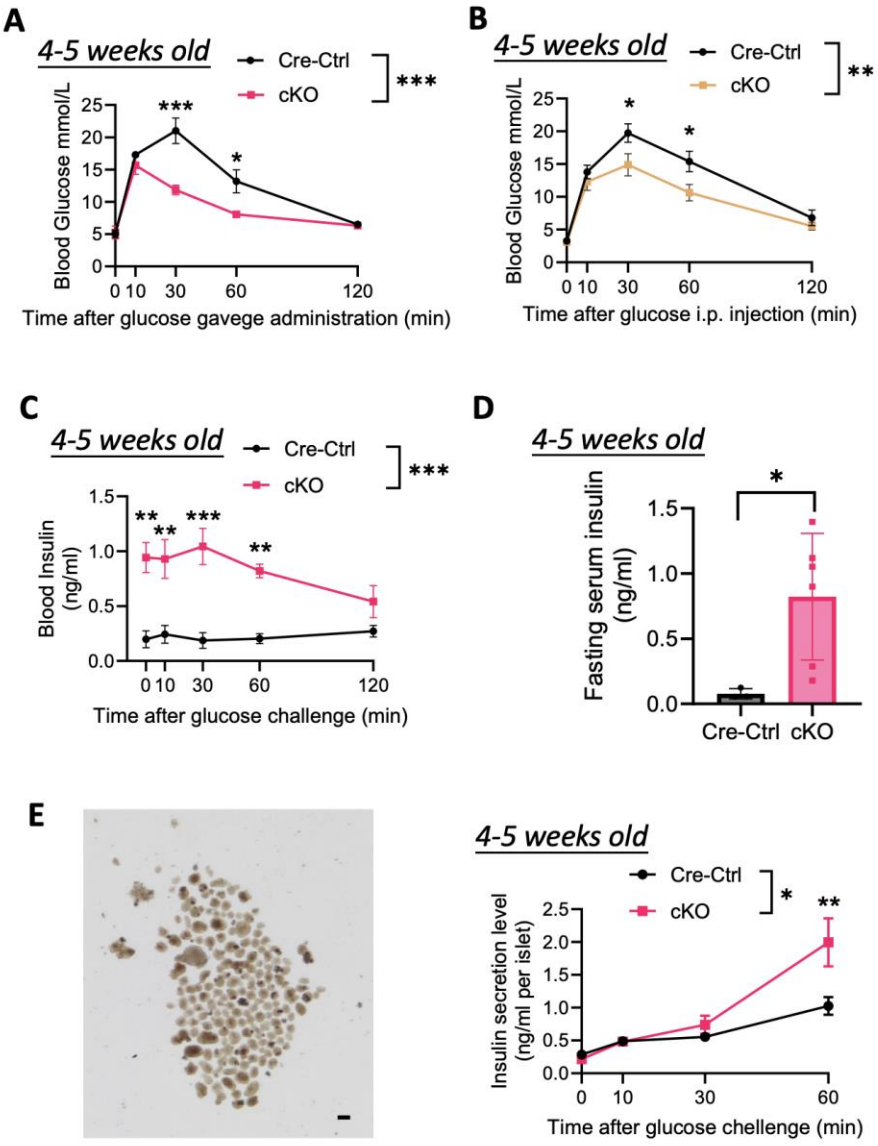

Figure 5.3 Effect of β-cell-specific knockout of ENaCα on glucose metabolism in young mice aged 4-5 weeks. (A-B) Time-course change of blood glucose level tested with oral glucose tolerance test (OGTT) (A) and intraperitoneal administration glucose tolerance test (IPGTT) (B) respectively. Measurement was done after glucose administration (2 g kg^{-1} body weight) in **4–5 weeks old** Cre-Ctrl (black, n = 5-10) and cKO mice (red or yellow, n = 4- 14). ** $p < 0.01$, *** $p < 0.001$. Two-way analysis of variance. (C) ELISA for blood insulin concentrations in Cre-Ctrl (n = 3) and cKO (n =

4) mice 120 min after glucose administration. ** $p < 0.01$, *** $p < 0.001$. Two-way analysis of variance. (D) ELISA for plasma insulin levels upon 16 h fasting in Cre-Ctrl ($n = 3$) and cKO ($n = 6$) mice. * $p < 0.05$ by unpaired *t*-tests. Data are mean ± s.e.m. (E) Representative figure of whole isolated islets from mouse and ELISA measurement of glucose-stimulated insulin secretion in 1 h in isolated islets from Cre-Ctrl ($n = 15$) and cKO ($n = 15$) mice. The results were achieved from 3 mice in each group. * $p < 0.05$, ** $p < 0.01$. Two-way analysis of variance. Scale bars are 100 μm.

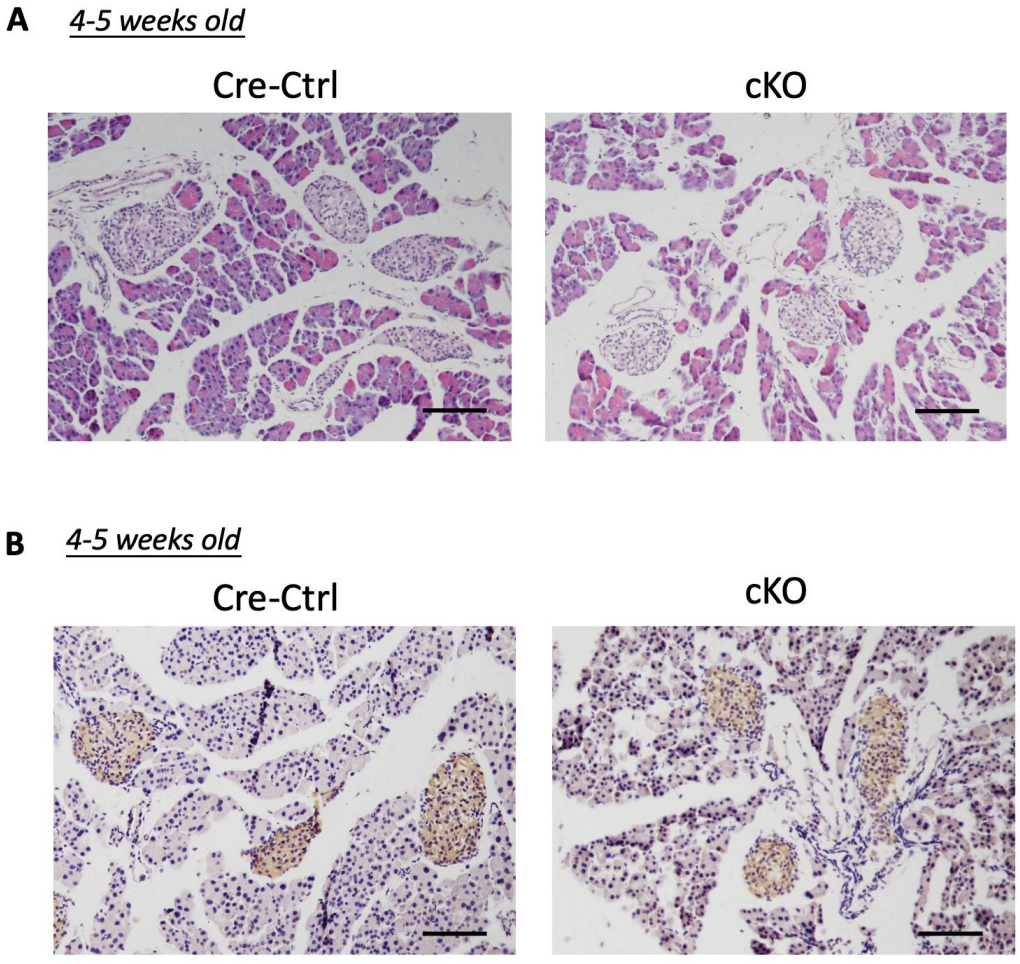

Figure 5.4 Pancreas morphology of young mice with β-cell-specific knockout of

ENaCα. (A) Hematoxylin and Eosin (H&E) (A) and immunohistochemistry (IHC) (B) staining for insulin (brown) in pancreas tissues from 4-5 weeks old Cre-Ctrl and cKO mice. Scale bars are 100 μm.

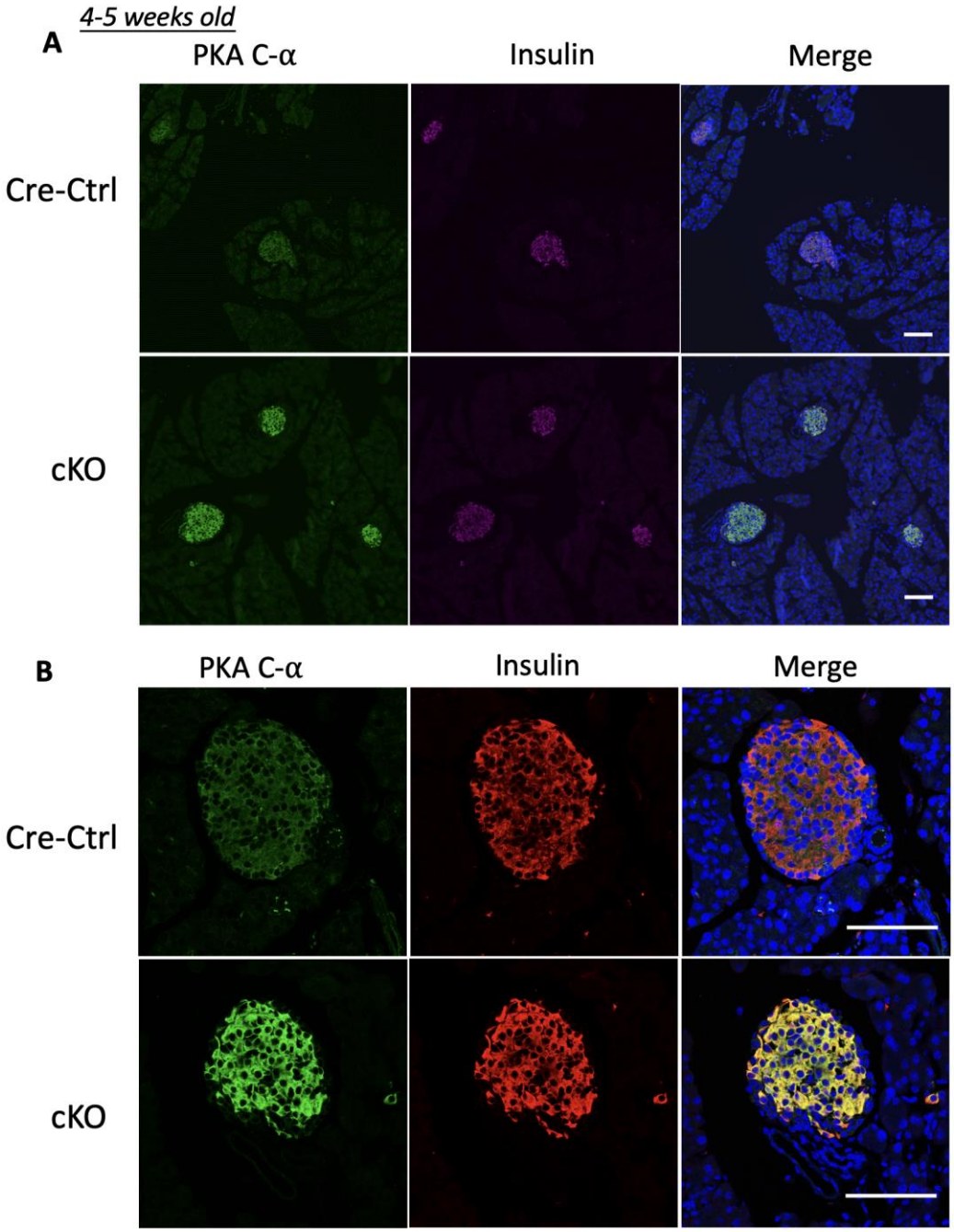

Figure 5.5 Immunofluorescence staining of PKA in young mice with β-cell-specific

knockout of ENaCα. Immunofluorescence staining for PKA (green) and insulin (purple in A, red in B) in pancreas tissues from 4-5 weeks old Cre-Ctrl and cKO mice. Scale bars in epifluorescence images (A) and confocal images (B) are 100 μm.

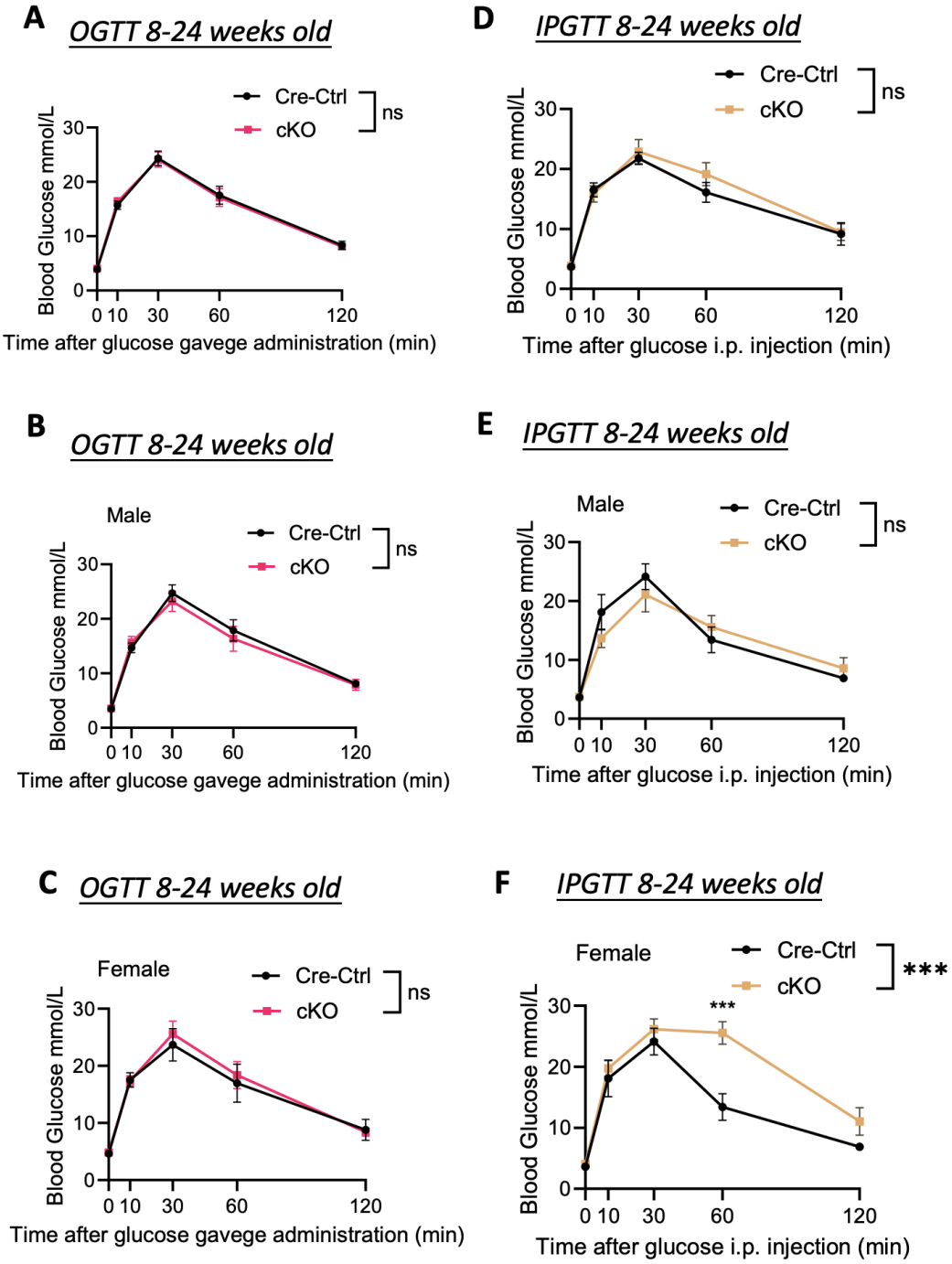

Figure 5.6 Effect of β-cell-specific knockout of ENaCα on glucose metabolism in mature mice aged 8-24 weeks. (A-C) Time-course change of blood glucose level with OGTT in 8-24 weeks old Cre-Ctrl (black, *n* = 17, male *n* =11, female *n* = 6) and cKO mice (red or yellow, *n* = 16, male *n* =10, female *n* = 6). (D-F) Time-course change of blood glucose level with IPGTT in 8-24 weeks old Cre-Ctrl (black, *n* = 12, male *n* =8,

female $n = 4$) and cKO mice (red or yellow, $n = 14$, male $n = 9$, female $n = 5$). Specific gender is indicated in the figure. * $p < 0.05$. Two-way analysis of variance.

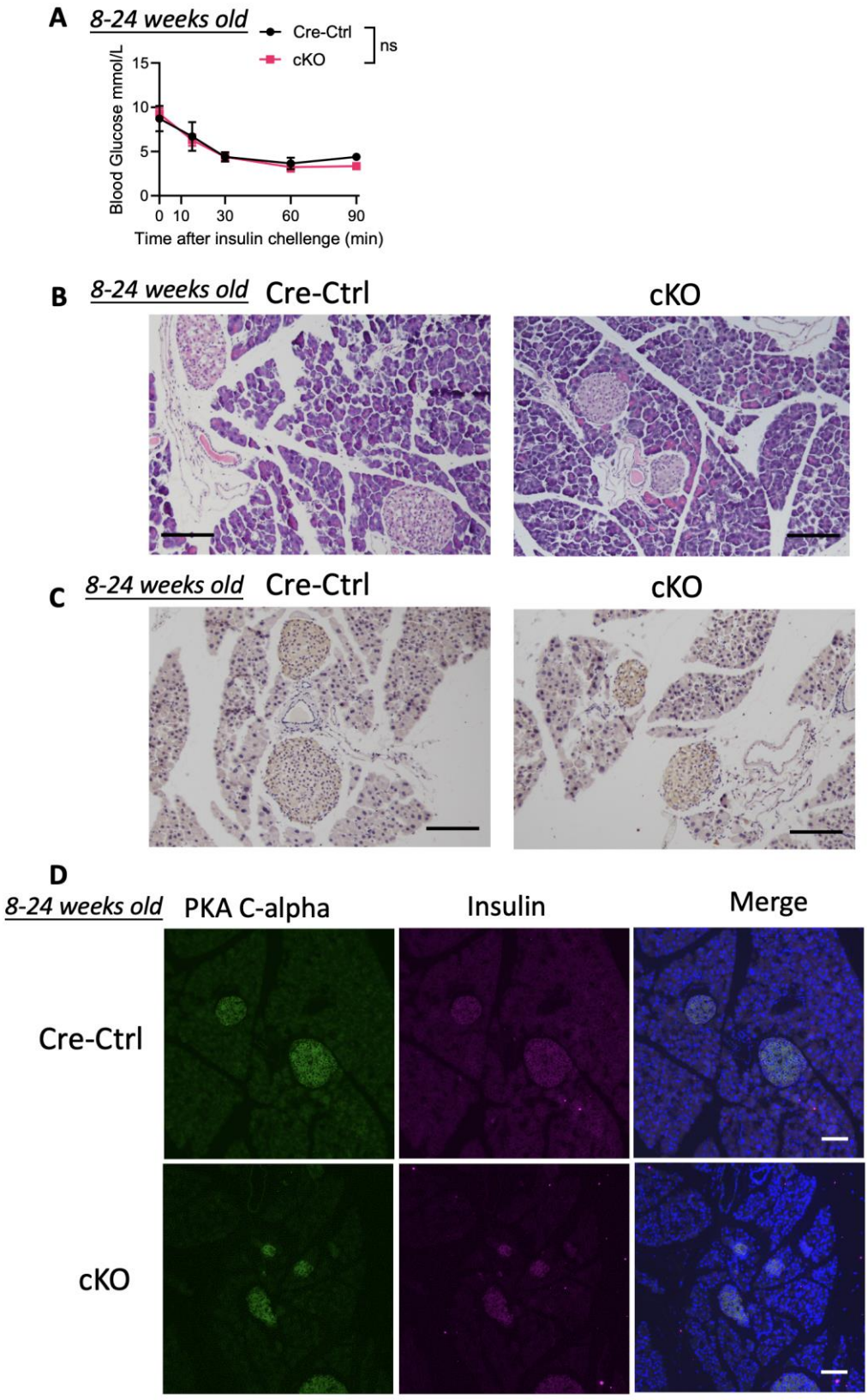

Figure 5.7 Multiple factors involved in mature mice with β-cell-specific ENaCα knockout at 8-24 weeks of age. (A) Insulin tolerance test (ITT) upon 4-h fasting in

response to 0.75 IU insulin injection within 90 min in mature Cre-Ctrl (n = 4) and cKO mice (n = 5). (B-C) H&E staining (B) and IHC staining for insulin (brown) (C) in pancreas tissues from mature Cre-Ctrl and cKO mice. (D) Immunofluorescence staining for PKA (green) and insulin (purple) in pancreas tissues from mature Cre-Ctrl and cKO mice. Scale bars are 100 μm.

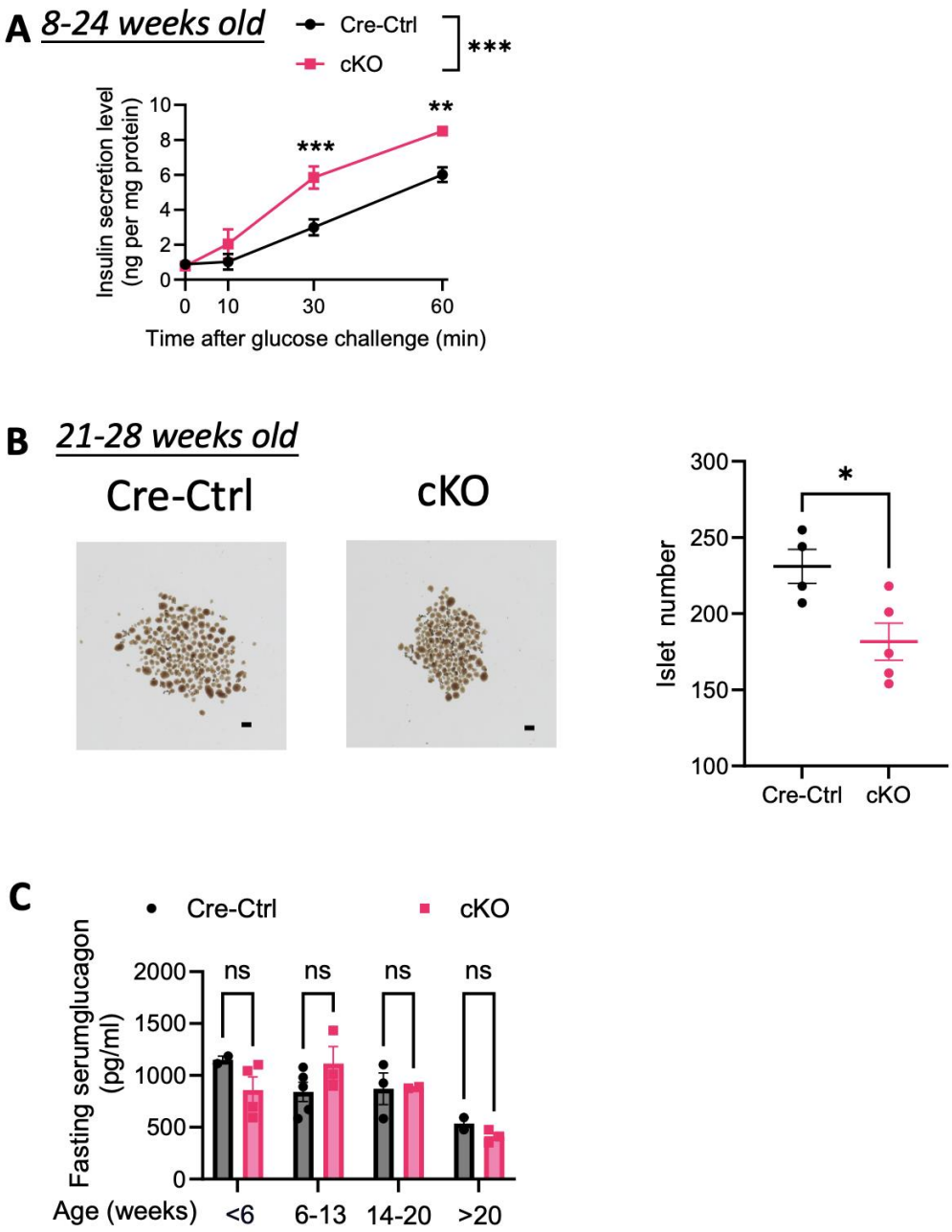

Figure 5.8 Islet function in mature mice with β-cell-specific knockout of ENaCα. (A) ELISA for glucose-stimulated insulin secretion in 1 h from isolated islets of Cre-Ctrl ($n = 15$) and cKO ($n = 15$) mice (8-24 weeks old). The results were achieved from 3 mice in each group. ** $p < 0.01$, *** $p < 0.001$. Two-way analysis of variance. (B) Representative figures and quantification of whole islets isolated from 21-28 weeks old Cre-Ctrl ($n = 4$) and cKO ($n = 5$) mice. Scale bars are 100 μm. (C) Glucagon ELISA

measurement upon 16 h fasting in Cre-Ctrl and cKO mice at different ages. *n* was shown in the figure. *ns* $p > 0.05$ by unpaired *t*-tests. Data are mean ± s.e.m.

5.3 Discussion

In summary, the present results have demonstrated that ENaC indeed plays a role in the regulation of insulin secretion and glucose metabolism *in vivo*: Mice with β-cell-specific knockout of ENaCα exhibited blood insulin elevation, hypoglycemia and hypoglycemia at young ages before puberty; However, all these changes were attenuated as the mice reached mature ages (> 8 weeks old). However, isolated islets from both young and old cKO mice consistently showed insulin hypersecretion.

The present findings in β-cell-specific knockout of ENaCα mice suggested a phenotype characterized by insulin hypersecretion in young mice, consistently demonstrating the role of ENaC in both *in vivo* and *in vitro*. The circulating insulin secretion levels, as measured by glucose tolerance test, fasting blood insulin levels, and glucose-stimulated insulin secretion from isolated islets were all significantly elevated in cKO mice compared to Cre-Ctrl before puberty, consistent with ENaC deficiency-promoted insulin hypersecretion in RINm5F cells. Also, ENaC deficiency did not affect insulin production, as evidenced by no difference in IHC staining for insulin consistent with no increased expression of Ins1 and Pdx1 in RINm5F cells with ENaCα knockdown. Besides, the significantly increased PKA fluorescence observed in cKO mice before

puberty aligns with the upregulated expression of cAMP signaling pathways found in RINm5F cells with ENaCα deficiency. Studies have reported that in rodents, the attainment of full GSIS function requires more than a month of postnatal development [236]. Hence, mice at 4-5 weeks of age, both in Cre-Ctrl and cKO groups, present the most ancestral metabolic functions [67]. These findings strongly indicate that the absence of ENaCα indeed eventuates the phenotype of insulin hypersecretion *in vivo*, consistently supporting the role of ENaC in promoting insulin hypersecretion observed *in vitro*.

Deletion of ENaC in β-cells over the long term in mice has been observed to diminish all the changes related to glucose metabolism. A disappeared phenotype in glycemia levels was observed in cKO mice aged 8 weeks and older, characterized by no difference in glucose tolerance compared to the Cre-Ctrl mice. However, the insulin levels in single islets of cKO mice still demonstrated hypersecretion substantially, indicating a continuous role of ENaC in promoting insulin secretion throughout the metabolism of these mice. These findings provide evidence that the absence of ENaC in β-cells leads to a phenotype of hyperinsulinemia (insulin hypersecretion) at young ages but finally is revised into normal glycemia. To be noted, the Cre-Ctrl consistently exhibited stable glucose tolerance and glucose-induced insulin secretion levels across different ages, suggesting that the Ins2-Cre line serves as a reliable control for comparative analyses.

The age-dependent glucose metabolism in cKO mice may account for some reasons. During the onset of puberty, hormone development and other environmental factors contribute to shaping whole-body metabolism [88]. These mice undergo a maturation process characterized bycβ-cell replication and expansion [237], which may vary overall metabolic profiles of these mice. The previously unstable glucose homeostasis gradually stabilizes until around 12 weeks, which is a critical age for the establishment of stable transgenic mice [238]. A compensation mechanism may occur over time in mice lacking ENaC, enabling them to adapt and restore their physiological responses, thereby overcoming the absence of ENaC and achieving a better alignment with their environmental homeostasis demands. Given the observed hypoglycemia in early life, which suggests the initial role of ENaC in promoting insulin hypersecretion, it is reasonable to consider that an immature and unfavorable environment such as unhealthy diet or irregular circadian rhythm could contribute to the dysregulation of glucose metabolism in β-cell-specific ENaC-deficient mice. This may lead to disturbances in regulatory mechanisms and compromised glucose homeostasis. Previous studies have reported that β-cell-specific barr1 knockout mice fed a standard chow diet did not exhibit significant impairments in glucose homeostasis. However, when exposed to an obesogenic diet, these mice displayed notable reductions in β-cell mass and proliferation rates, leading to pronounced impairments in glucose homeostasis [239]. Hence, it is crucial to investigate whether and how the absence of ENaC in β-cells contributes to metabolic disturbances in specific disordered metabolic environments.

Chapter 6: General Discussion and Conclusion

6.1 General discussion

Taken together, we have confirmed the functional expression of ENaC in pancreatic islet β-cells to be inversely correlated with insulin secretion (Chapter 3). We have demonstrated the mechanism underlying the regulatory role of ENaC in β-cells. ENaC exerts an inhibitory effect on ACs activity and thus restrains cAMP production affecting multiple downstream events/factors to suppress insulin secretion (Chapter 4). In Chapter 5, we have shown such a regulatory role of ENaC is significant *in vivo*. β-cell-specific knockout of ENaCα in mice resulted in insulin hypersecretion before puberty and in a long run led to normal glucose tolerance, suggesting ENaC to play a protective role in pancreatic islet β-cells.

6.1.1 A new mechanism underlying insulin secretion

The present study provides new insights into the understanding of insulin secretion. In the existing knowledge of insulin secretion, K_{ATP} and voltage-gated Ca^{2+} channels play dominant roles in the excitability of β-cells. Other ion channels such as CFTR, HCN, TRP are also documented to contribute to β-cell excitability. The demonstrated role of ENaC in β-cells is sophisticated. It allows Na^{+} entry to depolarize the membrane and is thus excitatory to some extent. However, its major effect is inhibitory, which is mediated by cAMP suppression. The two seemingly contradicting effects are possibly exerted in sequential order to contribute to the realization of the known biphasic feature

of insulin secretion -- an initial window for the surge of insulin followed with a period of restraining and recovery. In this regard, ENaC provides a mechanism for the homeostasis of insulin secretion, complementing existing understanding of glucose-stimulated and cAMP-amplified insulin secretion.

Moreover, different from typical excitable cell types such as neurons, β-cells use K^+ channels instead of Na^+ channels to generate action potentials. Previous studies reported that the voltage-sensitive Na^+ channel has limited/obscure role in action potential generation in β-cells [212]. The present study provides an explanation why β-cells use such a unique mechanism to generate action potentials since Na^+ plays an intriguing role in β-cells. Due to probably very different ACs and cAMP signalings from neurons, Na^+ entry functions mostly as a suppressor for insulin secretion.

6.1.2 A possible etiology for diabetes

Given the rising incidence and mortality rates of diabetes, it is of paramount importance to revisit the etiology and epidemiology of diabetes. Na^+ and Na^+ environment play a critical role in the physiological functioning of β-cells and have been implicated in the pathogenesis of diabetes. According to the human database, we found an increased expression of ENaC in the diabetic groups, suggesting the participation of this ion channel in pathophysiological development of this disease. Indeed, there is evidence suggesting that high salt intake can contribute to the development of obesity and metabolic syndromes, including diabetes [202]. It is reasonable to take ENaC as a

potential novel indicator for diabetes diagnosis and reference. On the other hand, diabetes as a chronic disease, is influenced by long-term exposure to environmental factors, such as diet and obesity. The present studies indicate a link between disturbed insulin secretion and ENaC deficiency in the long term. Furthermore, as previously discussed, diabetes and obesity are common factors in resistant hypertension. In clinical practice, the ENaC inhibitor amiloride is utilized as an adjunctive therapy for hypertension. Based on our research findings, which demonstrate that inhibition of ENaC facilitates insulin secretion and ultimately results in β-cell dysfunction, so it is imperative to investigate whether the administration of amiloride in hypertension has any adverse effects on pancreatic β-cells.

Recently, a new drug called semaglutide, a GLP-1 receptor agonist, has been approved as a second-line treatment for better glycemic control in type 2 diabetes [240]. In β-cells, GPCRs are activated by paracrine/endocrine factors like glucagon, GLP-1, and GIP stimulate ACs and cAMP activities [241]. ENaC has been reported to be regulated by GPCRs for extracellular signals transduction in epithelial cells [242]. ENaC activity could be stimulated by the alpha i-3 subunit of the Gi-3 protein in renal epithelial cell line A6 [243] and is also regulated by G protein and Gi1/Gi2 protein in mouse mandibular gland duct cells [244]. $G_{\beta\gamma}$ inhibits ENaC activity in A6 cells by activating PLC, leading to the activation of PKC and ERK1/2 [242]. While the involvement of ENaC in GPCR signaling has not been extensively studied in β-cells, our findings on ENaC-dependent inhibition of cAMP production indicated the potential role of ENaC

in this signaling pathways, including those related to GLP-1/GIP regulation of β-cell function. In addition, by analyzing human pancreas tissues from diabetes patients, we observed a significant upregulation on both ENaC and ADCY6 with a positive correlation, though ADCY8 did not show any difference in the pancreas from the two groups. However, Animal models of T2D have identified ADCYs [245], specifically ADCY8, as causal drivers of obesity and diabetes, with overexpression observed in the islets of diabetic animals [246]. In humans, significantly elevated levels of ADCY8 expression and cAMP have been found in the plasma of T2D patients compared to non-diabetic controls [247]. According to above evidence, ENaC and ADCY may serve as clinical diagnostic indicators for diabetes.

6.1.3 A new understanding of ENaC

Previously, we demonstrated in endometrial epithelial cells that the activation of ENaC promotes Ca^{2+} mobilization [182, 184]. Here, we demonstrate that ENaC can inhibit Ca^{2+} mobilization in a particular context as well, providing a new understanding of this channel. Possibly, ENaC may be exerting versatile roles under different physiological conditions. The revealed previously undefined capacity of ENaC in directly regulating cAMP production may have far-reaching implications beyond β-cells and insulin secretion.

An interesting aspect to note is the relationship between ENaC and CFTR. In a recent study, we revealed the biphasic regulatory role of ENaC in tuning CFTR expression

involving Ca^{2+}-modulated sAC-driven cAMP production in endometrial epithelial cells [192]. CFTR, the cAMP-regulated chloride channel, contributes to enhancing β-cell excitability and insulin secretion. In β-cells, the presence of CFTR inhibitor 172 led to decreased insulin secretion levels in both control and amiloride groups, with in amiloride group exhibiting a slightly enhancing effect compared to the control, suggesting CFTR was also involved in ENaC regulated β-cell function. By discovering ENaC-dependent inhibition of cAMP in β-cells, it provides a more comprehensive explanation for the relationship between ENaC and CFTR. We can also learn from that, the reciprocal relationship observed between CFTR and ENaC in various epithelial cell-enriched organ systems may be attributed to their distinct response to cAMP.

6.2 Conclusion

In conclusion, the present study has demonstrated for the first time a critical role of ENaC in insulin secretion and glucose metabolism in pancreatic islet β-cells (Figure 6). ENaC mediates glucose-independent Na^+ entry in β-cells, which inhibits adenylyl cyclase-dependent cAMP production following modulating multiple downstream events/factors to suppress insulin secretion in β-cells. Deficiency of ENaCα in mouse β-cells revealed problematic insulin secretion and defective glucose tolerance. These findings open up new avenues for understanding the interplay between Na^+ channels/environment and β-cell function. Abnormality of ENaC may serve as a possible etiology in glucose metabolism disorders and diabetes. The demonstrated role

of ENaC in the regulation of adenylyl cyclase-dependent cAMP production may also have further implications in other system diseases beyond β-cells.

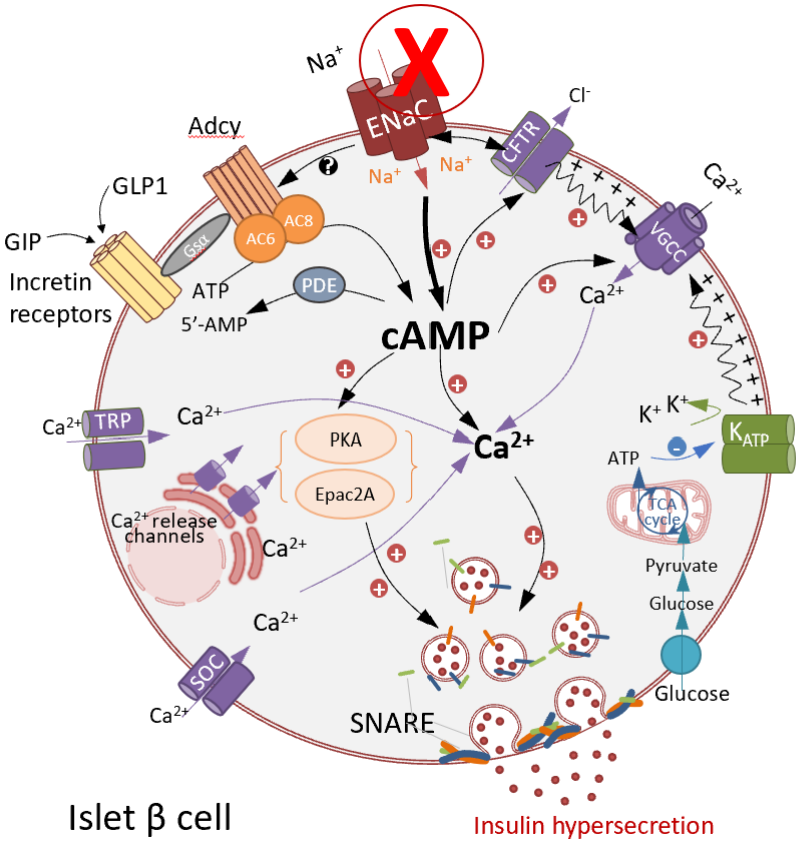

Figure 6 Schematic diagram demonstrating the role of ENaC in the regulation of β-cell function.

References:

1. Nakrani, M.N., R.H. Wineland, and F. Anjum, *Physiology, glucose metabolism.* 2020.
2. Lema-Pérez, L., *Main organs involved in glucose metabolism*, in *Sugar intake-risks and benefits and the global diabetes epidemic*. 2021, IntechOpen.
3. Chandel, N.S., *Glycolysis.* Cold Spring Harbor Perspectives in Biology, 2021. **13**(5): p. a040535.
4. Zierler, K., *Whole body glucose metabolism.* American Journal of Physiology-Endocrinology and Metabolism, 1999. **276**(3): p. E409-E426.
5. Adeva-Andany, M.M., et al., *Liver glucose metabolism in humans.* Bioscience reports, 2016. **36**(6): p. e00416.
6. Roach, P.J., *Glycogen and its metabolism.* Current molecular medicine, 2002. **2**(2): p. 101-120.
7. Akram, M., *Citric acid cycle and role of its intermediates in metabolism.* Cell biochemistry and biophysics, 2014. **68**(3): p. 475-478.
8. Farman, M., et al., *Stability analysis and control of the glucose insulin glucagon system in humans.* Chinese Journal of Physics, 2018. **56**(4): p. 1362-1369.
9. Bavitz, J.B., *Emergency management of hypoglycemia and hyperglycemia.* Dental Clinics of North America, 1995. **39**(3): p. 587-594.
10. Röder, P.V., et al., *Pancreatic regulation of glucose homeostasis.* Experimental & molecular medicine, 2016. **48**(3): p. e219-e219.
11. Tokarz, V.L., P.E. MacDonald, and A. Klip, *The cell biology of systemic insulin function.* Journal of Cell Biology, 2018. **217**(7): p. 2273-2289.
12. White, M.F. and C.R. Kahn, *The insulin signaling system.* Journal of Biological Chemistry, 1994. **269**(1): p. 1-4.
13. Cheatham, B. and C.R. Kahn, *Insulin action and the insulin signaling network.* Endocrine reviews, 1995. **16**(2): p. 117-142.
14. Mackenzie, R.W. and B.T. Elliott, *Akt/PKB activation and insulin signaling: a novel insulin signaling pathway in the treatment of type 2 diabetes.* Diabetes, metabolic syndrome and obesity: targets and therapy, 2014: p. 55-64.
15. Watson, R.T. and J.E. Pessin, *Intracellular organization of insulin signaling and GLUT4 translocation.* Recent progress in hormone research, 2001. **56**(1): p. 175-194.
16. Ren, Z., et al., *Insulin promotes mitochondrial respiration and survival through PI3K/AKT/GSK3 pathway in human embryonic stem cells.* Stem cell reports, 2020. **15**(6): p. 1362-1376.
17. Yang, L., et al., *The role of insulin/IGF-1/PI3K/Akt/GSK3β signaling in Parkinson's disease dementia.* Frontiers in neuroscience, 2018. **12**: p. 73.
18. Habegger, K.M., et al., *The metabolic actions of glucagon revisited.* Nature Reviews Endocrinology, 2010. **6**(12): p. 689-697.

19. Burcelin, R., E. Katz, and M. Charron, *Molecular and cellular aspects of the glucagon receptor: role in diabetes and metabolism.* Diabetes & metabolism, 1996. **22**(6): p. 373-396.
20. Jiang, G. and B.B. Zhang, *Glucagon and regulation of glucose metabolism.* American Journal of Physiology-Endocrinology and Metabolism, 2003. **284**(4): p. E671-E678.
21. Jiang, Y., et al., *Glucagon receptor activates extracellular signal-regulated protein kinase 1/2 via cAMP-dependent protein kinase.* Proceedings of the National Academy of Sciences, 2001. **98**(18): p. 10102-10107.
22. Mao, T., et al., *PKA phosphorylation couples hepatic inositol-requiring enzyme 1α to glucagon signaling in glucose metabolism.* Proceedings of the National Academy of Sciences, 2011. **108**(38): p. 15852-15857.
23. Beuers, U. and K. Jungermann, *Relative contribution of glycogenolysis and gluconeogenesis to basal, glucagon-and nerve stimulation-dependent glucose output in the perfused liver from fed and fasted rats.* Biochemistry International, 1990. **21**(3): p. 405-415.
24. Taborsky Jr, G.J., *The physiology of glucagon.* Journal of diabetes science and technology, 2010. **4**(6): p. 1338-1344.
25. Briant, L., et al., *Glucagon secretion from pancreatic α-cells.* Upsala journal of medical sciences, 2016. **121**(2): p. 113-119.
26. Bansal, P. and Q. Wang, *Insulin as a physiological modulator of glucagon secretion.* American Journal of physiology-endocrinology and metabolism, 2008. **295**(4): p. E751-E761.
27. Svendsen, B., et al., *Insulin secretion depends on intra-islet glucagon signaling.* Cell reports, 2018. **25**(5): p. 1127-1134. e2.
28. Hamilton, A., et al., *Adrenaline stimulates glucagon secretion by Tpc2-dependent Ca2+ mobilization from acidic stores in pancreatic α-cells.* Diabetes, 2018. **67**(6): p. 1128-1139.
29. Choi, J.H. and M.-S. Kim, *Homeostatic regulation of glucose metabolism by the central nervous system.* Endocrinology and Metabolism, 2022. **37**(1): p. 9-25.
30. Bratusch-Marrain, P.R., D. Smith, and R.A. Defronzo, *The effect of growth hormone on glucose metabolism and insulin secretion in man.* The Journal of Clinical Endocrinology & Metabolism, 1982. **55**(5): p. 973-982.
31. Aronoff, S.L., et al., *Glucose metabolism and regulation: beyond insulin and glucagon.* Diabetes spectrum, 2004. **17**(3): p. 183-190.
32. Kern, T.S., B.A. Berkowitz, and E.L. Feldman, *National Institute of Diabetes and Digestive and Kidney Diseases (NIDDK) meeting summary: Advances toward measuring diabetic retinopathy and neuropathy: from the bench to the clinic and back again (April 4–5, 2007, Baltimore, Maryland).* Journal of Diabetes and its Complications, 2009. **23**(3): p. 219-223.
33. Jungheim, K. and T. Koschinsky, *Glucose monitoring at the arm: risky delays of hypoglycemia and hyperglycemia detection.* Diabetes care, 2002. **25**(6): p. 956-960.

34. Goyal, A., et al., *Differential clinical outcomes associated with hypoglycemia and hyperglycemia in acute myocardial infarction.* Circulation, 2009. **120**(24): p. 2429-2437.
35. Cryer, P.E., et al., *Evaluation and management of adult hypoglycemic disorders: an Endocrine Society Clinical Practice Guideline.* The Journal of Clinical Endocrinology & Metabolism, 2009. **94**(3): p. 709-728.
36. Cryer, P.E., *Hypoglycemia, functional brain failure, and brain death.* The Journal of clinical investigation, 2007. **117**(4): p. 868-870.
37. Hoffman, R.G., et al., *Changes in cortical functioning with acute hypoglycemia and hyperglycemia in type I diabetes.* Diabetes Care, 1989. **12**(3): p. 193-197.
38. Petrides, A.S., et al., *Effect of physiologic hyperinsulinemia on glucose and lipid metabolism in cirrhosis.* The Journal of clinical investigation, 1991. **88**(2): p. 561-570.
39. Thomas, D.D., et al., *Hyperinsulinemia: an early indicator of metabolic dysfunction.* Journal of the Endocrine Society, 2019. **3**(9): p. 1727-1747.
40. Zimmet, P.Z., et al., *Diabetes: a 21st century challenge.* The lancet Diabetes & endocrinology, 2014. **2**(1): p. 56-64.
41. Deshpande, A.D., M. Harris-Hayes, and M. Schootman, *Epidemiology of diabetes and diabetes-related complications.* Physical therapy, 2008. **88**(11): p. 1254-1264.
42. Forouhi, N.G. and N.J. Wareham, *Epidemiology of diabetes.* Medicine, 2010. **38**(11): p. 602-606.
43. Rother, K.I., *Diabetes treatment—bridging the divide.* The New England journal of medicine, 2007. **356**(15): p. 1499.
44. Wang, J., et al., *Analysis of pathogenesis of juvenile new-onset diabetes.* Journal of diabetes, 2011. **3**(2): p. 132-137.
45. Guo, J.H., et al., *Glucose-induced electrical activities and insulin secretion in pancreatic islet β-cells are modulated by CFTR.* Nature communications, 2014. **5**(1): p. 1-10.
46. Care, D., *Classification and diagnosis of diabetes.* Diabetes Care, 2017. **40**(Suppl 1): p. S11-S24.
47. Melmed, S., et al., *Williams textbook of endocrinology E-Book*. 2015: Elsevier Health Sciences.
48. Kitabchi, A.E., et al., *Hyperglycemic crises in adult patients with diabetes.* Diabetes care, 2009. **32**(7): p. 1335.
49. Gardner, D.G. and D. Shoback, *Greenspan's basic & clinical endocrinology*. 2018: McGraw-Hill Education.
50. Williams, L., *Wilkins (ed.): Diabetes Mellitus: A Guide to Patient Care.* Springhouse Publishing, Philadelphia, 2007. **1**: p. 2-3.
51. Larsen, R. and H. Kronenberg, *et ad. Williams textbook of endocrinology 12th edition*. 2011, Elsevier Saunders.

52. Ellis, C., A. Ramzy, and T.J. Kieffer, *Regenerative medicine and cell-based approaches to restore pancreatic function.* Nature reviews Gastroenterology & hepatology, 2017. **14**(10): p. 612-628.
53. Leung, P.S. and P.S. Leung, *Overview of the pancreas.* The Renin-Angiotensin System: Current Research Progress in The Pancreas: The RAS in the Pancreas, 2010: p. 3-12.
54. Longnecker, D.S., *Anatomy and Histology of the Pancreas (version 1.0).* Pancreapedia: The Exocrine Pancreas Knowledge Base, 2014.
55. Kim, A., et al., *Islet architecture: A comparative study.* Islets, 2009. **1**(2): p. 129-136.
56. Andralojc, K., et al., *Ghrelin-producing epsilon cells in the developing and adult human pancreas.* Diabetologia, 2009. **52**: p. 486-493.
57. Williams, J.A. and I.D. Goldfine, *The insulin-pancreatic acinar axis.* Diabetes, 1985. **34**(10): p. 980-986.
58. Campbell, J.E. and C.B. Newgard, *Mechanisms controlling pancreatic islet cell function in insulin secretion.* Nature reviews Molecular cell biology, 2021. **22**(2): p. 142-158.
59. Michael, D.J., et al., *Pancreatic β-cells secrete insulin in fast-and slow-release forms.* Diabetes, 2006. **55**(3): p. 600-607.
60. Boland, B.B., C.J. Rhodes, and J.S. Grimsby, *The dynamic plasticity of insulin production in β-cells.* Molecular metabolism, 2017. **6**(9): p. 958-973.
61. Hodson, D.J., et al., *Lipotoxicity disrupts incretin-regulated human β cell connectivity.* The Journal of clinical investigation, 2013. **123**(10): p. 4182-4194.
62. Ferrannini, E. and A. Mari, *β-Cell function in type 2 diabetes.* Metabolism, 2014. **63**(10): p. 1217-1227.
63. Ferrannini, E. and A. Mari, *Beta cell function and its relation to insulin action in humans: a critical appraisal.* Diabetologia, 2004. **47**: p. 943-956.
64. Brereton, M.F., M. Rohm, and F.M. Ashcroft, *β-Cell dysfunction in diabetes: a crisis of identity?* Diabetes, obesity and metabolism, 2016. **18**: p. 102-109.
65. Eizirik, D.L., L. Pasquali, and M. Cnop, *Pancreatic β-cells in type 1 and type 2 diabetes mellitus: different pathways to failure.* Nature Reviews Endocrinology, 2020. **16**(7): p. 349-362.
66. Shanik, M.H., et al., *Insulin resistance and hyperinsulinemia: is hyperinsulinemia the cart or the horse?* Diabetes care, 2008. **31**(Supplement_2): p. S262-S268.
67. Basu, R., et al., *Mechanisms of the age-associated deterioration in glucose tolerance: contribution of alterations in insulin secretion, action, and clearance.* Diabetes, 2003. **52**(7): p. 1738-1748.
68. Cohrs, C.M., et al., *Dysfunction of persisting β cells is a key feature of early type 2 diabetes pathogenesis.* Cell Reports, 2020. **31**(1): p. 107469.
69. Panzer, J.K., A. Tamayo, and A. Caicedo, *Restoring glutamate receptor signaling in pancreatic alpha cells rescues glucagon responses in type 1 diabetes.* Cell Reports, 2022. **41**(11): p. 111792.

70. Kieffer, T.J. and J. Francis Habener, *The glucagon-like peptides.* Endocrine reviews, 1999. **20**(6): p. 876-913.
71. Stanojevic, V. and J.F. Habener, *Evolving function and potential of pancreatic alpha cells.* Best Practice & Research Clinical Endocrinology & Metabolism, 2015. **29**(6): p. 859-871.
72. Verberne, A.J. and B.M. Mussa, *Neural control of pancreatic peptide hormone secretion.* Peptides, 2022. **152**: p. 170768.
73. Yu, Q., et al., *Glucose controls glucagon secretion by directly modulating cAMP in alpha cells.* Diabetologia, 2019. **62**: p. 1212-1224.
74. Rutter, G.A., et al., *Intracellular zinc in insulin secretion and action: a determinant of diabetes risk?* Proceedings of the Nutrition Society, 2016. **75**(1): p. 61-72.
75. Kailey, B., et al., *SSTR2 is the functionally dominant somatostatin receptor in human pancreatic β-and α-cells.* American journal of physiology-endocrinology and metabolism, 2012. **303**(9): p. E1107-E1116.
76. Almaça, J., et al., *Human beta cells produce and release serotonin to inhibit glucagon secretion from alpha cells.* Cell reports, 2016. **17**(12): p. 3281-3291.
77. Collombat, P., et al., *The ectopic expression of Pax4 in the mouse pancreas converts progenitor cells into α and subsequently β cells.* Cell, 2009. **138**(3): p. 449-462.
78. Holter, M.M., M. Saikia, and B.P. Cummings, *Alpha-cell paracrine signaling in the regulation of beta-cell insulin secretion.* Frontiers in endocrinology, 2022. **13**: p. 934775.
79. Chung, C.-H., et al., *Pancreatic β-cell neogenesis by direct conversion from mature α-cells.* Stem cells, 2010. **28**(9): p. 1630-1638.
80. Braun, M., et al., *γ-Aminobutyric acid (GABA) is an autocrine excitatory transmitter in human pancreatic β-cells.* Diabetes, 2010. **59**(7): p. 1694-1701.
81. Renström, E., et al., *Neurotransmitter-induced inhibition of exocytosis in insulin-secreting β cells by activation of calcineurin.* Neuron, 1996. **17**(3): p. 513-522.
82. Brereton, M.F., et al., *Alpha-, delta-and PP-cells: are they the architectural cornerstones of islet structure and co-ordination?* Journal of Histochemistry & Cytochemistry, 2015. **63**(8): p. 575-591.
83. Masharani, U. and M.S. German, *17. Pancreatic Hormones and Diabetes Mellitus.* 2011.
84. Sakata, N., G. Yoshimatsu, and S. Kodama, *Development and characteristics of pancreatic epsilon cells.* International journal of molecular sciences, 2019. **20**(8): p. 1867.
85. Olszewski, P.K., et al., *Hypothalamic paraventricular injections of ghrelin: effect on feeding and c-Fos immunoreactivity.* Peptides, 2003. **24**(6): p. 919-923.
86. Horvath, T.L., et al., *Minireview: ghrelin and the regulation of energy balance—a hypothalamic perspective.* Endocrinology, 2001. **142**(10): p. 4163-4169.

87. Shiao, M.-S., et al., *Adaptive evolution of the insulin two-gene system in mouse.* Genetics, 2008. **178**(3): p. 1683-1691.
88. Fu, Y., et al., *Cellular composition characterizing postnatal development and maturation of the mouse brain and spinal cord.* Brain Structure and Function, 2013. **218**: p. 1337-1354.
89. Devaskar, S.U., et al., *Insulin gene expression and insulin synthesis in mammalian neuronal cells.* Journal of Biological Chemistry, 1994. **269**(11): p. 8445-8454.
90. Vaulont, S., M. Vasseur-Cognet, and A. Kahn, *Glucose regulation of gene transcription.* Journal of Biological Chemistry, 2000. **275**(41): p. 31555-31558.
91. D'Amour, K.A., et al., *Production of pancreatic hormone–expressing endocrine cells from human embryonic stem cells.* Nature biotechnology, 2006. **24**(11): p. 1392-1401.
92. Bohuslavova, R., et al., *NEUROD1 Is Required for the Early α and β Endocrine Differentiation in the Pancreas.* International Journal of Molecular Sciences, 2021. **22**(13): p. 6713.
93. Aguayo-Mazzucato, C., et al., *Mafa expression enhances glucose-responsive insulin secretion in neonatal rat beta cells.* Diabetologia, 2011. **54**: p. 583-593.
94. Wang, H., et al., *MAFA controls genes implicated in insulin biosynthesis and secretion.* Diabetologia, 2007. **50**: p. 348-358.
95. Zhang, C., et al., *MafA is a key regulator of glucose-stimulated insulin secretion.* Molecular and cellular biology, 2005. **25**(12): p. 4969-4976.
96. Henquin, J.-C., et al., *Shortcomings of current models of glucose-induced insulin secretion.* Diabetes, Obesity and Metabolism, 2009. **11**: p. 168-179.
97. Ashcroft, F., *KATP channels and insulin secretion: a key role in health and disease.* Biochemical Society Transactions, 2006. **34**(2): p. 243-246.
98. Navarro-Tableros, V., et al., *Physiological development of insulin secretion, calcium channels, and GLUT2 expression of pancreatic rat β-cells.* American Journal of Physiology-Endocrinology and Metabolism, 2007. **292**(4): p. E1018-E1029.
99. Rorsman, P. and E. Renström, *Insulin granule dynamics in pancreatic beta cells.* Diabetologia, 2003. **46**: p. 1029-1045.
100. Palumbo, P., et al., *Mathematical modeling of the glucose–insulin system: A review.* Mathematical biosciences, 2013. **244**(2): p. 69-81.
101. Wang, Z. and D.C. Thurmond, *Mechanisms of biphasic insulin-granule exocytosis–roles of the cytoskeleton, small GTPases and SNARE proteins.* Journal of cell science, 2009. **122**(7): p. 893-903.
102. Del Prato, S. and A. Tiengo, *The importance of first-phase insulin secretion: implications for the therapy of type 2 diabetes mellitus.* Diabetes/metabolism research and reviews, 2001. **17**(3): p. 164-174.

103. Kashyap, S., et al., *A sustained increase in plasma free fatty acids impairs insulin secretion in nondiabetic subjects genetically predisposed to develop type 2 diabetes.* Diabetes, 2003. **52**(10): p. 2461-2474.
104. Henquin, J.-C., *Regulation of insulin secretion: a matter of phase control and amplitude modulation.* Diabetologia, 2009. **52**(5): p. 739-751.
105. Henquin, J.-C., et al., *Signals and pools underlying biphasic insulin secretion.* Diabetes, 2002. **51**(suppl_1): p. S60-S67.
106. Barg, S., et al., *A subset of 50 secretory granules in close contact with L-type Ca2+ channels accounts for first-phase insulin secretion in mouse β-cells.* Diabetes, 2002. **51**(suppl_1): p. S74-S82.
107. Kahn, S.E., *The importance of β-cell failure in the development and progression of type 2 diabetes.* The Journal of Clinical Endocrinology & Metabolism, 2001. **86**(9): p. 4047-4058.
108. Thompson, B. and L.S. Satin, *Beta-cell ion channels and their role in regulating insulin secretion.* Comprehensive Physiology, 2021. **11**(4): p. 1.
109. Ashcroft, F.M. and P. Rorsman, *Electrophysiology of the pancreatic β-cell.* Progress in biophysics and molecular biology, 1989. **54**(2): p. 87-143.
110. Gloyn, A.L., et al., *Permanent neonatal diabetes due to paternal germline mosaicism for an activating mutation of the KCNJ11 gene encoding the Kir6. 2 subunit of the β-cell potassium adenosine triphosphate channel.* The Journal of Clinical Endocrinology & Metabolism, 2004. **89**(8): p. 3932-3935.
111. Aguilar-Bryan, L. and J. Bryan, *Molecular biology of adenosine triphosphate-sensitive potassium channels.* Endocrine reviews, 1999. **20**(2): p. 101-135.
112. Quan, Y., et al., *Current understanding of KATP channels in neonatal diseases: focus on insulin secretion disorders.* Acta Pharmacologica Sinica, 2011. **32**(6): p. 765-780.
113. Fridlyand, L.E., D.A. Jacobson, and L. Philipson, *Ion channels and regulation of insulin secretion in human β-cells: a computational systems analysis.* Islets, 2013. **5**(1): p. 1-15.
114. Eliasson, L., et al., *Novel aspects of the molecular mechanisms controlling insulin secretion.* The Journal of physiology, 2008. **586**(14): p. 3313-3324.
115. Pertusa, J.A., et al., *Effects of calcium buffering on glucose-induced insulin release in mouse pancreatic islets: an approximation to the calcium sensor.* The Journal of physiology, 1999. **520**(Pt 2): p. 473.
116. Ohara-Imaizumi, M., et al., *ELKS/Voltage-dependent Ca2+ channel-β subunit module regulates polarized Ca2+ influx in pancreatic β cells.* Cell Reports, 2019. **26**(5): p. 1213-1226. e7.
117. Yang, S.-N. and P.-O. Berggren, *The role of voltage-gated calcium channels in pancreatic β-cell physiology and pathophysiology.* Endocrine reviews, 2006. **27**(6): p. 621-676.
118. Namkung, Y., et al., *Requirement for the L-type Ca 2+ channel α 1D subunit in postnatal pancreatic β cell generation.* The Journal of clinical investigation, 2001. **108**(7): p. 1015-1022.

119. Schulla, V., et al., *Impaired insulin secretion and glucose tolerance in β cell-selective Cav1. 2 Ca2+ channel null mice.* The EMBO journal, 2003. **22**(15): p. 3844-3854.
120. Davalli, A., et al., *Dihydropyridine-sensitive and-insensitive voltage-operated calcium channels participate in the control of glucose-induced insulin release from human pancreatic β cells.* journal of Endocrinology, 1996. **150**(2): p. 195-203.
121. Jing, X., et al., *Ca V 2.3 calcium channels control second-phase insulin release.* The Journal of clinical investigation, 2005. **115**(1): p. 146-154.
122. Ashcroft, F.M., R. Kelly, and P. Smith, *Two types of Ca channel in rat pancreatic β-cells.* Pflügers Archiv, 1990. **415**: p. 504-506.
123. Göpel, S., et al., *Regulation of glucagon release in mouse α-cells by KATP channels and inactivation of TTX-sensitive Na+ channels.* The Journal of physiology, 2000. **528**(3): p. 509-520.
124. Gilon, P., et al., *Uptake and release of Ca2+ by the endoplasmic reticulum contribute to the oscillations of the cytosolic Ca2+ concentration triggered by Ca2+ influx in the electrically excitable pancreatic B-cell.* Journal of Biological Chemistry, 1999. **274**(29): p. 20197-20205.
125. Sabourin, J., et al., *Store-operated Ca2+ entry mediated by Orai1 and TRPC1 participates to insulin secretion in rat β-cells.* Journal of Biological Chemistry, 2015. **290**(51): p. 30530-30539.
126. Philippaert, K. and R. Vennekens, *12 The Role of TRP Channels in the Pancreatic Beta-Cell.* Neurobiology of TRP channels, 2017: p. 229.
127. Islam, M.S., *Transient receptor potential channels*. Vol. 704. 2011: Springer Science & Business Media.
128. Caterina, M.J., et al., *The capsaicin receptor: a heat-activated ion channel in the pain pathway.* Nature, 1997. **389**(6653): p. 816-824.
129. Perraud, A.-L., et al., *ADP-ribose gating of the calcium-permeable LTRPC2 channel revealed by Nudix motif homology.* Nature, 2001. **411**(6837): p. 595-599.
130. Hodgkin, A.L. and A.F. Huxley, *Currents carried by sodium and potassium ions through the membrane of the giant axon of Loligo.* The Journal of physiology, 1952. **116**(4): p. 449.
131. Goldin, A.L., *Resurgence of sodium channel research.* Annual review of physiology, 2001. **63**(1): p. 871-894.
132. Nita, I.I., et al., *Pancreatic β-cell Na+ channels control global Ca2+ signaling and oxidative metabolism by inducing Na+ and Ca2+ responses that are propagated into mitochondria.* The FASEB Journal, 2014. **28**(8): p. 3301-3312.
133. Fridlyand, L.E., N. Tamarina, and L.H. Philipson, *Modeling of Ca2+ flux in pancreatic β-cells: role of the plasma membrane and intracellular stores.* American Journal of Physiology-Endocrinology and Metabolism, 2003. **285**(1): p. E138-E154.

134. Zhang, Q., et al., *Na+ current properties in islet α-and β-cells reflect cell-specific Scn3a and Scn9a expression.* The Journal of physiology, 2014. **592**(21): p. 4677-4696.
135. Rizzetto, R., *Pathophysiology of the late sodium current: from myocardium to pancreatic beta cells.* 2013.
136. Best, L., et al., *Electrical activity in pancreatic islet cells: the VRAC hypothesis.* Islets, 2010. **2**(2): p. 59-64.
137. Edlund, A., et al., *CFTR and Anoctamin 1 (ANO1) contribute to cAMP amplified exocytosis and insulin secretion in human and murine pancreatic beta-cells.* BMC medicine, 2014. **12**(1): p. 1-12.
138. Davidson, H.W., C.J. Rhodes, and J.C. Hutton, *Intraorganellar calcium and p H control proinsulin cleavage in the pancreatic β cell via two distinct site-specific endopeptidases.* Nature, 1988. **333**(6168): p. 93-96.
139. Edlund, A., et al., *Defective exocytosis and processing of insulin in a cystic fibrosis mouse model.* Journal of Endocrinology, 2019. **241**(1): p. 45-57.
140. Huang, W.Q., et al., *Glucose-sensitive CFTR suppresses glucagon secretion by potentiating KATP channels in pancreatic islet α cells.* Endocrinology, 2017. **158**(10): p. 3188-3199.
141. Baggio, L.L. and D.J. Drucker, *Biology of incretins: GLP-1 and GIP*. Gastroenterology, 2007. **132**(6): p. 2131-2157.
142. Kreymann, B., et al., *Glucagon-like peptide-1 7-36: a physiological incretin in man.* The Lancet, 1987. **330**(8571): p. 1300-1304.
143. Rorsman, P. and M.O. Huising, *The somatostatin-secreting pancreatic δ-cell in health and disease.* Nature Reviews Endocrinology, 2018. **14**(7): p. 404-414.
144. Insel, P.A. and R.S. Ostrom, *Forskolin as a tool for examining adenylyl cyclase expression, regulation, and G protein signaling.* Cellular and molecular neurobiology, 2003. **23**: p. 305-314.
145. Wang, W., H. Oberleithner, and F. Lang, *The effect of cAMP on the cell membrane potential and intracellular ion activities in proximal tubule of rana esculenta.* Pflügers Archiv, 1983. **396**: p. 192-198.
146. Chen, J., et al., *Ca2+-stimulated adenylyl cyclases as therapeutic targets for psychiatric and neurodevelopmental disorders.* Frontiers in Pharmacology, 2022. **13**: p. 949384.
147. Tengholm, A. and E. Gylfe, *cAMP signalling in insulin and glucagon secretion.* Diabetes, obesity and metabolism, 2017. **19**: p. 42-53.
148. Adame-García, S.R., et al., *cAMP-dependent activation of the Rac guanine exchange factor P-REX1 by type I protein kinase A (PKA) regulatory subunits.* Journal of Biological Chemistry, 2019. **294**(7): p. 2232-2246.
149. Gaisano, H.Y., *Recent new insights into the role of SNARE and associated proteins in insulin granule exocytosis.* Diabetes, Obesity and Metabolism, 2017. **19**: p. 115-123.

150. Shibasaki, T., et al., *Essential role of Epac2/Rap1 signaling in regulation of insulin granule dynamics by cAMP.* Proceedings of the National Academy of Sciences, 2007. **104**(49): p. 19333-19338.
151. Tengholm, A., *Cyclic AMP dynamics in the pancreatic β-cell.* Upsala journal of medical sciences, 2012. **117**(4): p. 355-369.
152. Lu, T.-W., et al., *Two PKA RIα holoenzyme states define ATP as an isoform-specific orthosteric inhibitor that competes with the allosteric activator, cAMP.* Proceedings of the National Academy of Sciences, 2019. **116**(33): p. 16347-16356.
153. Song, W.-J., et al., *Snapin mediates incretin action and augments glucose-dependent insulin secretion.* Cell metabolism, 2011. **13**(3): p. 308-319.
154. Song, W.-J., et al., *Pancreatic β-cell response to increased metabolic demand and to pharmacologic secretagogues requires EPAC2A.* diabetes, 2013. **62**(8): p. 2796-2807.
155. Blanchet, E., et al., *Feedback inhibition of CREB signaling promotes beta cell dysfunction in insulin resistance.* Cell reports, 2015. **10**(7): p. 1149-1157.
156. Hanukoglu, I. and A. Hanukoglu, *Epithelial sodium channel (ENaC) family: Phylogeny, structure–function, tissue distribution, and associated inherited diseases.* Gene, 2016. **579**(2): p. 95-132.
157. Hanukoglu, I., et al., *Expression of epithelial sodium channel (ENaC) and CFTR in the human epidermis and epidermal appendages.* Histochemistry and cell biology, 2017. **147**: p. 733-748.
158. Enuka, Y., et al., *Epithelial sodium channels (ENaC) are uniformly distributed on motile cilia in the oviduct and the respiratory airways.* Histochemistry and cell biology, 2012. **137**: p. 339-353.
159. Voilley, N., et al., *The lung amiloride-sensitive Na+ channel: biophysical properties, pharmacology, ontogenesis, and molecular cloning.* Proceedings of the National Academy of Sciences, 1994. **91**(1): p. 247-251.
160. Shimkets, R.A., et al., *Liddle's syndrome: heritable human hypertension caused by mutations in the β subunit of the epithelial sodium channel.* Cell, 1994. **79**(3): p. 407-414.
161. Brooker, D.R., C.A. Kozak, and T.R. Kleyman, *Epithelial Sodium Channel GenesScnn1bandScnn1gAre Closely Linked on Distal Mouse Chromosome 7.* Genomics, 1995. **29**(3): p. 784-786.
162. Canessa, C.M., et al., *Amiloride-sensitive epithelial Na+ channel is made of three homologous subunits.* Nature, 1994. **367**(6462): p. 463-467.
163. Deval, E. and E. Lingueglia, *Acid-Sensing Ion Channels and nociception in the peripheral and central nervous systems.* Neuropharmacology, 2015. **94**: p. 49-57.
164. Fechner, S., et al., *DEG/ENaC/ASIC channels vary in their sensitivity to anti-hypertensive and non-steroidal anti-inflammatory drugs.* Journal of General Physiology, 2021. **153**(4): p. e202012655.

165. Moore, P.J. and R. Tarran, *The epithelial sodium channel (ENaC) as a therapeutic target for cystic fibrosis lung disease.* Expert opinion on therapeutic targets, 2018. **22**(8): p. 687-701.
166. Litwack, G., *Hormonal Regulation of Epithelial Sodium Channel (ENaC) and Other Nonneuronal Epithelial Ion Channels.* Hormonal Signaling in Biology and Medicine, 2020: p. 283-309.
167. Garty, H. and L.G. Palmer, *Epithelial sodium channels: function, structure, and regulation.* Physiological reviews, 1997. **77**(2): p. 359-396.
168. Bhalla, V. and K.R. Hallows, *Mechanisms of ENaC regulation and clinical implications.* Journal of the American Society of Nephrology, 2008. **19**(10): p. 1845-1854.
169. Hummler, E., et al., *Early death due to defective neonatal lung liquid clearance in α ENaC-deficient mice.* Nature genetics, 1996. **12**(3): p. 325-328.
170. Mérillat, A.-M., et al., *Conditional gene targeting of the ENaC subunit genes Scnn1b and Scnn1g.* American Journal of Physiology-Renal Physiology, 2009. **296**(2): p. F249-F256.
171. McDonald, F.J., et al., *Disruption of the β subunit of the epithelial Na+ channel in mice: hyperkalemia and neonatal death associated with a pseudohypoaldosteronism phenotype.* Proceedings of the National Academy of Sciences, 1999. **96**(4): p. 1727-1731.
172. Barker, P.M., et al., *Role of gammaENaC subunit in lung liquid clearance and electrolyte balance in newborn mice. Insights into perinatal adaptation and pseudohypoaldosteronism.* The Journal of clinical investigation, 1998. **102**(8): p. 1634-1640.
173. Boiko, N., V. Kucher, and J.D. Stockand, *Pseudohypoaldosteronism type 1 and Liddle's syndrome mutations that affect the single-channel properties of the epithelial Na+ channel.* Physiological Reports, 2015. **3**(11): p. e12600.
174. Edelheit, O., et al., *Truncated beta epithelial sodium channel (ENaC) subunits responsible for multi-system pseudohypoaldosteronism support partial activity of ENaC.* The Journal of Steroid Biochemistry and Molecular Biology, 2010. **119**(1-2): p. 84-88.
175. Chang, S.S., et al., *Mutations in subunits of the epithelial sodium channel cause salt wasting with hyperkalaemic acidosis, pseudohypoaldosteronism type 1.* Nature genetics, 1996. **12**(3): p. 248-253.
176. Enslow, B.T., J.D. Stockand, and J.M. Berman, *Liddle's syndrome mechanisms, diagnosis and management.* Integrated Blood Pressure Control, 2019: p. 13-22.
177. Liu, F., et al., *Associations of epithelial sodium channel genes with blood pressure: the GenSalt study.* Journal of human hypertension, 2015. **29**(4): p. 224-228.
178. Matalon, S., R. Bartoszewski, and J.F. Collawn, *Role of epithelial sodium channels in the regulation of lung fluid homeostasis.* American Journal of Physiology-Lung Cellular and Molecular Physiology, 2015. **309**(11): p. L1229-L1238.

179. Helve, O., et al., *Expression of the epithelial sodium channel in airway epithelium of newborn infants depends on gestational age.* Pediatrics, 2007. **120**(6): p. 1311-1316.
180. Hamm, L.L., Z. Feng, and K.S. Hering-Smith, *Regulation of sodium transport by ENaC in the kidney.* Current opinion in nephrology and hypertension, 2010. **19**(1): p. 98.
181. Firsov, D., N. Tokonami, and O. Bonny, *Role of the renal circadian timing system in maintaining water and electrolytes homeostasis.* Molecular and cellular endocrinology, 2012. **349**(1): p. 51-55.
182. Ruan, Y.C., et al., *Activation of the epithelial Na+ channel triggers prostaglandin E2 release and production required for embryo implantation.* Nature medicine, 2012. **18**(7): p. 1112-1117.
183. Sun, X., et al., *Regulation of miR-101/miR-199a-3p by the epithelial sodium channel during embryo implantation: involvement of CREB phosphorylation.* Reproduction (Cambridge, England), 2014. **148**(6): p. 559-568.
184. Sun, X., et al., *Activation of the epithelial sodium channel (EN aC) leads to cytokine profile shift to pro-inflammatory in labor.* EMBO molecular medicine, 2018. **10**(10): p. e8868.
185. Chen, H., et al., *Regulation of male fertility by CFTR and implications in male infertility.* Human reproduction update, 2012. **18**(6): p. 703-713.
186. Collawn, J.F., et al., *The CFTR and ENaC debate: how important is ENaC in CF lung disease?* American Journal of Physiology-Lung Cellular and Molecular Physiology, 2012. **302**(11): p. L1141-L1146.
187. Gaillard, E.A., et al., *Regulation of the epithelial Na+ channel and airway surface liquid volume by serine proteases.* Pflügers Archiv-European Journal of Physiology, 2010. **460**: p. 1-17.
188. Graham, A., et al., *No added benefit from nebulized amiloride in patients with cystic fibrosis.* European Respiratory Journal, 1993. **6**(9): p. 1243-1248.
189. Pons, G., et al., *French multicenter randomized double-blind placebo-controlled trial on nebulized amiloride in cystic fibrosis patients.* Pediatric pulmonology, 2000. **30**(1): p. 25-31.
190. Chan, H.C., et al., *Physiology and pathophysiology of the epithelial barrier of the female reproductive tract: role of ion channels.* Biology and Regulation of Blood-Tissue Barriers, 2013: p. 193-217.
191. Ruan, Y.C., H. Chen, and H.C. Chan, *Ion channels in the endometrium: regulation of endometrial receptivity and embryo implantation.* Human reproduction update, 2014. **20**(4): p. 517-529.
192. Wuchu, F., et al., *Biphasic regulation of CFTR expression by ENaC in epithelial cells: The involvement of Ca2+-modulated cAMP production.* Frontiers in Cell and Developmental Biology, 2022. **10**: p. 781762.
193. Pearce, D., *Aldosterone: its receptor, target genes, and actions.* Vitam Horm, 2003. **66**: p. 29-76.

194. Masilamani, S., et al., *Aldosterone-mediated regulation of ENaC α, β, and γ subunit proteins in rat kidney.* The Journal of clinical investigation, 1999. **104**(7): p. R19-R23.
195. Rossier, B.C. and M.J. Stutts, *Activation of the epithelial sodium channel (ENaC) by serine proteases.* Annual review of physiology, 2009. **71**: p. 361-379.
196. Pitzer, A.L., et al., *ENaC in salt-sensitive hypertension: kidney and beyond.* Current Hypertension Reports, 2020. **22**(9): p. 1-10.
197. Hinrichs, G.R., et al., *Amiloride resolves resistant edema and hypertension in a patient with nephrotic syndrome; a case report.* Physiological reports, 2018. **6**(12): p. e13743.
198. Saha, C., et al., *Improvement in blood pressure with inhibition of the epithelial sodium channel in blacks with hypertension.* Hypertension, 2005. **46**(3): p. 481-487.
199. Matthesen, S.K., et al., *Effect of amiloride and spironolactone on renal tubular function and central blood pressure in patients with arterial hypertension during baseline conditions and after furosemide: a double-blinded, randomized, placebo-controlled crossover trial.* Clinical and Experimental Hypertension, 2013. **35**(5): p. 313-324.
200. Sowers, J.R., M. Epstein, and E.D. Frohlich, *Diabetes, hypertension, and cardiovascular disease: an update.* Hypertension, 2001. **37**(4): p. 1053-1059.
201. Gillespie, C.D., et al., *Prevalence of hypertension and controlled hypertension—United States, 2007–2010.* MMWR Suppl, 2013. **62**(3): p. 144-148.
202. Kim, M.-K., *Dietary sodium intake in patients with type 2 diabetes mellitus.* Diabetes & Metabolism Journal, 2016. **40**(4): p. 280-282.
203. He, F.J., J. Li, and G.A. MacGregor, *Effect of longer term modest salt reduction on blood pressure: Cochrane systematic review and meta-analysis of randomised trials.* Bmj, 2013. **346**.
204. Hu, G., et al., *Urinary sodium and potassium excretion and the risk of type 2 diabetes: a prospective study in Finland.* Diabetologia, 2005. **48**: p. 1477-1483.
205. Zhao, Y., et al., *Sodium intake regulates glucose homeostasis through the PPARδ/adiponectin-mediated SGLT2 pathway.* Cell Metabolism, 2016. **23**(4): p. 699-711.
206. Taki, K., et al., *Dietary sodium chloride attenuates increased β-cell mass to cause glucose intolerance in mice under a high-fat diet.* Plos one, 2021. **16**(3): p. e0248065.
207. Ogihara, T., et al., *Insulin resistance with enhanced insulin signaling in high-salt diet–fed rats.* Diabetes, 2001. **50**(3): p. 573-583.
208. Li, D.-S., et al., *A protocol for islet isolation from mouse pancreas.* Nature protocols, 2009. **4**(11): p. 1649-1652.

209. Waxman, S.G., et al., *Sodium channels, excitability of primary sensory neurons, and the molecular basis of pain.* Muscle & nerve, 1999. **22**(9): p. 1177-1187.
210. Guo, J.H., et al., *Glucose-induced electrical activities and insulin secretion in pancreatic islet β-cells are modulated by CFTR.* Nature communications, 2014. **5**(1): p. 4420.
211. Bondarava, M., et al., *α-ENaC is a functional element of the hypertonicity-induced cation channel in HepG2 cells and it mediates proliferation.* Pflügers Archiv-European Journal of Physiology, 2009. **458**: p. 675-687.
212. Plant, T., *Na+ currents in cultured mouse pancreatic B-cells.* Pflügers Archiv, 1988. **411**: p. 429-435.
213. Rossier, B.C., *The epithelial sodium channel (ENaC): new insights into ENaC gating.* Pflügers Archiv-European Journal of Physiology, 2003. **446**(3): p. 314.
214. Soundararajan, R., M. Lu, and D. Pearce, *Organization of the ENaC-regulatory machinery.* Critical reviews in biochemistry and molecular biology, 2012. **47**(4): p. 349-359.
215. Pochynyuk, O., et al., *Binding and direct activation of the epithelial Na+ channel (ENaC) by phosphatidylinositides.* The Journal of physiology, 2007. **580**(2): p. 365-372.
216. Shi, S., et al., *ENaC regulation by proteases and shear stress.* Current molecular pharmacology, 2013. **6**(1): p. 28-34.
217. Butterworth, M.B., et al., *Acute ENaC stimulation by cAMP in a kidney cell line is mediated by exocytic insertion from a recycling channel pool.* The Journal of general physiology, 2005. **125**(1): p. 81-101.
218. Straub, S.G. and G.W. Sharp, *Glucose-stimulated signaling pathways in biphasic insulin secretion.* Diabetes/metabolism research and reviews, 2002. **18**(6): p. 451-463.
219. Huypens, P., et al., *Glucagon receptors on human islet cells contribute to glucose competence of insulin release.* Diabetologia, 2000. **43**: p. 1012-1019.
220. Mayendraraj, A., M.M. Rosenkilde, and L.S. Gasbjerg, *GLP-1 and GIP receptor signaling in beta cells–a review of receptor interactions and co-stimulation.* Peptides, 2022. **151**: p. 170749.
221. Stožer, A., et al., *The role of cAMP in beta cell stimulus–secretion and intercellular coupling.* Cells, 2021. **10**(7): p. 1658.
222. Wang, L., et al., *A high-performance genetically encoded fluorescent indicator for in vivo cAMP imaging.* Nature communications, 2022. **13**(1): p. 5363.
223. Chheda, M.G., et al., *Phosphorylation of Snapin by PKA modulates its interaction with the SNARE complex.* Nature cell biology, 2001. **3**(4): p. 331-338.
224. Henquin, J.-C. and M. Nenquin, *Activators of PKA and Epac distinctly influence insulin secretion and cytosolic Ca2+ in female mouse islets stimulated by glucose and tolbutamide.* Endocrinology, 2014. **155**(9): p. 3274-3287.

225. Stutts, M.J., et al., *CFTR as a cAMP-dependent regulator of sodium channels.* Science, 1995. **269**(5225): p. 847-850.
226. Steer, M.L. and A. Wood, *Inhibitory effects of sodium and other monovalent cations on human platelet adenylate cyclase.* Journal of Biological Chemistry, 1981. **256**(19): p. 9990-9993.
227. Kiroytcheva, M., et al., *Effect of cAMP on the activity and the phosphorylation of Na+, K+-ATPase in rat thick ascending limb of Henle.* Kidney international, 1999. **55**(5): p. 1819-1831.
228. Thomas, A., et al., *AC6 is the major adenylate cyclase forming a diarrheagenic protein complex with cystic fibrosis transmembrane conductance regulator in cholera.* Journal of Biological Chemistry, 2018. **293**(33): p. 12949-12959.
229. Peercy, B.E., A.S. Sherman, and R. Bertram, *Modeling of glucose-induced cAMP oscillations in pancreatic β cells: cAMP rocks when metabolism rolls.* Biophysical journal, 2015. **109**(2): p. 439-449.
230. Renström, E., L. Eliasson, and P. Rorsman, *Protein kinase A-dependent and-independent stimulation of exocytosis by cAMP in mouse pancreatic B-cells.* The Journal of physiology, 1997. **502**(Pt 1): p. 105.
231. Erion, K. and B.E. Corkey, *β-Cell failure or β-cell abuse?* Frontiers in endocrinology, 2018. **9**: p. 532.
232. Esser, N., K.M. Utzschneider, and S.E. Kahn, *Early beta cell dysfunction vs insulin hypersecretion as the primary event in the pathogenesis of dysglycaemia.* Diabetologia, 2020. **63**: p. 2007-2021.
233. Hummler, E., et al., *Early death due to defective neonatal lung liquid clearance in αENaC-deficient mice.* Nature genetics, 1996. **12**(3): p. 325-328.
234. Postic, C., et al., *Dual roles for glucokinase in glucose homeostasis as determined by liver and pancreatic β cell-specific gene knock-outs using Cre recombinase.* Journal of Biological Chemistry, 1999. **274**(1): p. 305-315.
235. Lee, J.-Y., et al., *RIP-Cre revisited, evidence for impairments of pancreatic β-cell function.* Journal of Biological Chemistry, 2006. **281**(5): p. 2649-2653.
236. Bliss, C.R. and G. Sharp, *Glucose-induced insulin release in islets of young rats: time-dependent potentiation and effects of 2-bromostearate.* American Journal of Physiology-Endocrinology and Metabolism, 1992. **263**(5): p. E890-E896.
237. Dalbøge, L.S., et al., *Characterisation of age-dependent beta cell dynamics in the male db/db mice.* PloS one, 2013. **8**(12): p. e82813.
238. Lou, D., et al., *Does age matter? Comparison of neurobehavioral effects of paraquat exposure on postnatal and adult C57BL/6 mice.* Toxicology Mechanisms and Methods, 2016. **26**(9): p. 667-673.
239. Barella, L.F., et al., *β-Arrestin-1 is required for adaptive β-cell mass expansion during obesity.* Nature Communications, 2021. **12**(1): p. 3385.
240. Mahapatra, M.K., M. Karuppasamy, and B.M. Sahoo, *Semaglutide, a glucagon like peptide-1 receptor agonist with cardiovascular benefits for*

management of type 2 diabetes. Reviews in Endocrine and Metabolic Disorders, 2022. **23**(3): p. 521-539.
241. Holst, J.J., L.S. Gasbjerg, and M.M. Rosenkilde, *The role of incretins on insulin function and glucose homeostasis.* Endocrinology, 2021. **162**(7): p. bqab065.
242. Yu, L., et al., *The inhibitory effect of Gβγ and Gβ isoform specificity on ENaC activity.* American Journal of Physiology-Renal Physiology, 2013. **305**(9): p. F1365-F1373.
243. Ausiello, D.A., et al., *Purified epithelial Na+ channel complex contains the pertussis toxin-sensitive G alpha i-3 protein.* Journal of Biological Chemistry, 1992. **267**(7): p. 4759-4765.
244. Komwatana, P., et al., *Cytosolic Na+ controls and epithelial Na+ channel via the Go guanine nucleotide-binding regulatory protein.* Proceedings of the National Academy of Sciences, 1996. **93**(15): p. 8107-8111.
245. Abdel-Halim, S.M., et al., *Mutations in the promoter of adenylyl cyclase (AC)-III gene, overexpression of AC-III mRNA, and enhanced cAMP generation in islets from the spontaneously diabetic GK rat model of type 2 diabetes.* Diabetes, 1998. **47**(3): p. 498-504.
246. Guenifi, A., et al., *Adenylyl cyclase isoform expression in non-diabetic and diabetic Goto-Kakizaki (GK) rat pancreas. Evidence for distinct overexpression of type-8 adenylyl cyclase in diabetic GK rat islets.* Histochemistry and cell biology, 2000. **113**: p. 81-89.
247. Abdel-Halim, S.M., et al., *Increased plasma levels of adenylate cyclase 8 and cAMP are associated with obesity and type 2 diabetes: Results from a cross-sectional study.* Biology, 2020. **9**(9): p. 244.